UNIVERSITY OF CALIFORNIA
RIVERSIDE

Uncovering Arbuscular Mycorrhizal Fungi and Microbiome Responses to Dryland Fires

A Dissertation submitted in partial satisfaction
of the requirements for the degree of

Doctor of Philosophy

in

Microbiology

by

Arik Joukhajian

September 2025

Dissertation Committee:
Dr. Sydney I. Glassman, Chairperson
Dr. Quinn S. McFrederick
Dr. Joel L. Sachs

The Dissertation of Arik Joukhajian is approved:

_____

_____

_____

Committee Chairperson

University of California, Riverside

Acknowledgements

I would like to extend my sincerest gratitude to the many people who helped me achieve the work in this dissertation. To my advisor Sydney Glassman, thank you for all the guidance and help not only in shaping my projects but shaping my skillset, and trust while I explored many interesting side projects, alternate analyses, and one-off ideas along the way. To my Glassman lab predecessors Dylan and Fabi, thank you for the endless answers to my endless questions before during and after your tenure in the lab. To Basubi and Esbeiry, thank you for your unique perspectives and fresh ideas, I look forward to reading your publications. To James and Maria, thank you for all the work behind the scenes allowing me to focus on research. To Ryan and Aishwarya, thank you both for the work you did maintaining the lab and the vibes. To Victoria and Justin, thank you for the hours you spent looking through microscopes with me. To Marcos, thank you for providing a fresh perspective on the world outside of California. To our neighbors in Boyce Hall from the Gachomo, Vidalakis, Aronson, Roper, and Manosalva labs, as well as the Homyak, Sweet, and Stajich labs, thank you for maintaining a friendly environment for interdisciplinary research. To my friends Patty, Claudia, and Tania, thank you for challenging my notions of what is and isn't achievable, and to Arsen and our colleagues in Armenia who took us on an adventure and continue to impress. And to my parents, Manoug and Lucy, thank you for constant support of my interest in the sciences through my winding journey of a dozen different topics, I would not have made it here without your lessons and encouragement.

ABSTRACT OF THE DISSERTATION

Uncovering Arbuscular Mycorrhizal Fungi and Microbiome Responses to Dryland Fires

by

Arik Joukhajian

Doctor of Philosophy, Graduate Program in Microbiology
University of California, Riverside, September 2025
Dr. Sydney I. Glassman, Chairperson

Drylands cover 40% of the Earth's land surface, and this is expected to expand under climate change. These ecosystems are increasingly affected by wildfire, yet the responses of microbes to wildfire remain far less studied than forests and chaparral. In the Mojave Desert, most plants, including the iconic Eastern Joshua tree (*Yucca jaegeriana*), depend on symbioses with arbuscular mycorrhizal fungi (AMF). However, the AMF of *Y. jaegeriana* have not been characterized. To establish a baseline of symbiosis, I seasonally sampled and sequenced soil and root microbes from healthy, unburned counterparts to the heavily impacted *Y. jaegeriana* in the region and identified high overlap in root and soil samples yet greater divergence between the two in Winter and Spring. Overall richness and abundance was lowest in Summer, making Fall the best time to identify AMF

diversity. I then characterized soil microbial communities impacted by the nearby Dome Fire, which burned a million trees of *Y. jaegeriana* and displayed unusually high-severity for a desert fire. Over three years, archaeal, bacterial, and fungal diversity remained stable or even increased. Yet, this fire still caused emergence of known pyrophilous bacteria such as *Massilia* and *Noviherbaspirillum*, and fungi such as *Naganishia, Coniochaeta*, and *Penicillium*, overlapping with microbes found in fire-adapted forest and chaparral fires. To compare outcomes of this low-intensity, high-severity fire with a high-intensity, high-severity chaparral wildfire, I constructed cross-kingdom association networks to identify trends beyond diversity and abundance which varied over time. I saw trends in cohesion consistent with long-term disturbance in burned plots in both desert and chaparral plots, despite only chaparral plots showing signs of decreased richness and biomass post-fire. I also identified potential keystone taxa in the burned plots, including two closely related pyrophilous bacteria *Noviherbaspirillum* and *Massilia,* a Pyronemataceae fungus *Pseudotricharina*, and taxa identified as potential keystones in other systems like *Candidatus Udaeobacter* and *Crossiella*. Taken together, I report AMF diversity, minimal shifts in diversity, and yet widespread emergence of pyrophilous microbes in a sensitive post-fire desert community.

Table of Contents

List of Figures

List of Tables

1 Chapter I.
Introduction to the Dissertation

1.1 Introduction

Drylands cover 40% of the Earth's land surface and are projected to expand further due to climate change (Zeng and Yoon 2009). Despite their low precipitation and sparse vegetation (Huang et al. 2016), these ecosystems are increasingly subject to wildfires, driven by altered rainfall patterns and rising temperatures (Stanton et al. 2023). Although deserts have historically experienced infrequent fire, the increasing occurrence of large, high-severity wildfires raises concerns about long-term impacts on desert ecosystems (Stanton et al. 2023). Soil microbial communities, which mediate nutrient cycling, plant interactions, and ecosystem recovery, are particularly sensitive to the disturbance of wildfires (Certini et al. 2021; Pulido-Chavez et al. 2023; Nelson et al. 2024), yet their responses to desert wildfires are underexplored. Understanding how fire affects these communities is essential for predicting ecosystem resilience and recovery under future climate scenarios.

California habitats have historically been managed by fire, whether through human intervention or plant-induced fire encouragement (Vale 2013), but a century of fire suppression now converges with climate change resulting in increasingly frequent and unusually large wildfires across the state (Turco et al. 2023). Fires in forests and chaparral shrublands have historically occurred at a high return interval, establishing fire

adaptations like serotinous pinecones and excess buildup of oily secretions on shrubs to promote occasional clearance of the overstory in chaparrals (Keeley et al. 2011). These conditions were sustained by early human inhabitants, and fire suppression only began in 1850 to simplify management (Martinez et al. 2023). While growing human expansion and a growing wildland-urban interface can impact wildfire occurrence through fire suppression and accidental fires, climate change appears to be a more widespread cause of this growing fire regime (Vachula et al. 2019). Cycles of drought and downpour, combined with buildup of plant matter, led to 2018 and 2020 to be some of the largest wildfire years in California history. The 2018 Mendocino Complex Fire burned 459,123 acres (1,858 km^2) and was only surpassed by the 2020 August Complex Fire which burned 1,032,648 acres (4,180 km^2), roughly 1% of California's total land (Keeley and Syphard 2021).

Meanwhile, Southern California was impacted by the 2018 Holy Fire in Cleveland National Forest, split between Orange and Riverside counties. The Holy Fire served as an early template to document microbial secondary succession following wildfire (Pulido-Chavez et al. 2023), similar to the consistent secondary succession found in chaparral plants in which certain early colonizers establish soon post-fire and eventually give way to long-term inhabiting late colonizers (Keeley et al. 2011). Chaparral wildfires are often high-intensity, or producing extreme levels of thermal energy, as a result of dense woody vegetation and volatile oils of plant surfaces (Wilkin et al. 2017), but it was also high-severity, or extreme in its impact on plant communities, evidenced by an ash depth of up to 11cm in certain areas (Pulido-Chavez et al. 2023).

Despite suppression of microbial diversity soon after fire, early colonizing bacteria and fungi identified through DNA sequencing were represented by well-known documented pyrophilous, or fire-loving, microbes which rapidly grew in dominance within the soil microbial community (Pulido-Chavez et al. 2023). These included *Pyronema*, a genus of "phoenicoid" fungus that was long-since identified fruiting in large quantities in burned areas (Seaver 1909), and a variety of bacteria that have also showed up in other burned ecosystems (Whitman et al. 2019; Enright et al. 2022; Nelson et al. 2024). These pyrophilous microbes often replace those killed by the direct effects of fire on heat-sensitive microbes, but several indirect effects can cause further shifts in microbial communities allowing pyrophilous microbes to thrive.

Indirect effects such as shifting aboveground plant communities and nutrient deposition can have long-lasting effects on soil microbes such as mycorrhizal fungi (Lekberg et al. 2013). In particular, arbuscular mycorrhizal fungi (AMF) can show immediate and long-term shifts in response to desert wildfires (Chimal-Sánchez et al. 2015). However, they can also be highly resilient to wildfires, partly due to their chlamydospores, which can vary in spore size (11 μm up to 685 μm) and volume (3,363 μm^3 to 88,173,798 μm^3) (Chaudhary et al. 2020, 2025). Concerns over such indirect effects and the long-term sustainability of *Y. jaegeriana* habitat prompted my assessment of their association with AMF. Since AMF can enhance drought tolerance and facilitate direct water transport to plants along fungal hyphae (Augé 2001; Kakouridis et al. 2020), AMF are ubiquitous among desert plants, especially in the Mojave. Further, AMF inoculum was the most abundant under the Mojave Yucca, *Y. schidigera*, in a 2002

assessment of 34 Mojave desert plants (Titus et al. 2002b), and a diverse AMF community was recently identified to be associated with the closely related sister species Western Joshua tree (*Y. brevifolia*) (Harrower and Gilbert 2021). In contrast, the AMF associated with the more recently described Eastern Joshua tree (*Y. jaegeriana*) had never been described. In Chapter II, we characterized AMF from *Y. jaegeriana* near the Cima Dome to establish a baseline of this symbiosis. We sampled trees seasonally to identify year-round variations in spore abundance and a temporal core community of AMF, in order to identify potential mycorrhizal partners in any potential inoculation efforts.

The long-term analysis of soil microbial communities inspired a similar investigation of the 2020 Dome Fire, which burned 43,273 acres (175 km^2) of Joshua tree grassland around the Cima Dome. Unlike the Holy Fire, the Dome Fire occurred in the Mojave Desert, which does not have a frequent fire return interval. This wildfire burned a million Eastern Joshua trees (*Yucca jaegeriana*), which formed a dense stand of trees across this high-elevation region in the desert, causing high-severity impact on grasses and shrubs as well (Smith et al. 2023). Assessments of desert microbial communities after fire have primarily been done in controlled burn settings (Liu et al. 2000; Aanderud et al. 2019; Zhang et al. 2025), and the dry nature of desert sand has been thought to buffer most of the impacts of fire (Allen et al. 2011). Coupled with the fact that the understory grasses burn away quickly, fast-moving desert fires are thought to leave little impact on the soil microbial community as the direct effects of fire are attenuated. In Chapter III, we investigate the plant and microbial community shifts following this desert wildfire across 5 sampling timepoints ranging from 17 days to 3-years post-fire.

With the wealth of data following long-term analyses of microbial communities in the Holy Fire and the Dome Fire, I aimed to better understand the overall microbial response in these contrasting fires of low- and high-intensity, which both showed high-severity impacts on the aboveground plant community, using network analysis. Networks can be generated from compositional data of microbial communities based on associations of taxa with each other, and can be expanded to multiple datasets allowing for cross-kingdom analyses, useful for inferring interactions between microbes in the network (Kurtz et al. 2015). Wildfires can vary to uniform depression of diversity in bacteria and fungi, as in the Holy Fire (Pulido-Chavez et al. 2023), or uneven depression of only fungi often seen in forest fires (Whitman et al. 2019). However, a cross-kingdom approach towards network metrics allows for examination of wider-scale understanding of concepts such as sensitivity and resilience, already tested in contexts of salt-stress (Hernandez et al. 2021) and controlled burns (Birch et al. 2025). Further, highly connected nodes in networks may correlate to microbial keystone species, and identifying differences in important network nodes across burned and unburned networks may help expand our understanding of pyrophilous microbes and their activity in soil post-fire.

Thus, over the course of three chapters, I first described the seasonal variations in the association between *Y. jaegeriana* and the AMF community through sampling of both soil and root using assessments of spore abundance and high-throughput sequencing. Further, I investigated the impact on surviving trees within the burn scar. Second, I described how the plant community and microbial community responded to wildfire over the course of three years of sampling, using plant assessments and soil samples collected

from 9 plots across the Cima Dome. Finally, I compared my findings with the Holy Fire, which was studied with an identical sampling regime and DNA sequencing methodology. In my comparison, I will employ both a comparison of the impact of the fire on soil edaphic properties and microbial diversity in response to fire, but also an analysis of microbial association networks using archaeal, bacterial, and fungal data together. Using these comparisons, I can better understand how desert wildfires impact soil microbial communities in both direct and indirect ways with a severely impacted chaparral community as a benchmark.

2 Chapter II.
Eastern Joshua Tree Arbuscular Mycorrhizal Fungi Largely Consistent Across Roots, Soils, and Seasons

2.1 Abstract

The Mojave Desert is home to iconic Joshua trees threatened by climate change. Most desert plants form mutually beneficial partnerships with arbuscular mycorrhizal fungi (AMF), yet the AMF of the Eastern Joshua tree (*Yucca jaegeriana*) remain completely uncharacterized. We tested how *Y. jaegeriana* AMF spore abundance, richness, and composition varied when sampling 20 trees across 4 seasons from roots versus soils. We confirmed root colonization via staining, assessed spore abundance via microscopy, and used Illumina MiSeq to sequence AMF virtual taxa (VT) with WANDA AML2 primers. We identified 12 spore morphotypes and 47 VTs across 5 families within Glomeromycotina and the most abundant VT *Glomus VTX00294* appeared in 87% of soil and root samples. The majority of VTs (26/47) were present across all seasons and were shared among soil and roots (38/47) with more VTs unique to soil. In soil, per tree mean spore abundance and AMF richness was lowest in Summer but consistent across other seasons with richness ranging from 8.8 to 11.5 VTs and mean root richness consistent across seasons. We conclude that sampling from soils rather than roots and any season other than Summer will yield the most diverse AMF communities.

2.2 Introduction

Mycorrhizal fungi enable many desert plants to survive at the edge of climatic extremes, particularly by increasing access to water (Augé 2001; Miriti et al. 2007). Yet, many desert plant species face contraction of their reproductive ranges as climate change exacerbates desert conditions (Guida et al. 2014). The iconic Joshua trees are among the many desert plants facing such threats, and the Western Joshua tree, *Yucca brevifolia*, has shown both long-term predicted declines and observed range shrinkage in reproductive viability due to climate change (Sweet et al. 2019). Yuccas, like most desert plants, associate with symbiotic arbuscular mycorrhizal fungi (AMF) within the Glomeromycotina (Titus et al. 2002b; James et al. 2020) for increased access to nutrients and water (Smith and Read 2010). As parts of the Joshua tree habitat become unsuitable for reproduction, it is critical to understand their microbial associations in the cooler climate refugia where Joshua trees are expected to thrive.

Despite the iconic nature of Joshua trees, many open questions remain about the basic biology of these plants and their associated microbiomes. *Yucca jaegeriana*, the Eastern Joshua tree, which is densest in cooler climate refugia (Esque et al. 2023), was recently recognized as a distinct species from the Western Joshua tree based on morphology (Lenz 2007), its unique species of obligate pollinator moth (Smith et al. 2008), and genomic sequencing (Royer et al. 2016). AMF have been found in desert ecosystems across the globe (Vasar et al. 2021), including 3 species of *Yucca* (Titus et al. 2002b; Tawaraya 2003; Harrower and Gilbert 2021), yet the AMF of *Y. jaegeriana* remain completely uncharacterized. One existing study found 37 AMF virtual taxa (VTs,

or roughly the equivalent of AMF species based on 18S rRNA sequences (Öpik et al. 2010)), associated with the roots of sister species *Y. brevifolia* within Joshua Tree National Park (JTNP). AMF taxa in *Y. brevifolia* roots were clustered phylogenetically by elevation, and experimental seedling inoculation showed that all sources of native AMF inoculum increased plant biomass after six months (Harrower and Gilbert 2021). This suggests that *Y. jaegeriana* will be similarly colonized with diverse AMF taxa important to its growth and survival, potentially aiding future restoration goals as wildfires increasingly threaten these trees (Wilkening et al. 2022).

Beyond being completely uncharacterized within *Y. jaegeriana*, little is known in general about how AMF vary in richness and composition across seasons or in roots versus soils. AMF families show differing investment in root colonization and extra-radical hyphae, and these lifestyle differences can result in greater nutrient access or enhanced pathogen resistance for the plant depending on AMF lifestyle preferences (Camenzind et al. 2024). Similarly, AMF in the same region can display varying seasonal trends while associating with different plants (Hopkins and Bever 2024). The impact of seasons on richness and community composition of AMF can vary from weak to strong in temperate grasslands (Dumbrell et al. 2011; Sepp et al. 2019). Seasonality also had no effect on AM community composition in a temperate forest (Davison et al. 2012) but a strong effect in an arid shrubland and a subtropical forest (Sánchez-Castro et al. 2012; Maitra et al. 2019). Finally, AMF richness remained stable throughout the year in semi-arid shrublands (Chaudhary et al. 2014). Moreover, sample type (root, soil, spore, or rhizosphere) drove significant differences of community composition in grasslands,

wheat prairies, agricultural sorghum fields, and a subtropical forest (Hempel et al. 2007; Ellouze et al. 2018; Sepp et al. 2019; Gao et al. 2019), suggesting that sampling root or soil can also lead to differing AMF communities. Therefore, a comprehensive characterization of *Y. jaegeriana* AMF communities should sample across seasons and sample types.

AMF can also vary in spore abundance and root colonization across seasons. If host plants have different active seasons, then AMF species can show seasonal preferences for sporulation (Bever et al. 2001). Sporulation can also vary based on climate. For example, sporulation trended with precipitation in a water limited semi-arid region in Brazil (Da Costa et al. 2021). However, this seasonality of spore abundance disappeared in a Brazilian rainforest with high humidity (Kemmelmeier et al. 2022). AMF root colonization of the perennial Mojave desert shrubs *Larrea tridentata* and *Ambrosia dumosa* showed strong seasonal changes after cool-season rains (Apple et al. 2005) but these seasonal changes in colonization went away during drought (Titus et al. 2002b; Clark et al. 2009). Therefore, it is likely that AMF sporulation and colonization would vary across seasons in a desert plant like *Y. jaegeriana*.

Since AMF species can vary seasonally, there may only be a few AMF species present in the core community year-round. Core microbiomes can either refer to a few taxa repeatedly identified across time within the same host individual, or to core taxa that are shared across all host individuals within a population (Risely 2020). Some evidence points to AMF occurring as core community members. For example, 4 AMF sequence phylotypes formed a temporal core community for two plants in an arid shrubland

(Sánchez-Castro et al. 2012), potatoes appear to have a core community of AMF partners across the Andes mountains despite a wide geographic range (Senés-Guerrero and Schüßler 2016), and some AMF species were consistently found with the Western Joshua tree across long physical distances (Harrower and Gilbert 2021). Dominance within a particular season does not necessarily indicate membership of the core microbiome. For example, 2 AMF taxa that were highly dominant in June disappeared by September in sorghum fields (Gao et al. 2019). Thus, sampling across both time and space is necessary to identify a core microbiome.

Finally, another factor potentially impacting the AMF of *Y. jaegeriana* is fire. A mix of intermittent drought, exotic grasses (McAuliffe 2016), and Winter rains (Tagestad et al. 2016) primed the Cima Dome, which was home to the densest population of *Y. jaegeriana*, for the 2020 Dome Fire, killing > 1 million trees (NPS. 2020). High-elevation regions like the Cima Dome are among the 10% of habitat expected to continually support Joshua tree reproduction in the face of ongoing climate change (Sweet et al. 2019) making it a particularly important location to characterize *Y. jaegeriana* AMF. While AMF are typically more resistant to high temperatures than other soil microbes (Allen et al. 2011), post-fire communities of AMF may be shaped by the succession of their plant hosts (Neuenkamp et al. 2018) and the varying survival rates of initial community members based on their differing spore traits (Hopkins and Bennett 2023). There may not be any correlation between traits that allow AMF to support early successional plants and traits for fire survivorship, so turnover of AMF following fire is possible.

Here, we comprehensively characterize the *Y. jaegeriana* AMF community via both traditional microscopy and modern next-generation sequencing methods in root and soils and across seasons. We collected root and soil samples from 20 healthy Eastern Joshua trees from each of the four seasons spanning from June 2021 to March 2022 with 16 trees outside and 4 surviving but scarred trees within the 2020 Dome Fire burn scar. We asked if AMF spore abundance, richness, and composition varied across seasons and sample types (roots versus soil) and if a core community exists across roots/soils and seasons. We further tested if being within a burn patch affected AMF richness and composition. We predicted that spore abundance would significantly increase during seasons of high precipitation, corresponding to Summer and Winter samplings, which would also vary in AMF community composition. However, we predicted that AMF richness would be lower in Eastern Joshua trees within the burn scar due to reduction of surrounding desert shrubs and grasses. We also predicted that roots would provide greater AMF species richness than soil since Glomeraceae, which were abundant in Western Joshua tree *Y. brevifolia* (Harrower and Gilbert 2021), preferred roots over rhizosphere or extra-radical mycelium in semi-arid plants (Varela-Cervero et al. 2015; Alguacil et al. 2016). Finally, we predicted that a *Y. jaegeriana* AMF core community would consist of members of the Glomeraceae and *Ambispora* from Ambisporaceae, corresponding to taxa that were abundant at a similar elevation band for *Y. brevifolia* (Harrower and Gilbert 2021).

2.3 Experimental Procedures

Sampling: We selected 20 healthy *Yucca jaegeriana* trees (Fig. 1A) with a minimum of 5 florets and 1m height as our focal plants in Mojave National Preserve, CA (Table S1). Sixteen trees (#1-16) were selected east of the Morningstar Mine Rd which acted as a barrier for the Dome Fire, while four fire-scarred but surviving trees (#17-20) were selected within the burn perimeter (Fig. 1B). We sampled at the beginning of each season with Summer on June 23, 2021, Fall on September 9, 2021, Winter on December 21, 2021, and Spring on March 30, 2022. We collected and extracted DNA from both roots and surrounding soil for a total of 160 samples (2 types (roots vs soil) X 4 seasons (Summer, Fall, Winter, Spring) x 20 trees). We used releasable bulb planters and wiped off debris with 70% ethanol between trees to collect 2-3 soil cores of the top 10 cm of soil from close to the base of the trunk of each tree at each season, avoiding previously sampled edges of the base when possible (Fig. 1A). We ensured that roots came directly from Eastern Joshua tree roots due to the distinct red color and also sampling directly from beneath the tree trunk and away from other grasses and shrubs (Fig. S1). We stored soil on ice and returned to UC Riverside where it was sieved (2mm) within 24-48 hours of collection, during which we separated roots from within the soil sample. We stored approximately 10g of soil and 1g of roots at -80°C for downstream DNA extraction and air-dried the remaining soil. We stored additional roots in -80°C or in 50% ethanol solution in 4°C for staining and visualization of fungal structures.

AMF Spore Count and Colonization Analysis: We extracted and counted spore number and estimated morphotype diversity from all 20 trees from all seasons. We used

25g of dried soil for sucrose-Calgon spore extractions (Ianson and Allen 1986) collected with 15mL distilled water. We dispensed 1mL aliquots of well-mixed spore extracts onto filter paper and counted all spores at 40X magnification four times per sample. We identified AMF spores based on color, size, morphology, and based on INVAM (Stürmer et al. 2021), the AMF spore guide in *Glomeromycota* (Błaszkowski 2012), and following expert opinion by Dr Michael Allen. We averaged those 4 spore counts, multiplied by 15 (mL) to extrapolate the total count, and divided by 25 (g) to estimate spore content per gram of soil (Fig. 1C). We assessed spores for their relative size and color and assigned them to 12 different morphotypes (McKenney and Lindsey 1987). We confirmed the presence of AMF colonization in the roots (Fig. 1D) through trypan blue staining and microscopy (Koske and Gemma 1989; McGonigle et al. 1990). We rinsed roots in distilled water and cleared overnight in 2.5% KOH. We then rinsed roots in water again and bleached with 15% peroxide with 0.05% KOH for 5 minutes at room temperature to reduce red coloration in the roots. We then acidified roots with 2% HCl for 2 minutes and moved roots to a 0.05% Trypan Blue solution at 90°C for 30 minutes. Finally, we destained the roots in a 1:1 solution of lactic acid and glycerol for 24 hours. We mounted roots on slides in PVLG to detect AMF structures but did not quantify colonization rates due to inconsistent clearance of red coloration from the roots.

DNA Extractions: To extract DNA from soil, we used Qiagen DNeasy Powersoil Pro kits following the manufacturer's protocol, except we replaced 100µL C1 solution with 100µL ATL buffer and incubated with 0.30g soil overnight at 4°C to improve yields. We followed an established protocol to extract DNA from roots (Glassman et al.

2015), where we lyophilized roots for 24 hours (Labconco FreeZone 4.5L, Kansas City, MO, USA), used sterilized steel beads to grind 0.1g of roots using a 1 minute Fast-Prep 24™ (MP Biomedicals, Santa Ana, USA) cycle at 6.5m/sec, then added 1 ml of 1:1000 beta-mercaptoethanol:cetyltrimethyl ammonium bromide 2X (CTAB) and incubated one hour at 65°C. We then used 600µL of chloroform to remove lipids and mixed 700µL of the aqueous solution with 350µL 95% EtOH then proceeded with the Qiagen DNeasy Blood and Tissue Kit starting with buffer AW1.

PCR and Sequencing: We used a two-step PCR to amplify the AMF-specific WANDA-AML2 primer pair (Lee et al. 2008; Dumbrell et al. 2011) adapting from established methods (Weber et al. 2019). We mixed 3 µL DNA from roots or soil with 0.5µL of 10 µM of each primer, 8.5 µL of Ultra-Pure Sterile Molecular Biology Grade water (Genesee Scientific), and 12.5 µl Accustart ToughMix (2× concentration; Quantabio). We amplified at the following settings: 94°C for 2 minutes, followed by 30 cycles of denaturing at 94°C for 30 s, annealing at 60°C for 30 s, elongating at 68°C for 45 s, and a final elongation step at 68°C for 2 minutes. We ran a 1.2% agarose gel to check for bands and increased to 35 cycles for samples with no visible bands. We cleaned PCR products with AMPure XP magnetic beads (Beckman Coulter Inc.) following manufacturer instructions. We used a second PCR to add DIP barcodes (Kozich et al. 2013) and adaptors for Illumina sequencing with a 94°C heating step for 2 minutes and 10 cycles at 94°C for 30 s, 60°C for 30 s, and 72°C for 1 min, using 12.5 µL Accustart Toughmix, 2.5µL of 1 µM DIP PCR2 primers, 6.5µL of ultra-pure water, and 1µL of PCR product. Following established protocols from our lab (Pulido-Chavez et al. 2023;

Glassman et al. 2023), we pooled samples based on band intensity in an agarose gel by aliquoting 1 µL, 2 µL, or 3 µL per sample, then cleaned the pool with AMPure prior to checking concentration and quality with Agilent Bioanalyzer 210. We sequenced with Illumina Miseq 2x250 bp Nano kit, which provided sufficient sequence coverage due to low richness of AMF communities (Öpik et al. 2010), at the UC Riverside Institute for Integrative Genome Biology in 2 libraries to accommodate all samples. We included multiple negative controls for DNA extraction and PCRs in each library.

Bioinformatics: We analyzed sequencing data using QIIME2 version 2022.2 (Bolyen et al. 2019). We removed forward and reverse adaptors using the QIIME2 cutadapt trim-paired plugin, demultiplexed, and denoised using DADA2 with the denoise-single plugin based on the quality of forward reads to ensure median quality scores over 30. We assigned taxonomy exclusively using forward reads, since the forward reads contain more of the informative variable region (Dumbrell et al. 2011; Davison et al. 2012). We matched sequences to the MaarjAM database (Öpik et al. 2010) using virtual taxa (VT) numbers and removed singletons to minimize the impact of erroneous reads. Since a portion of reads did not match to any VTs, they were subjected to a lower threshold BLAST against the MaarjAM database which retained matches with the highest e-value lower than 1e-50, a percent identity over 90%, and less than 10 nucleotide mismatches (Chaudhary *et al.*, 2020). Sequences not matching one VT with these constraints were excluded from analysis as non-AMF reads.

Statistical analysis: We performed statistical analysis in R version 4.1 (R Core Team 2020). We generated a species accumulation curve and rarefaction curve to

determine cutoffs for sample numbers and sequencing depth using functions specaccum and rarecurve in "vegan" (Oksanen et al. 2022). We tested the impact of different rarefaction levels on number of samples, total number of VTs, and mean and median per sample AMF richness using the using the rrarefy.perm function in "EcolUtils" (Salazar 2015) and taking the mean of 10,000 permutations of rarefaction. We found that normalizing to 754 reads per sample allowed us to retain the most samples (143/150) and yield the same total number of VTs as non-rarefied data (47 VTs) but also account for uneven sequencing depth to accurately compare sample richness across treatments (Weiss et al. 2017; Table S2). Prior to rarefaction, our samples ranged from 202 reads to 39,799 reads with an average of 7,266 reads per sample, and this level of variance can skew results without a rarefaction method that maintains species counts through multiple permutations (Schloss 2024). We calculated diversity indices using the estimateR and diversity functions in "vegan".

To identify significant drivers of species richness across our trees, we used generalized linear mixed models from the "lme4" package (Bates et al. 2024). We used Poisson distributions after testing several distributions in the "MASS" package (Ripley et al. 2024) using the "car" (Fox et al. 2023) function qqp. We used reverse model selection to identify the lowest Akaike's Information Criterion (AIC) value amongst differing generalized linear models incorporating season, type, and burn status, while comparing library and tree number held as random effects. Sequence libraries had an uneven sample type distribution (Fig. S2) so final models only incorporated tree number as a random effect. To analyze seasonality of AMF VT richness and spore abundance, we used

separate models for roots and soils due to differing levels of variance in the two groups. We confirmed normal distributions and low variance with the Shapiro-Wilk test and Levene's test, respectively (Shapiro and Wilk 1965; Schultz 1985). Then we compared seasons with repeated measures ANOVA. We used the R package "modelsummary" (Arel-Bundock et al. 2022) to export tables of statistics.

We analyzed differences in beta-diversity using Bray-Curtis dissimilarity matrices calculated with the "vegan" function avgdist rarefied to 754 sequences per sample, then applied a PERMANOVA analysis using the "vegan" functions adonis2 and betadisper for differences between centroids and variation in mean distance of samples to centroids, respectively. We visualized beta diversity using non-metric multi-dimensional scaling (NMDS) plots with the "vegan" function metaMDS.

We generated masked sequence alignments of representative sequences of our forward read VTs and the Mucoromycota outgroup *Endogone botryocarpus* (Genbank accession LC431079). We made a phylogenetic tree of identified VTs using the QIIME2 plugin iq-tree-ultrafast-bootstrap which compared models to identify TIM+F+I+G4 (Transitional Model, Frequency, Invariant, rate 4 Gamma distribution) as the best fit model for tree construction based on the Bayesian Information Criterion.

We used heat maps and Venn diagrams to test and visualize the impact of sampling type (roots versus soils) and season on AMF richness and frequency and to identify a core microbiome. We used frequency of VTs in root and soil to generate Venn diagrams and made graphics using the "VennDiagram" package (Chen 2022). We used base R to create heatmaps based on prevalence of taxon appearance and selected color

palettes from the “viridis” package (Garnier et al. 2024). We used the rankabundance function in the “BiodiversityR” package (Kindt 2024) to calculate the abundance and prevalence of VTs in our filtered and rarefied dataset.

Sequences were deposited to NCBI SRA PRJNA1196672. All scripts can be found at github.com/arik-chou/YJAMF.

2.4 Results

After merging two Illumina libraries consisting of 2,399,441 reads, and filtering for quality, we obtained 1,264,130 sequences corresponding to 1,269 amplicon sequence variants (ASVs) from 150 samples, as 10 samples did not amplify. ASVs that matched a MaarjAM database VT were combined into 47 distinct VTs. Species saturation curves showed that sampling roughly 10 trees yielded most of the AMF VT diversity present (Fig. S3A). Rarefaction curves showed that all samples saturated at roughly 15 species per 0.1g root and under 20 species per 0.30g soil regardless of sequencing depth up ranging from 754 to 40,000 reads per sample (Fig. S3B). We compared library effects across sample types (Fig. S2) and saw no significant differences in root (LMM, $t(62.34) = 1.43$, $p = 0.16$) or soil (LMM, $t(52.07) = 1.12$, $p = 0.27$).

Spore abundance variation across seasons*:* Spore abundance averaged at a mean ± standard error (SE) of 12.06 ± 0.71 spores/1g soil, with 12 distinct morphotypes detected (Table S3). Summer had significantly fewer spores per gram than the other seasons (Table 1, Fig. 2A; ($F_{3,57} = 10.3$, $p < 0.001$). The Summer sampling (June 2021) followed the months with the lowest levels of precipitation (Fig. 2C). Spore abundance

was correlated to precipitation at each sampling time as a sum of the prior 3 months' rainfall ($F_{1,76} = 4.17$, $p < 0.0001$, Table S4). Two morphotypes dominated in abundance (M3 and M4) across all seasons, followed by 2 more morphotypes (M5 and M8), which all had lowest abundances in the Summer with M4 and M8 peaking in Spring, M3 in Winter, and M5 in Fall. The remaining eight spore morphotypes showed similar abundance values, most peaking in abundance in Fall (Fig. S4).

Impact of being in a burn patch on AMF richness and composition*:* Whether the tree was within the burn scar versus outside the burn scar did not significantly impact AMF VT richness (GLMM, $z = 0.39$, $p = 0.70$; Fig. 3A), so the burn effect was not included in our final model. There was also no significant difference in the mean spore abundance for trees within the burn scar versus outside the burn scar (Fig. 3B), but there was a small impact of burn on AMF VT community composition (PERMANOVA, $F_{1,1}$= 2.53, $R^2 = 0.018$, $p = 0.01$).

AMF richness and composition in roots versus soil*:* Averaged across seasons, soils yielded more AMF VTs per tree (10.63 ± 0.40 (n = 71)) than roots (9.18 ± 0.33 (n = 72)), (Fig. 3C, GLMM, $z = 2.86$, $p = 0.004$). Although soils yielded more AMF VTs than roots, 80% of AMF VTs were shared across soils and roots, with 38 of the 47 VT found in both sample types, and with 6 AMF VT exclusive to soil and only 3 to roots (Fig. 4A). *Glomus VTX00294* was the most frequent AMF VT in both roots and soils (Fig. 5), detected in 87% of all samples. AMF VT communities showed small but significant differences between roots and soils in both the location of centroids (PERMANOVA, $F_{1,1}$ = 15.0, $R^2 = 0.096$, $p = 0.001$) and mean distance to centroids per sample (betadisper, $F_{1,1}$

= 21.1, $p < 0.001$) when all seasons were considered together. Considering seasons separately, differences between AMF community composition of roots versus soils ranged from R^2 of 0.07 in Summer and 0.08 in Spring to 0.13 in Fall and 0.19 in Winter (Fig. 6).

AMF richness and composition across seasons*:* While there was no significant impact of season on per tree mean AMF richness in roots ($F_{3,46} = 0.84$, $p = 0.48$), soil samples did vary by season ($F_{3,45} = 5.2$, $p = 0.004$) with Summer having the lowest AMF VT richness (Table 1; Fig. 2B). Per tree mean AMF richness in soil was correlated with the sum of the prior 3 months' rainfall in soil (GLMM, $z = 3.03$, $p = 0.003$) but not in roots (GLMM, $z = 0.44$, $p = 0.66$). When combining total per tree AMF richness from soil and roots, richness was significantly higher in all seasons compared to Summer (LMM, Fall: $t = 2.65$, $p = 0.011$; Winter: $t = 2.66$, $p = 0.010$; Spring: $t = 2.77$, $p = 0.0078$; Fig. S5).

The majority (55%) of AMF VTs were found in all four seasons (Fig. 4B) and this pattern held for both roots (Fig. 4C) and soils (Fig. 4D). Seasons also had similar amounts of VTs detected overall when combining soil and roots, with 36 present in Fall and Spring, and 38 in Summer and Winter. However, each season had at least 1 VT that was not present in the other seasons (Fig. 4B), so season had a minor but significant impact on AMF community composition (Fig. S6, PERMANOVA, $F_{1,3} = 2.00$, $R^2 = 0.04$, $p = 0.004$). In soil, community composition differed between Summer and Fall ($F_{1,34} = 3.8$, $R^2 = 0.10$, $p = 0.003$), and Summer and Winter ($F_{1,32} = 2.2$, $R^2 = 0.06$, $p = 0.027$). Meanwhile, roots differed only between Fall and Spring ($F_{1,37} = 3.1$, $R^2 = 0.07$, $p =$

0.025), with no seasonal differences in beta-dispersion within root or soil. Heatmaps from root and soil samples (Fig. 5) highlight seasonal dominance for VTs highly prevalent across all samples, as the ten most prevalent VTs are also present in all seasons, representing 58% of the proportion of VT detection frequency. Some VTs were highly prevalent overall such as *Glomus VTX00294* and *Glomus VTX00063*, and others had clear seasonal preferences for Summer (*Glomus VTX00099* and *Glomus VTX00114*) or Fall (*Glomus VTX00177* and *Glomus VTX00442*). Sample-type specific trends included higher prevalence of *Paraglomus VTX00444* in Summer soils, *Diversispora VTX00306* in Summer roots, *Glomus VTX00409* and *Glomus VTX00098* in Fall soils, *Glomus VTX00214 and Diversispora VTX00306* in Winter soils, and *Claroideoglomus VTX00056* in Spring roots.

Core community across roots/soil and seasons*:* A core community of 26 out of 47 VT primarily from the Glomeraceae was present across all seasons from roots and soils (Fig. 4B), with 20 out of 41 detected in roots (Fig. 4C) and 25 out of 44 in soil (Fig. 4D). A total of 19 VTs were present across all seasons in both roots and soils. Season-exclusive taxa included *Glomus VTX00150* in Fall, *Glomus VTX00067* and *Diversispora VTX00355* in Summer, *Glomus VTX00105* and *Paraglomus VTX00375* in Spring, and *Archaeospora VTX00375*, *Glomus VTX00093*, and *Glomus VTX00077* in Winter samples. While many of these exclusive taxa often only appeared in a few samples in one season with low overall prevalence (Fig. 5), other non-core community members appeared more frequently in other seasons but were completely absent in one season, such as *Glomus VTX00069, Glomus VTX00165, Glomus VTX00174, Glomus VTX00414, Glomus*

VTX00416, and *Glomus VTX00326*. Of the 47 VT sequenced from roots and soil from *Y. jaegeriana*, only 9 VT overlapped with the 37 VTs associating with the closely related *Y. brevifolia* (Harrower and Gilbert 2021), those being *Glomus VTX00114, Claroideoglomus VTX00193, Claroideoglomus VTX00056, Diversispora VTX00061, Diversispora VTX00306, Glomus VTX00092, Glomus VTX00069, Glomus VTX00093,* and *Glomus VTX00105*, in descending order of frequency across all samples in this study. Of these, only *Glomus VTX00114* showed high prevalence, as the eighth most prevalent taxa in our study.

2.5 Discussion

Here, we present the first study of Eastern Joshua tree *Yucca jaegeriana* AMF and perform a comprehensive analysis of how AMF spore abundance, richness, and composition varies across seasons in roots versus soil among the same 20 trees sampled via both traditional microscopy and modern next generation sequencing methods. We confirmed AMF colonization in roots via staining and using Illumina MiSeq of WANDA-AML2 primers and identified 47 VTs overall from 5 families within the Glomeromycotina with a core AMF microbiome of 26 VTs across all seasons. AMF communities of *Y. jaegeriana* were diverse, with each tree harboring an average of ~10 VTs per tree per sample type. Contrary to our predictions, AMF richness was unaffected by being within a burn scar, and roots did not yield greater AMF species richness than soil. In fact, soils yielded more AMF taxa than roots overall, although the vast majority of AMF VTs were shared by soil and roots. While one VT, *Glomus VTX00294*, showed

dominance across sample types, trees, and seasons, the community showed high temporal stability. Further, AMF richness did not vary in roots across seasons but was lowest in Summer for soils and spore abundance. Notably, the AMF community was distinct from that of the sister species *Y. brevifolia*, with only 9 shared VTs between hosts, suggesting more host diversity than expected based on previous research indicating low host specificity and low global endemism among AMF (Davison et al. 2015).

We detected the lowest AMF spore abundance and richness in Summer soils following the driest months, but AMF spore abundance was constant from Fall to Spring. Similar trends regarding abundance and richness were reported in arid and semi-arid steppes (Bencherif et al. 2016), with richness and spore abundance at their lowest in the Summer. Precipitation leading up to the Summer sampling was minimal (Fig. 2C), likely slowing plant and AMF growth. Sustained precipitation may have supported the increase in spore abundance we detected in Fall, similar to a study that detected a correlation between precipitation and spore density in semiarid shrublands (Chaudhary et al. 2014).

While we identified 4X as many AMF VT from next generation sequencing than from spore morphotyping, both followed similar trends. Overall richness of VTs and spore abundance were both lowest in summer and both showed high dominance by 1-2 taxa. Similar to our trends in VT prevalence, each of the four seasons represented a peak in abundance for at least one morphotype. This trend is consistent with prior studies in which spore abundance rose after precipitation when water is limiting, with some morphotypes still peaking in abundance outside of the most spore-dense season (Gemma et al. 1989; Bever et al. 2001; Da Costa et al. 2021; Kemmelmeier et al. 2022). While

patterns of seasonality in spore morphotypes may be skewed by morphological plasticity of spores and other difficulties in species identification, a recent study of spore dispersal showed congruence between spore morphotyping and next-generation sequencing trends of aerial spores captured at a 20m height near agricultural fields (Chaudhary et al. 2020). While two morphotypes drove a peak in their post-harvest Summer spore counts, an overall diverse variety of 20 morphotypes and 17 VTs continued to follow their own seasonal trends with little change to VT richness, indicating that seasonal variation in spore dispersal is likely. Grasslands can show strong seasonal differences between summer and winter root AMF communities (Dumbrell et al. 2011), however the century-spanning lifetimes of Joshua trees supported a more consistent AMF community similar to those seen in forests (Kemmelmeier et al. 2022; Djotan et al. 2024).

Eastern Joshua trees sampled within the burn scar did not show a decrease in AMF spore abundance or taxa richness, indicating that burning away the surrounding shrubs and grasses did not drastically impact the AMF associated with surviving trees. While we did not sample trees killed by the fire in this study, it is possible that spores would still be detected amongst the surrounding soil and dead roots, since AMF survive in storage after long periods of time (Allen 1992), and some burn conditions can even increase spore abundance (Aguilar-Fernández et al. 2009; Moura et al. 2022). Further, AMF beyond the top 10cm are thought to be buffered from low-intensity fires (Allen et al. 2011), thus seeding recolonization of shallow roots. While ectomycorrhizal fungi appear to die off by 1 month post-fire (Pulido-Chavez et al. 2023), the longevity of AMF spores in the wild is not known. While it is possible that post-fire nutrient pulses reduce

the need for AMF associations (Kennedy et al. 2002), other studies indicate that fast moving low intensity fires do not typically lead to long lasting impacts on mycorrhizal fungal richness (Chimal-Sánchez et al. 2015; Stürmer et al. 2022; Espinosa et al. 2023).

Most AMF taxa were shared by soil and roots, with AMF taxa exclusive to one sample type being rare. Indeed, 80% of AMF taxa were shared by soils and roots, and none of the sample-type exclusive taxa were found in any substantial frequency, often appearing in one sample. Six AMF VTs (*Paraglomus VTX00375, Glomus VTX00093, Glomus VTX00077, Diversispora VTX00354, Diversispora VTX00355, and Archaeospora VTX00376*) were detected in soil exclusively. These soil-exclusive taxa may have different colonization structures and strategies for soil or root, like *Glomus intraradices* and *Glomus etunicatum* (Hart and Reader, 2005). Further, Diversisporales AMF are well-known for their "edaphophilic" lifestyle of abundant extraradical hyphae and sparse hyphae in roots (Powell et al. 2009; Weber et al. 2019). This soil preference was supported by increased prevalence of *Diversispora VTX00263* and *Diversispora VTX00*306 in Winter soils, but no corresponding increase of the same taxa in roots (Fig. 5). While some studies have shown substantial compositional differences in root and soil AM taxa (Hempel et al. 2007), we report significant overlap of root and soil communities with some variation in low abundance taxa.

Differing trends in seasonality across sample types led to some AMF compositional differences across seasons both between roots and soils and within roots and soils across seasons, likely driven by abundant edaphophilic Diversispora members fluctuating across seasons. For example, the differences between AMF composition in

roots versus soils was higher in Fall and Winter (13-19%) compared to Summer and Spring (7-8%). Moreover, within soil AMF communities, they only differed between Summer-Fall and Summer-Winter, and within root AMF communities, they only differed between Fall-Spring but were consistent across other seasons. A study highlighting seasonal preference of AMF in nearby Palm Desert surveyed multiple plant species' roots to assess microbial responses to the Winter and Summer rains (Taniguchi et al. 2023). AMF taxa were a larger percentage of the fungal ITS1 sequence relative abundance after Summer rain but not Winter rains. Root AMF in wet-season months appeared to be structured based on associations with host plants rather than stochastic processes, consistent with community assembly patterns seen in sorghum fields after the removal of drought stress (Gao et al. 2020). Those patterns were reflected here in this study, as AMF VT richness in Spring was not significantly different from the lowest season, Summer, despite prior Winter rain (Fig. 2B). It is possible that ending the drought stress with Summer monsoons leads to more root growth and more opportunities for diverse AMF community structure in Fall. Another shallow-rooted succulent, *Yucca angustissima*, showed preferential Summer rain uptake while nearby perennials used both Summer and Winter rain sources (Ehleringer et al. 1991). Thus, root growth in Fall could support new root-specific mycorrhizal associations, while post-Winter rains do not, driving the compositional difference in Fall and Spring roots and resulting in differing amounts of variation across roots and soil.

AMF VT richness and community composition was otherwise largely consistent across seasons, with the majority of AMF VTs found across all seasons and with soil

AMF richness reducing only in Summer. Our rarefaction curve shows that 10 *Y. jaegeriana* trees was sufficient for capturing most of the AMF community. Since we sampled double that, we were able to detect more rare taxa that either had some preference for roots versus soils or seasons, or were simply identified in one season versus another due to stochasticity. For example, *Glomus VTX00104* was prevalent in Summer soils but not detected in Winter soils, but was detected in roots in the Spring. Other taxa share their peak in prevalence in both sample types at the same season, such as *Glomus VTX00114* and *Glomus VTX00099* in Summer, *Glomus VTX00177* and *Glomus VTX00442* in Fall, and *Glomus VTX00155* in Spring. These trends are consistent with observations of *Cryptomeria japonica* root and soil sampled monthly in different forests, which revealed monthly stochastic changes in the plant's AMF communities but consistency in overall trends of richness across forests (Djotan et al. 2024). Aided by dispersal of AMF through spores, hyphal fragments, or infected plant roots (Paz et al. 2021), AMF maintain arbuscules for nutrient exchange over the course of multiple days (Kobae and Hata 2010) while the fungus remains as viable infective extraradical mycelium in the soil for up to 5 months after removal of a host (Pepe et al. 2018).

We found 26 out of 47 VTs that were present in at least one root or soil sample from our 20 *Y. jaegeriana* trees at every season, forming a temporal core community. These include VTs from 4 of the 5 genera detected in this study including *Glomus, Claroideoglomus, Paraglomus,* and *Diversispora* ordered from most to least abundant. Whether these taxa are functionally critical or simply resilient is not known. It is possible that functional redundancies exist across the AMF community, but the high rate of

genetic diversity across just one species of AMF suggests differing roles for each mycorrhizal association with implications for wider ecosystem functioning (Powell and Rillig 2018). Unlike other yuccas with deep taproots, Joshua tree roots are fibrous and shallow (Rundel and Gibson 1997), so they likely invest in a broad range of mycorrhizal partners to search for a variety of nutrients (Johnson 2010). This reliance on AMF may increase resource allocation towards many AMF species regardless of their benefit, potentially explaining the high diversity and low overlap of species between *Y. jaegeriana* and *Y. brevifolia* (Harrower and Gilbert 2021). However, the constant presence of 5-10 AMF virtual taxa may support resilience against increasing temperature maxima, since Summer heat did not drastically alter species composition, and did not obstruct an increase in soil AMF species richness between Summer and Fall. Better understanding the dynamics of the core community will require investigations into differing contributions of AMF species to their plant host, as AMF communities often exhibit rare taxa appearing and disappearing with unclear consequences (Sánchez-Castro et al. 2012). AMF also display intra-specific genomic differences that contribute to their interactions with hosts (Schoen et al. 2021) and mutualistic bacteria within AMF spores that modulate mycorrhizal drought responses (Chávez-González et al. 2024), adding further layers of complexity to these multilevel interactions.

Surprisingly, despite their close genetic relationship and the general lack of host specificity among AMF (Davison et al. 2015), only 9 of 47 VTs overlapped between *Y. jaegeriana* and *Y. brevifolia*, even while targeting the same V3 portion of the fungal 18S rRNA and assigning taxonomy with the same MaarjAM database (Harrower and Gilbert,

2021). The nearest *Y. brevifolia* individuals are located 100-200 Km away from our site (Wilkening et al. 2022), and they lacked *Glomus VTX00294*, which was the most abundant VT that we found on *Y. jaegeriana.* However, *Glomus VTX00294* has also been detected associating with perennial grasses and herbs nearby in the Chihuahuan Desert in New Mexico (Porras-Alfaro et al. 2007), and as far as Australia (Davison et al. 2015). Expected genera that were detected in JTNP with *Y. brevifolia* such as *Ambispora* as well as *Scutellospora* were not present in the Cima Dome at their corresponding elevations from JTNP (Harrower and Gilbert 2021). This suggests that climatic or edaphic characteristics vary enough to support diverging AMF communities in closely related plants, potentially lending further support for host specificity of AMF (Kajihara et al. 2022; d'Entremont and Kivlin 2023).

2.6 Conclusion

Although we focus narrowly on the AMF of a single desert tree, our comprehensive sampling across space, time, and roots versus soils provide valuable insight into the dynamics of host-associated microbiomes. We characterized for the first time the AMF the iconic Eastern Joshua tree and found that a single desert tree species associates with a diverse assemblage of 47 AMF taxa from 5 families within the Glomeromycotina. In addition, there is low overlap of AMF VTs shared between closely related sister genera of *Yucca,* indicating high levels of desert biodiversity are found belowground. Sampling soils is typically less effort than searching for roots especially in deep rooted desert plants, and our findings indicate that sampling from soils is preferred

since most AMF taxa were shared but soils had higher richness and more unique VTs than roots. Further, these similarities suggest that in instances where root collection can be prohibitively difficult, root samples are more informative for quantification of fungal structures when near-identical communities can be sequenced via soil. In our limited testing of fire, burning surrounding grasses did not alter AMF spore abundance or species richness when compared to unburned trees, suggesting that dynamics were tied to *Y. jaegeriana* or fine-scale soil properties. We also identified all seasons besides Summer as equally viable options for sampling, since we found high consistency in AMF spore abundance, richness, and composition across Fall, Winter, and Spring. Finally, our in-depth examination of both root and soil from the same 20 trees across seasons gives insight into generalized principles of host-associated microbiome turnover across space and time, indicating that a diverse core AMF microbiome persists across seasons and sampling type.

Acknowledgments: We acknowledge Mojave National Preserve and the Mojave Desert Land Trust for allowing us to sample and Debra Hughson, Annasofia Andeski, and Andrew Kaiser for help with permitting. We thank Tasha La Doux and Jim Andre at the Sweeney Granite Mountains Desert Research Center for assistance with field sampling. We thank Edie and Mike Allen for their extensive help and training with methods for AMF spore extractions and root colonization and help with identification via spore morphology. We thank Sohrab Bodaghi, Gerardo Uribe, and Georgios Vidalakis for assistance and use of their lyophilizer. We thank Victoria Sloot and Justin Diab for their assistance with spore counting and identification. We thank Aishwarya Veerabahu,

Marcos Vinicius Caiafa Sepulveda, Dylan Enright, Anna Nguyen, and Basubi Binti Zhilik for assistance with field work. We thank Joel Sachs and Quinn McFrederick for their input on the manuscript and the anonymous reviewers for their suggestions and revisions. We thank the Shipley Skinner Riverside County Endowment to AJ and SIG and the USDA Hatch fund #CA-R-MPP-5232-H to SIG for funding.

2.7 Figures

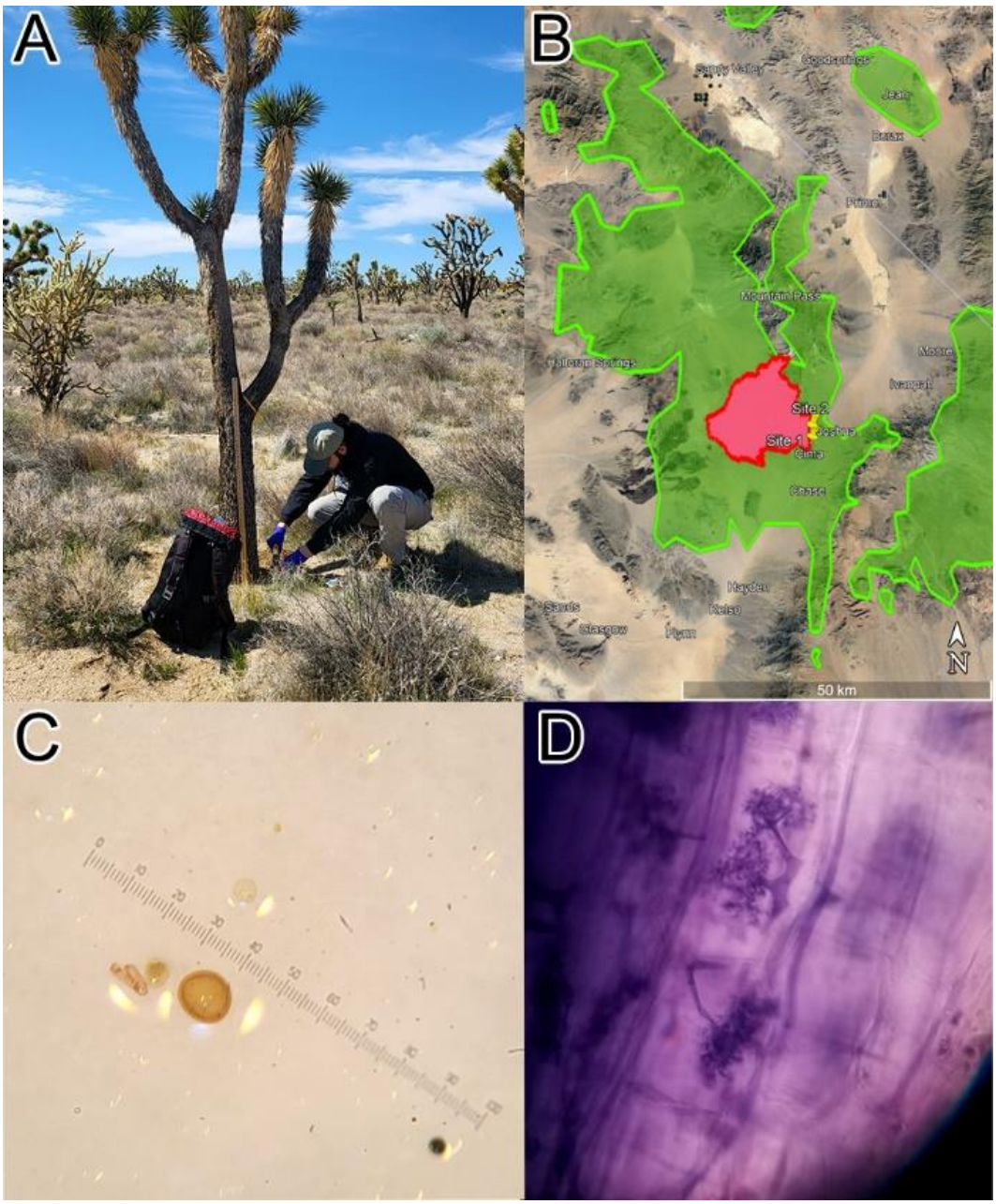

Figure 2.7.1 (A) Spring sampling of Y. jaegeriana soil and roots. (B) Y. jaegeriana habitat near the USA California-Nevada border (green). Location of the Dome Fire within California (red). Pins indicate general sampling sites for 20 trees. (C) AMF Spores at 65x magnification. (D) AMF arbuscules stained with Trypan Blue within Y. jaegeriana root.

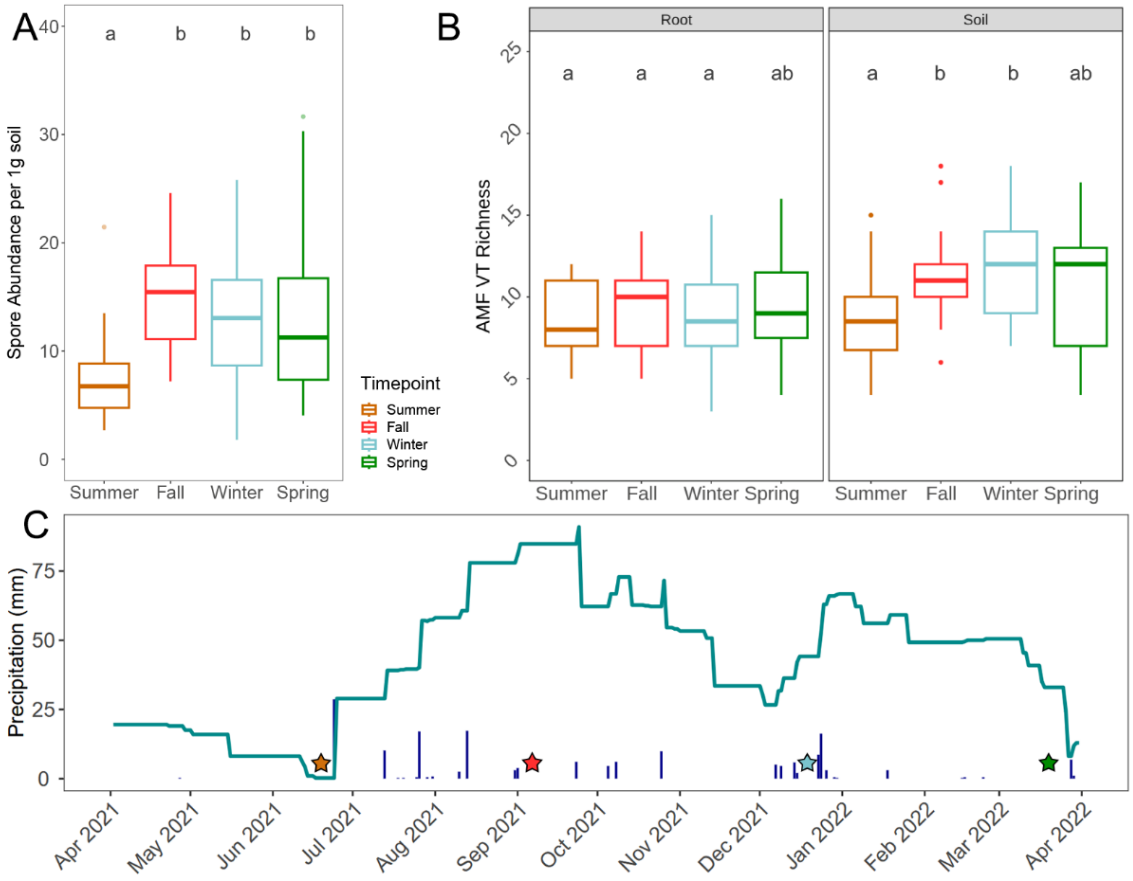

Figure 2.7.2 (A) Spore abundance in 1g of soil from 20 trees per season. (B) Richness of AMF virtual taxa in all trees per season in roots versus soils as detected by 18S sequencing. The median of each boxplot is indicated by the middle horizontal line, the bottom of the box indicates the first quartile, the top indicates the third quartile, and whiskers above and below indicate minimum and maximum values not considered outliers. Points beyond whiskers are outliers. We have also visualized the model predicted means as the points within each boxplot ± standard error. Letters indicate statistically significant differences between least-squares means in our generalized mixed effects model. (C) Precipitation measured at the Mojave Mid Hills Station from April 2021 to March 2022. Bars indicate daily precipitation listed in mm, and the line indicates the sum of the prior 3 months of precipitation. Stars indicate our four seasonal sampling timepoints.

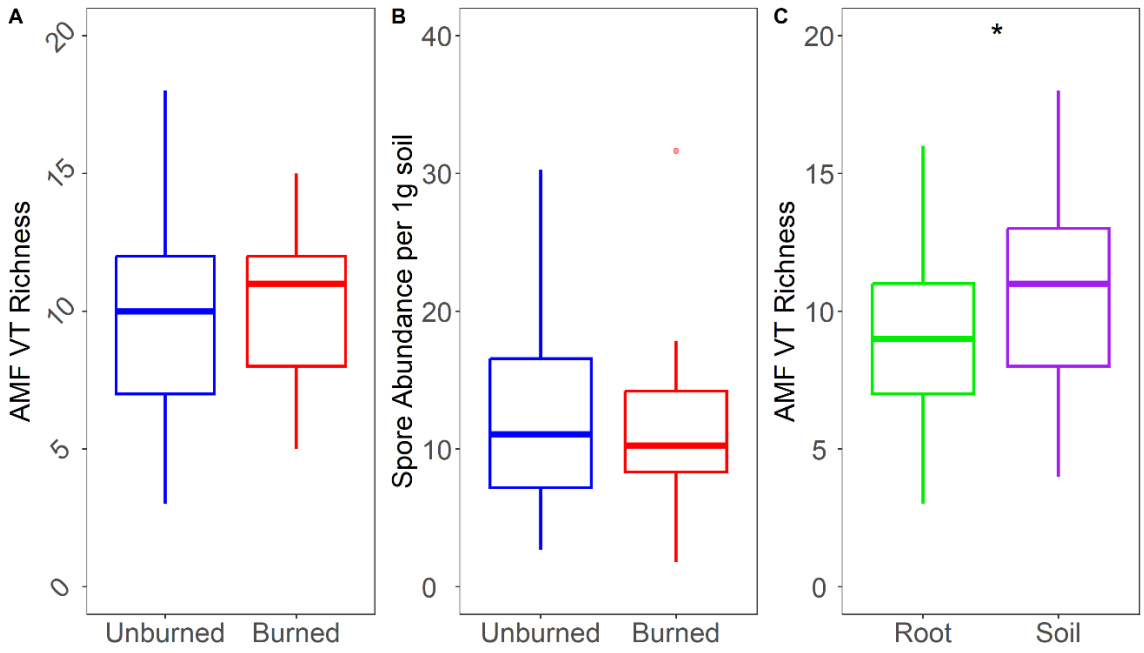

Figure 2.7.3 Comparison of burned and unburned Eastern Joshua trees and their AMF A) virtual taxa (VT) richness and B) spore abundance per 1g of soil. Blue represents unburned (n=16) and red represents burned (n=4) trees. Box plots show medians with the middle horizontal line, the bottom of the box indicating the first quartile, the top indicating the third quartile, and whiskers above and below indicating minimum and maximum values not considered outliers. Points beyond whiskers are outliers. We have also visualized the model predicted means as the points within each boxplot ± standard error. No significant difference was found between either group. C) AMF Virtual taxa richness in root (n=71) and soil (n=72) samples combined across seasons. Stars indicate significantly greater richness in soil ($p < 0.01$).

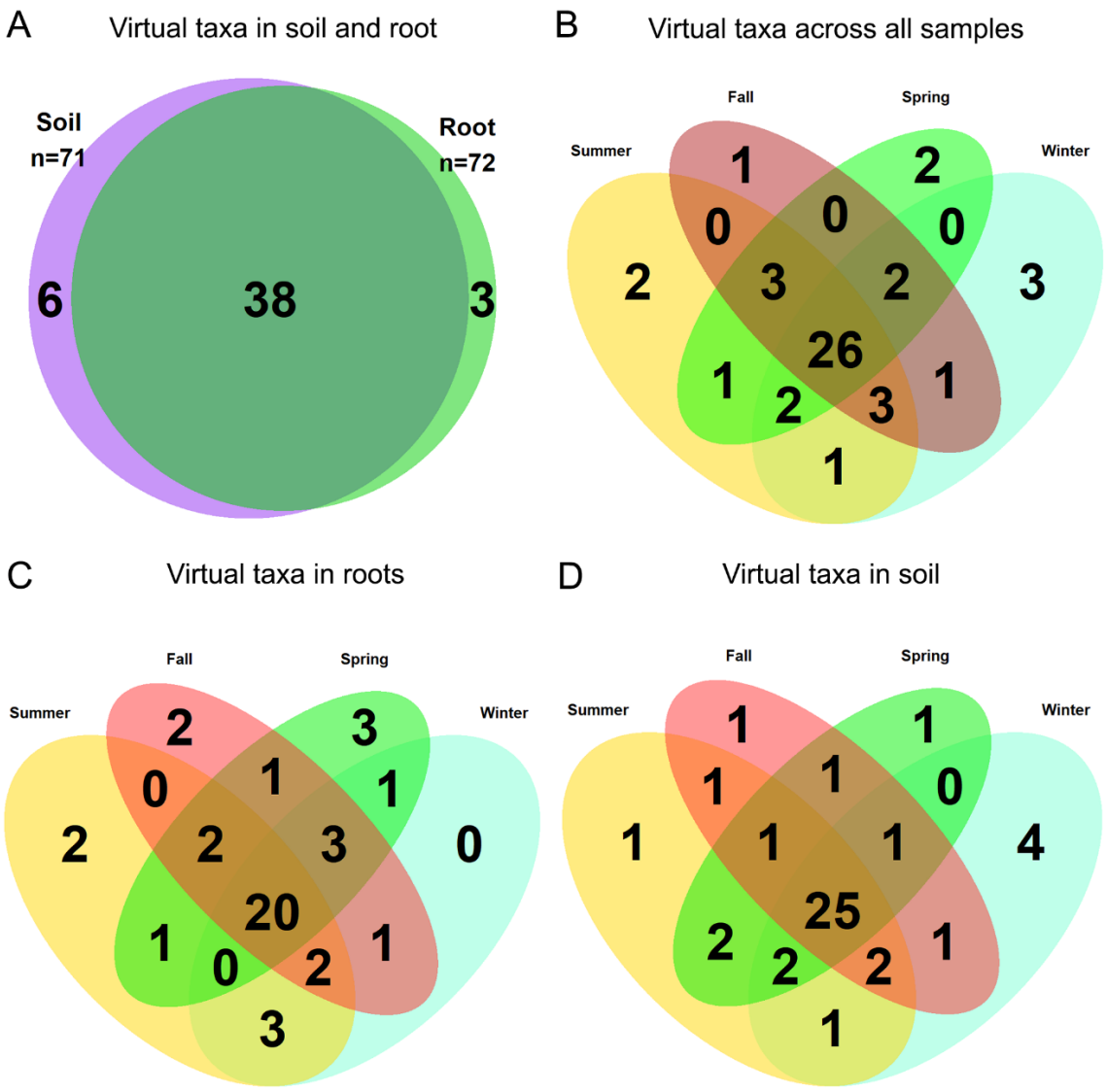

Figure 2.7.4 (A) Venn Diagram comparing virtual taxa in root and soil samples. (B) Venn Diagram indicating overlap of 47 detected virtual taxa in all root and soil samples. (C) Venn Diagram of 41 AMF VTs from roots and D) 44 soil VTs from each season.

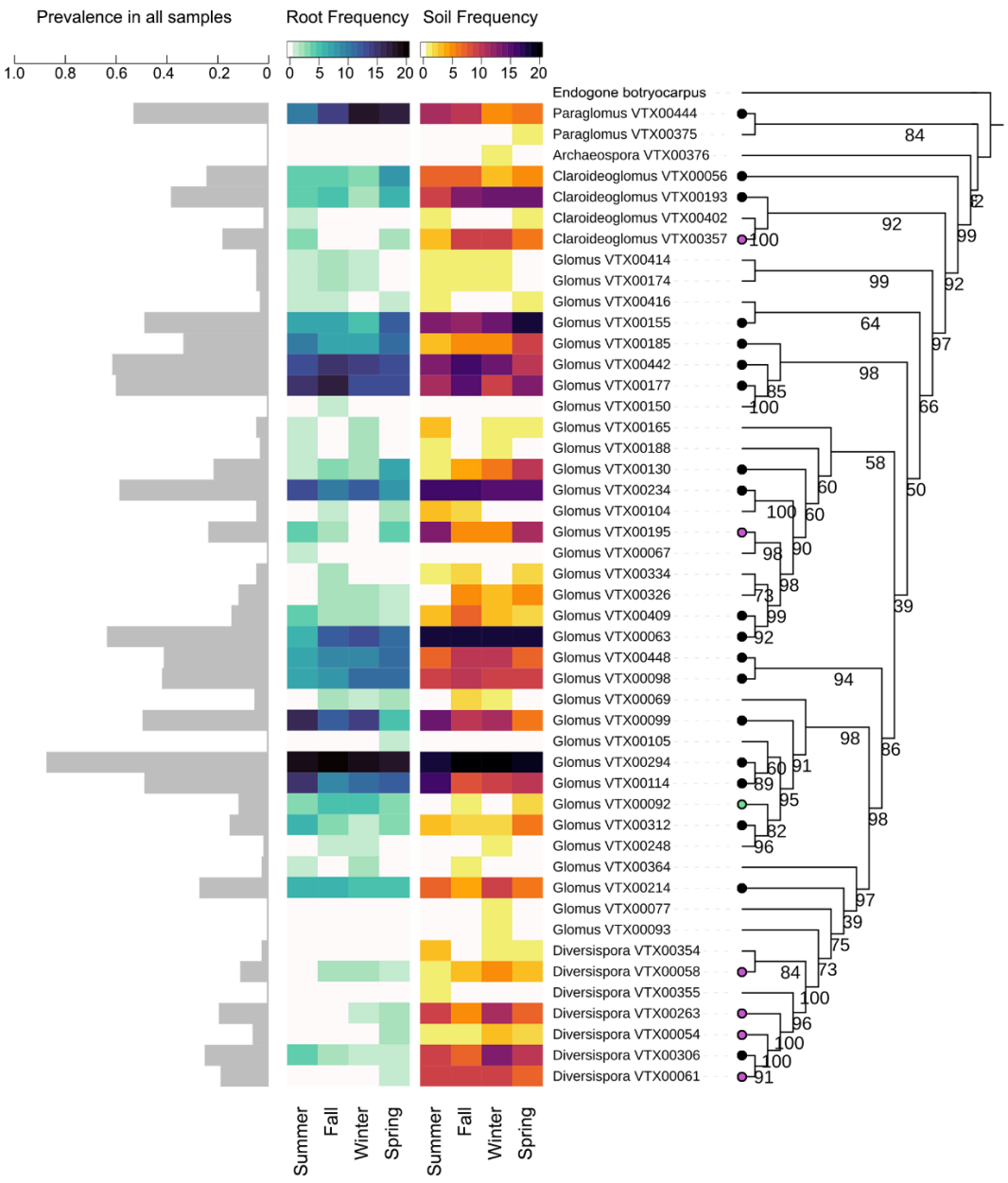

Figure 2.7.5 Prevalence of virtual taxa across 143 samples (gray). Heatmaps indicate AMF VT frequency across twenty trees in each season from roots (center-left) and soil (center-right). Root color scale in blue and soil color scale in red indicating frequency in up to 20 trees sampled per season. White cells are absences, and white rows indicate an absence of that VT from the sample type. A phylogenetic tree of 47 detected virtual taxa (with *Endogone botryocarpus* as an outgroup) was constructed based on forward reads. Numbers on the tree indicate bootstrap values. Tree-tip nodes indicate temporal core community members which are present in all 4 seasons in roots (green), in soils (purple), or in both (black).

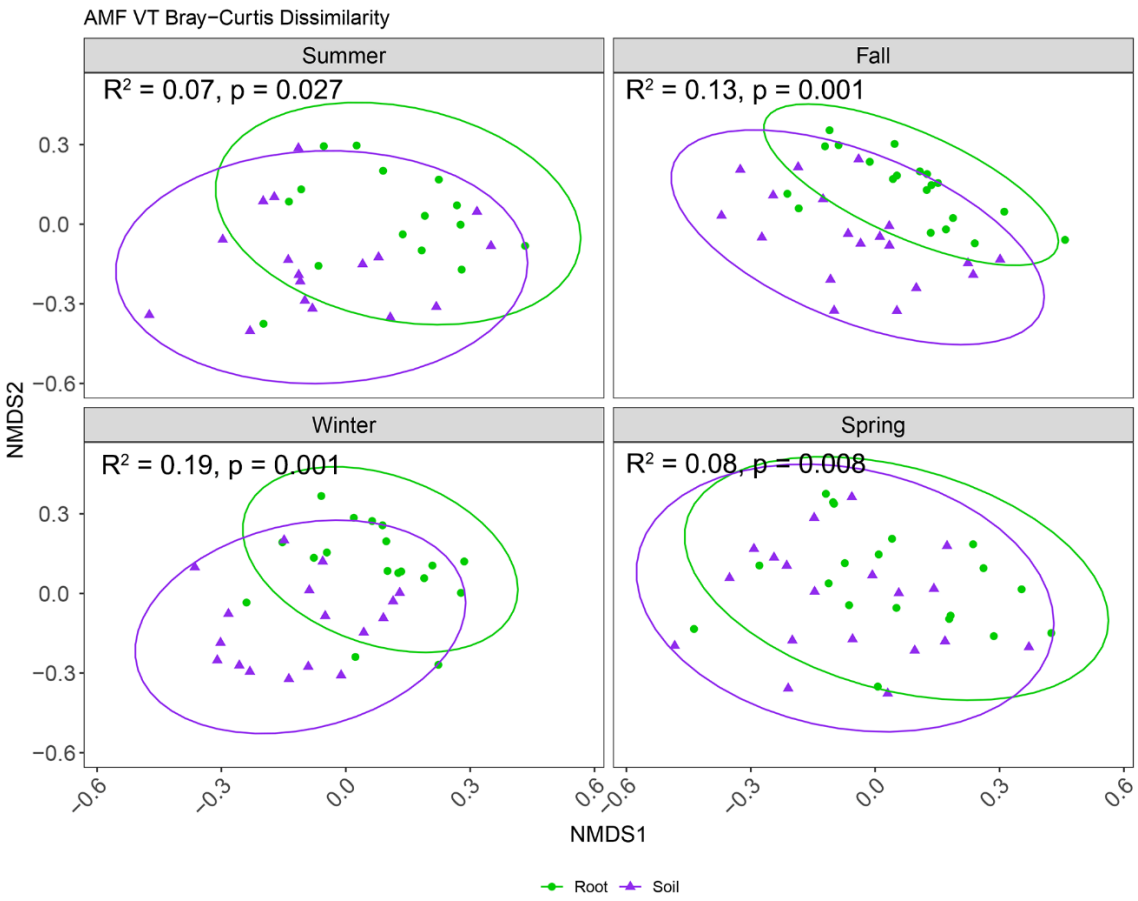

Figure 2.7.6 Bray-Curtis dissimilarity of AMF VTs across root (green circles) and soil (purple triangles) samples per season visualized as non-metric multidimensional scaling plots (k=3, stress = 0.18). Ellipses around each group represent 95% confidence intervals around the centroid of each sample type.

2.8 Supplementary Materials

Table S1. GPS Location of Joshua trees sampled for root and soil.

Tree Number	Latitude	Longitude	Height (cm)
1	35.251275	-115.497708	325
2	35.251261	-115.49756	302
3	35.250905	-115.497428	420
4	35.251377	-115.497459	335
5	35.251398	-115.497396	249
6	35.251412	-115.497392	230
7	35.251411	-115.497686	422
8	35.25169	-115.497233	567
9	35.268193	-115.498134	577
10	35.268291	-115.498224	308
11	35.267998	-115.497597	434
12	35.268044	-115.497910	506
13	35.267713	-115.497311	281
14	35.268048	-115.497525	588
15	35.267264	-115.497235	356
16	35.267647	-115.497137	272
17	35.250607	-115.502029	402
18	35.250872	-115.501821	343
19	35.251253	-115.501689	173
20	35.250872	-115.501821	294

Table S2. Sequence rarefaction levels of our sample-VT table of 150 samples and 47 virtual taxa. Prior to rarefaction, each sample had a median 5,565 reads and median 10 VTs. Low rarefaction levels were tested to maintain sample numbers and VTs. Increasing rarefaction to over 1,000 sequence reads per sample removed samples below that threshold which were low in species abundance, increasing the mean species richness.

	Mean Species	Median Species	Mean Seq	Median Seq	Total Taxa	N (samples)
Pre-rarefaction	10.1	10	7266	5565	47	150
418 Reads	9.6	9	418	418	45	146
754 Reads	9.9	10	754	754	47	145
889 Reads	9.9	10	899	899	47	143
10% - 1488 Reads	10.3	10	1488	1488	47	135

Thus 754 reads were selected for maintaining the total VT count and preserving the most sample numbers.

Table S3. Spore morphotypes based on single spore photos measured for identification purposes. Potential identifications based on expert opinion from Dr. Michael Allen.

Type	Size	Color	Note	Potential Taxon
M1	500 µm	Hyaline		*Gigaspora*
M2	250 µm	Orange-red		*Acaulospora*
M3	24 µm	Hyaline		*Glomus mosseae*
M4	24 µm	Yellow-orange		*Glomus*
M5	10 µm	Yellow to hyaline	Clustered	*Glomus aggregatum*
M6	85 µm	Yellow	Clustered	*Glomus*
M7	200 µm	Hyaline	1-2 spots within spore	*Scutellospora*
M8	10 µm	Red to purple		
M9	250 µm	Yellow	Budding	
M10	20 µm	Red to purple	Clustered	
M11	50 µm	Hyaline with red inside		
M12	300 µm	Translucent brown		

Table S4. A comparison of generalized mixed effects models of spore abundance, comparing a model with Fall, Winter, and Spring to the Summer reference level (Model 1), a model replacing seasons with a sum of the prior 3 months' precipitation (Model 2), and a model with a sum of 1 years' precipitation (Model 3). Precipitation values were scaled around zero. Bold p-values show significance. Both models use root and Summer as the Sample type and Season reference value, respectively.

Spore Abundance ~ Season + (1|TreeNum) +family = Gamma(link = "log")

term	estimate	std.error	z-value	p.value
(Intercept)	1.93172	0.00407	474.9005	<2e-16
Fall	0.74866	0.00406	184.3275	**<2e-16**
Winter	0.56444	0.00406	139.0090	**<2e-16**
Spring	0.56735	0.00406	139.6720	**<2e-16**

Spore Abundance ~Precipitation (3 months) + (1|TreeNum) +family = Gamma(link = "log")

term	estimate	std.error	z-value	p.value
(Intercept)	2.41962	0.09068	26.68235	<0.0001
Precipitation (3-month's sum)	0.20924	0.05018	4.16949	**0.00003**

Spore Abundance ~Precipitation (1 year) + (1|TreeNum) +family = Gamma(link = "log")

term	estimate	std.error	z-value	p.value

term	estimate	std.error	z-value	p.value
(Intercept)	2.405	0.004	568.620	<2 e-16
Precipitation (1-year's sum)	0.277	0.004	65.596	**<2 e-16**

Table S5. Models of seasonality on VT richness in soil and root samples. Seasons drove significant differences in soil but not root samples. Bold p-values show significance. Summer is used as the reference level for comparison.

Root Richness - S.obs ~ Timepoint+(1| TreeNum) , family = poisson(link = "log")

term	estimate	std.error	z-value	p.value
(Intercept)	2.145	0.094	22.757	0.000
Fall	0.092	0.115	0.799	0.424
Winter	0.030	0.119	0.253	0.800
Spring	0.121	0.115	1.052	0.293

Soil Richness - S.obs ~ Timepoint+(1| TreeNum) , family = poisson(link = "log")

term	estimate	std.error	z-value	p.value
(Intercept)	2.153	0.093	23.129	0.000
Fall	0.279	0.109	2.560	**0.010**
Winter	0.291	0.111	2.609	**0.009**
Spring	0.180	0.111	1.618	0.106

Figure 2.8.1 A distinct red root emerging from below the base of *Yucca jaegeriana*, indicating the bottom of the Eastern Joshua tree trunk. Saturation modified to highlight the root.

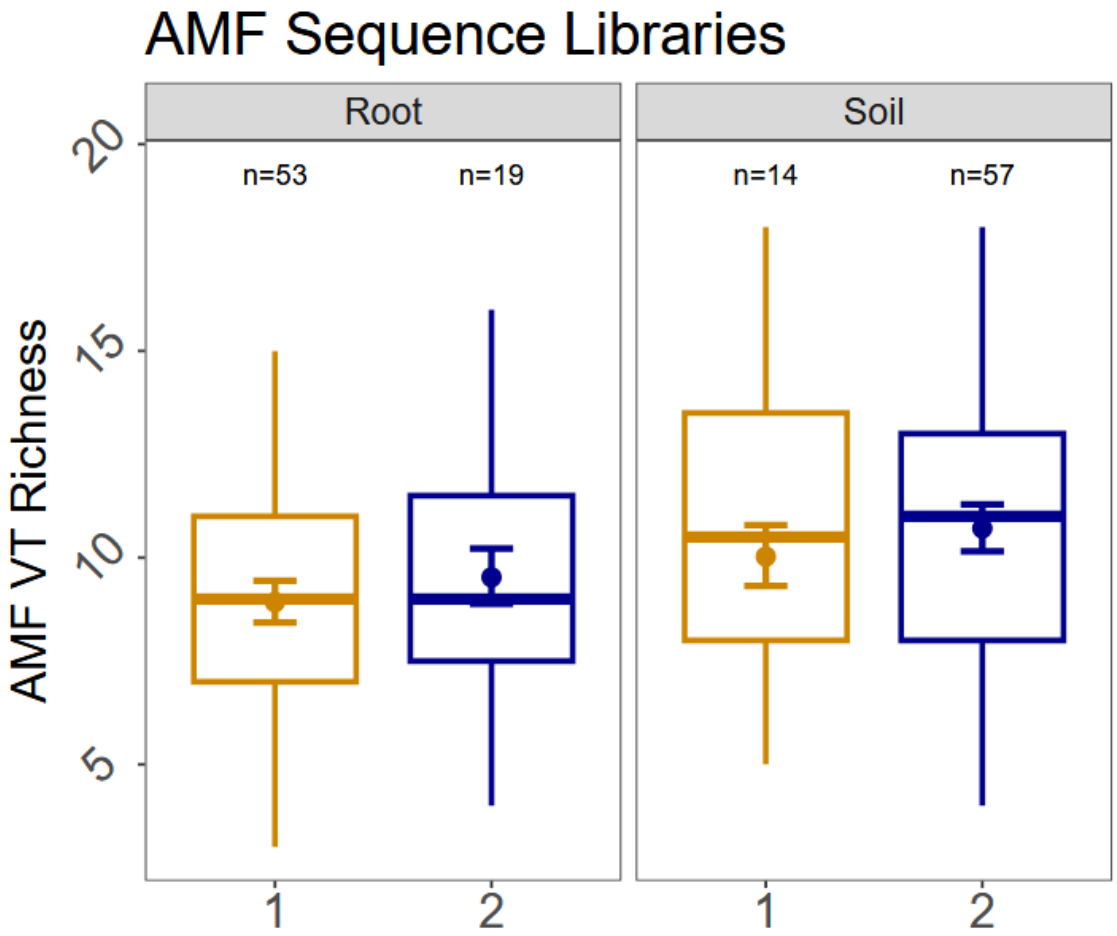

Figure 2.8.2 A comparison of richness per sample type between two sequence libraries. Library 1 was primarily root samples and seasons Summer, Fall, and Winter, while Library 2 was primarily soil samples across all seasons. Points and bars within each box indicate model-predicted means ± standard error. Box plots show medians with the middle horizontal line, the bottom of the box indicating the first quartile, the top indicating the third quartile, and whiskers above and below indicating minimum and maximum values not considered outliers.

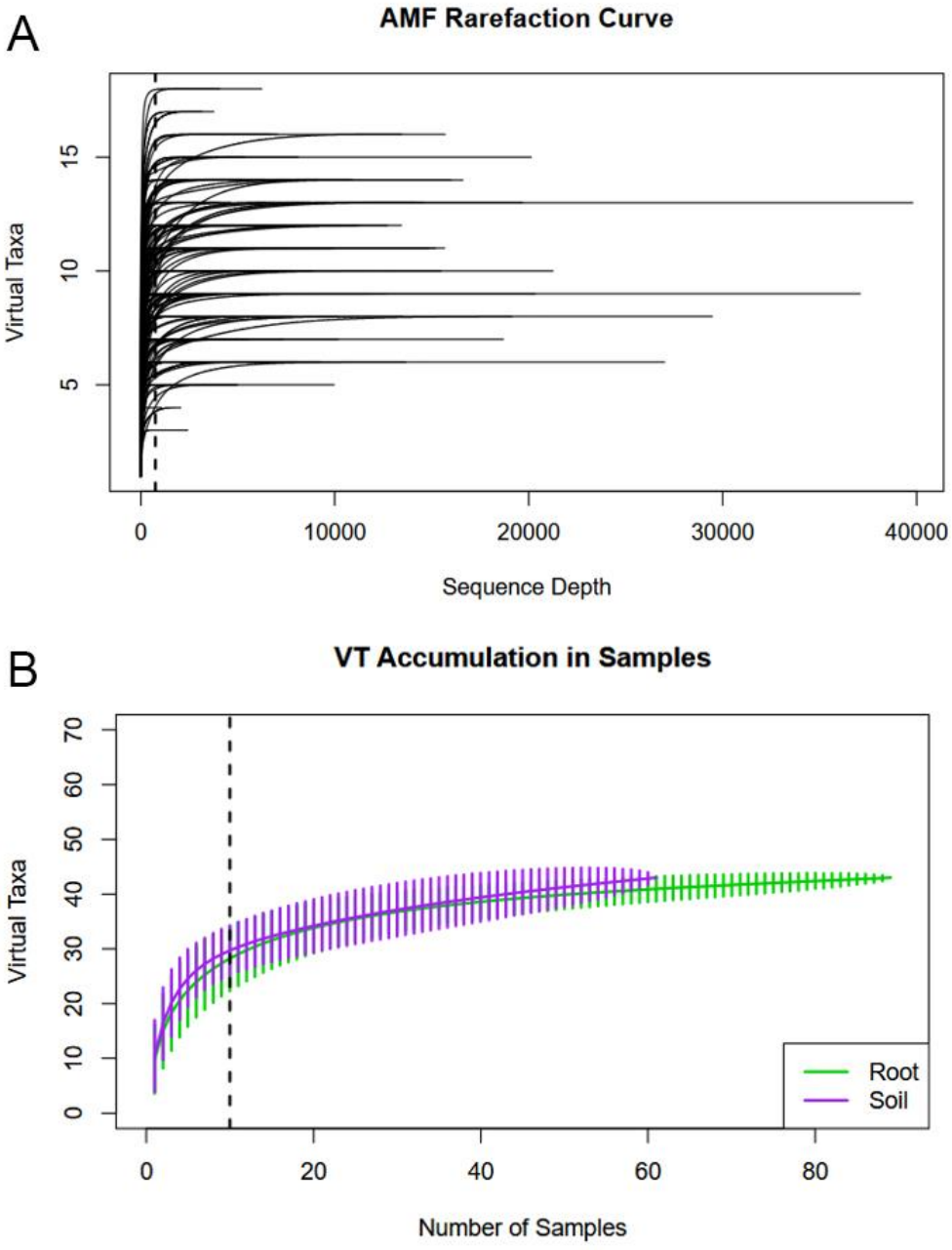

Figure 2.8.3 A) Species saturation curves based on 47 virtual taxa detected in all our samples across 1 year. Soil samples are depicted as purple and root samples are depicted in green. The curve indicates how many samples are sufficient for capturing most of the species present in the community. The dashed line at 10 samples shows approximately where taxa accumulation levels off. B) Sequence depth compared to the amount of species detected. Each line is one sample. Our rarefaction level of 754 sequences (dashed line) allows most samples to saturate and importantly, preserves the total number of VT detected without removing any.

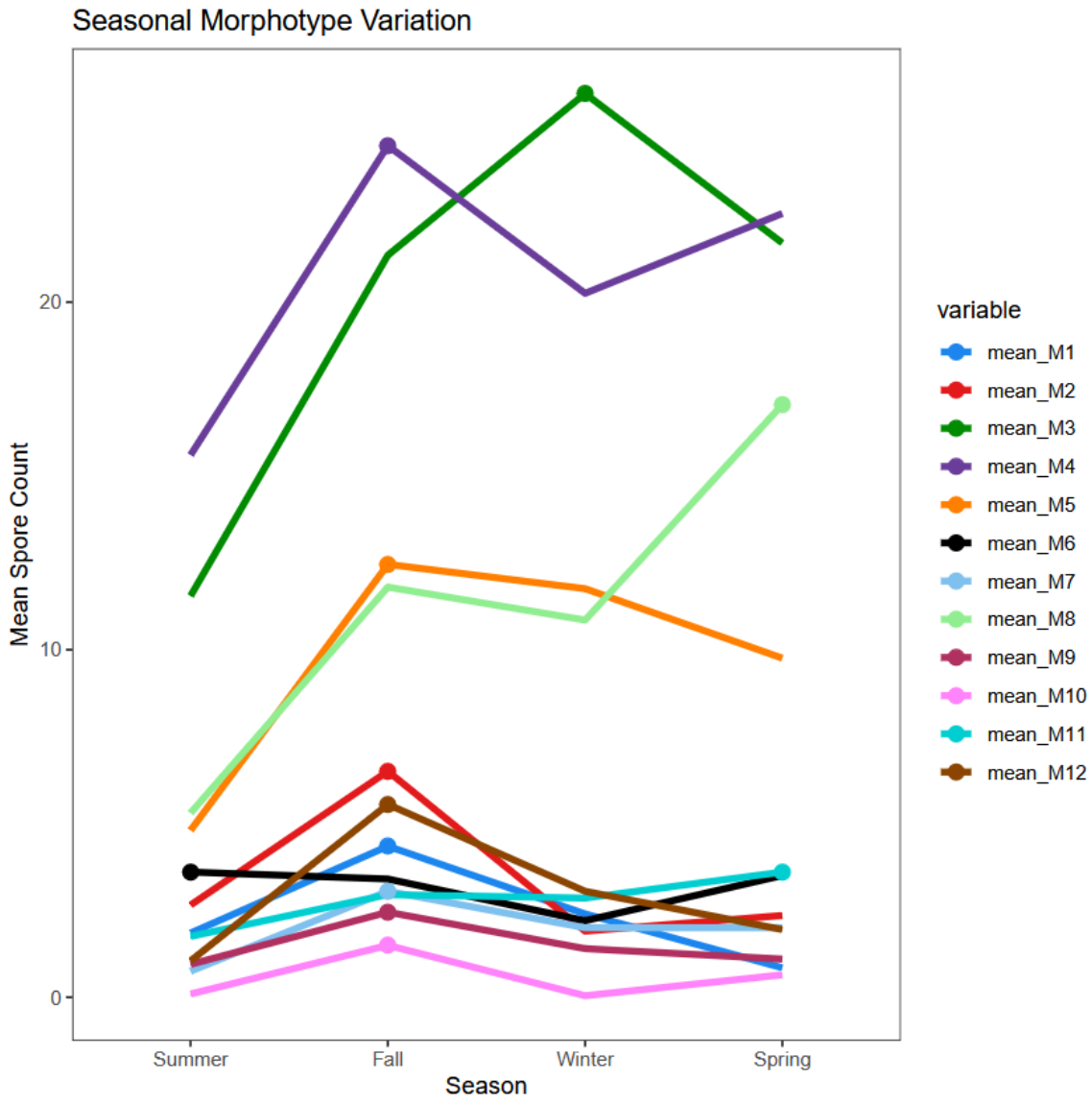

Figure 2.8.4 Mean spore morphotype count in twenty trees across each season. Circles indicate the season in which each morphotype was most abundant.

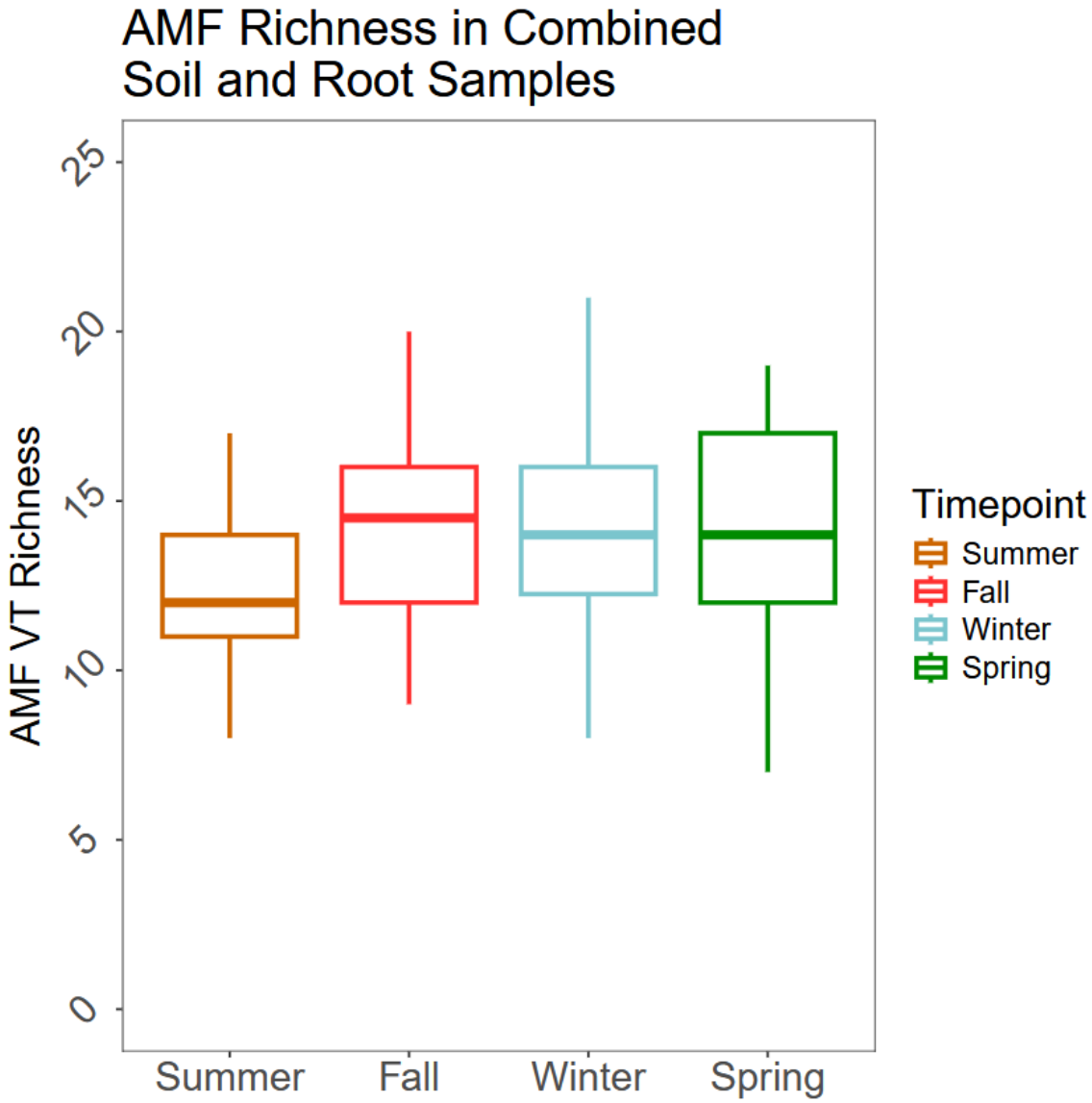

Figure 2.8.5 Richness comparisons of each season (from both root and soil combined per tree). Box plots show medians with the middle horizontal line, the bottom of the box indicating the first quartile, the top indicating the third quartile, and whiskers above and below indicating minimum and maximum values not considered outliers.

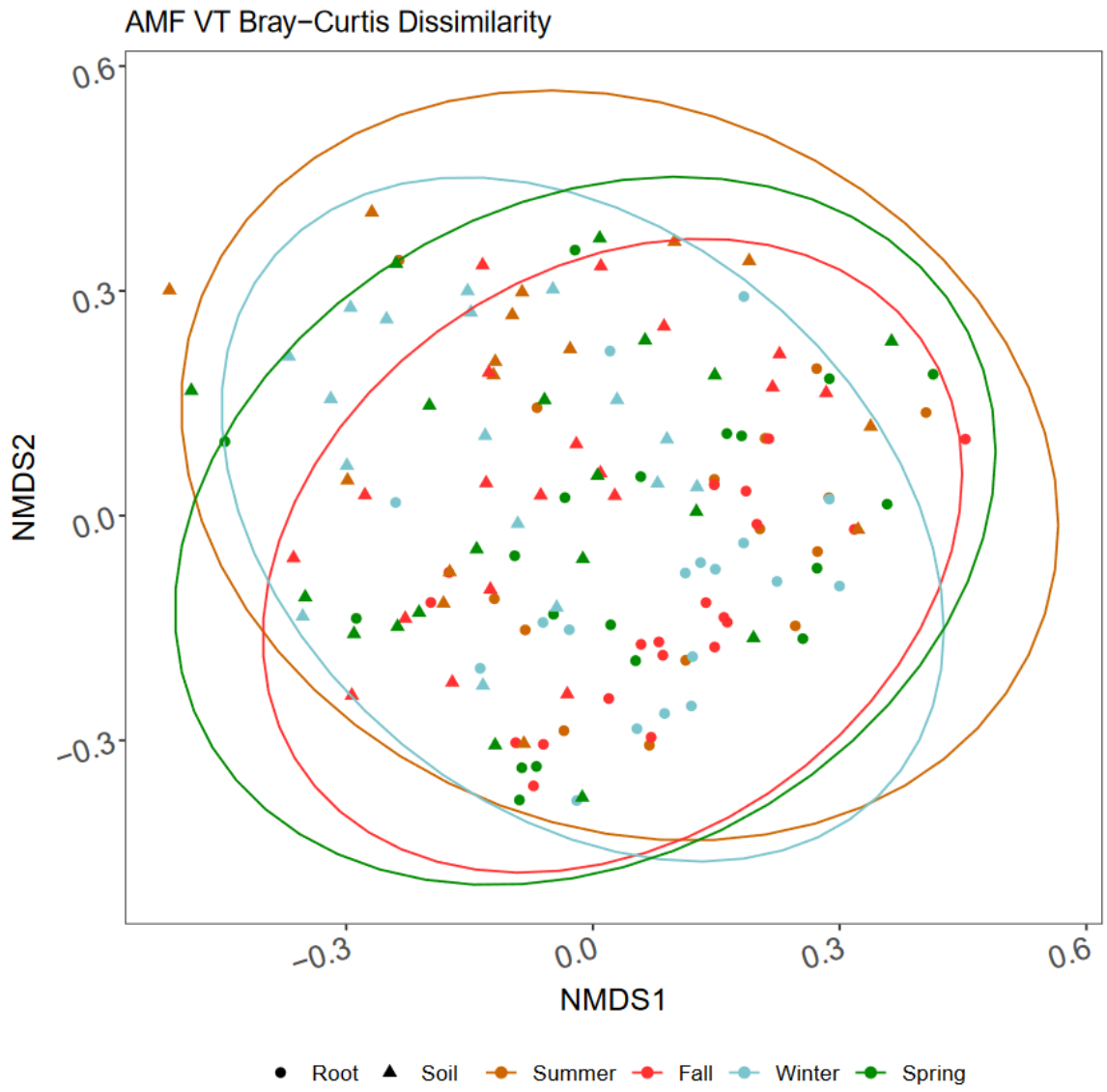

Figure 2.8.6 Bray-Curtis dissimilarity of samples based on VT sequences across seasons visualized as non-metric multidimensional scaling plots (k = 3, stress = 0.18). Triangles indicate soil samples and circles indicate root samples. Ellipses around each season represent 95% confidence intervals around the centroid of combined sample types per season.

3 Chapter III.

Mojave Desert microbial communities show resilience over three years despite widespread plant mortality following the Dome Fire

3.1 Abstract

High severity desert fires are uncommon but typically chart a new successional trajectory altering plant communities for at least 65 years. These aboveground vegetation shifts can have large implications for belowground microbial communities that maintain soil structure and nutrient cycling. High severity wildfires in forests or shrublands can severely reduce microbial species richness and biomass and alter microbiomes for decades but impacts on desert soil microbiomes are virtually unknown. The 2020 Mojave Desert Dome Fire burned 43,000 acres of Eastern Joshua tree *(Yucca jaegeriana*) habitat, burning roughly 1 million trees. To track aboveground and belowground impacts of the Dome Fire, we established 9 plots (6 burned; 3 unburned) and sampled 4 subsamples per plot for 5 time points ranging from 2 weeks to 3 years post-fire. We measured initial ash depth as a proxy of soil burn severity and assessed plant mortality, plant richness, soil chemical characteristics, estimated soil microbial biomass with qPCR, and microbial richness and composition with Illumina MiSeq of 16S and ITS2 amplicons. Belowground communities were highly diverse, containing 25,444 bacterial, 269 archaeal, and 6,683

fungal ASVs amplicon sequence variants (ASVs) or microbial taxa. We identified at least 65 plants across 3 years. Fire caused 80% Eastern Joshua tree mortality and reduced plant richness except during a bloom of annual herbs at 1-year post-fire, yet the fire did not significantly reduce microbial biomass or richness at any time point. Microbial communities for both bacteria and fungi showed small but significant changes, enriching for pyrophilous microbes in burned plots. We identified increases of pyrophilous microbes such as *Nitrososphaera*, *Massilia*, *Noviherbaspirillum* bacteria and *Penicillium, Alternaria, Coniochaeata* and *Naganishia* fungi. We present the first comprehensive above and belowground examination following a natural desert wildfire including Archaea, Bacteria, and Fungi. Despite the widespread mortality of Eastern Joshua trees across 3 years, microbial biomass, richness, and community composition were mostly resistant to change, like microbial responses to low-intensity fast-moving grassland fires. Despite high resistance overall, wildfire still increased several pyrophilous bacterial and fungal taxa common after high severity shrubland and forest wildfires.

3.2 Introduction

Drylands make up 46% of the terrestrial biosphere and are expected to expand to 56% by 2100 due to climate change (Cherlet et al. 2018). Increased mean temperatures, variability in precipitation, and invasive plants are increasing wildfire risks with long-lasting impacts on soil resources (Ravi et al. 2022). Frequently burned environments such as California chaparral shrublands (Hanes 1971) and pine forests (Habeck and Mutch 1973) have well understood vegetational responses to fire, but desert wildfires are infrequent and relatively understudied (Schussman et al. 2006; Klinger et al. 2021). Specifically, the Mojave Desert of Western North America has experienced increasingly large wildfires in recent decades (Brooks and Matchett 2006; Klinger et al. 2021) with slow regenerating plants exhibiting century-scale secondary successional patterns (Abella 2010). Moreover, fire impacts on desert soil microbiomes are nearly unknown (Allen et al. 2011), but could have critical implications for desert biogeochemical cycling (Homyak et al. 2016) and plant regeneration, since above- and below-ground communities are intimately linked (Van Der Heijden et al. 2008).

Desert plants like the iconic Joshua trees (*Yucca brevifolia* Engelm. and *Yucca jaegeriana* (McKelvey) L.W. Lenz) of the Mojave Desert are dependent on root-associated fungal communities for survival (Allen 1989), yet these symbiotic associations are vulnerable to disturbances from fire (Dove and Hart 2017). Arbuscular mycorrhizal fungi (AMF) are obligate symbionts associated with 70-80% of plant species (Brundrett and Tedersoo 2018). AMF are critical partners for desert plants, especially *Yucca* (Titus et al. 2002b), since AMF increase plant access to water (Augé 2001; Kakouridis et al.

2020) and enhance drought tolerance (Augé et al. 2015). Both the Western Joshua tree *Yucca brevifolia* (Harrower and Gilbert 2021) and Eastern Joshua tree *Y. jaegeriana* (Joukhajian and Glassman 2025) host diverse AMF from 8 Glomeromycotina families. Fungi can be either resistant (insensitive) or resilient (recover quickly to original status) to fire (Shade et al. 2012). However, most long-term studies show that AMF have high post-fire resilience (Bellgard et al. 1994; Aguilar-Fernández et al. 2009; Espinosa et al. 2023) although fires can select for changes in AMF spore traits both immediately post-fire and 6-months later (Hopkins et al. 2024). Fires also damage biological soil crusts that house AMF and other root-associated fungi such as dark septate endophytes (DSEs) (Aanderud et al. 2018; Brianne et al. 2020), thus reducing sources of fungal spore dispersal (Warren et al. 2019). These indirect effects may lead to both short- and long-term restructurings of plant-associated fungal communities.

Although most fungal species are negatively impacted by fire, some pyrophilous "fire-loving" fungi that are rare or undetectable pre-fire massively increase in abundance post-fire (Fox et al. 2022). Several genera in Pyronemataceae are referred to as "phoenicoid fungi" for their abundant fruiting via ascocarps post-fire (Carpenter and Trappe 1985). Studies in pine forests (Jacobson et al. 2004; Glassman et al. 2016; Bruns et al. 2020; Caiafa et al. 2023), shrublands (Pérez-Valera et al. 2017; Pulido-Chavez et al. 2023), boreal forests (Whitman et al. 2019), and eucalyptus forests (Warcup 1990; McMullan-Fisher et al. 2002) highlight pyrophilous ascomycete species in the genera *Pyronema*, *Neurospora, Penicillium* and *Aspergillus*. In contrast, little is known about how pyrophilous fungi might respond in desert ecosystems, where high temperatures

might pre-adapt common desert fungi like *Naganishia* (Wei et al. 2022; Lopez et al. 2024) and *Alternaria* (Pombubpa et al. 2020; Malicka et al. 2022) to survive wildfire. Studies on microbial community responses to desert fires are limited to controlled fires (Liu et al. 2000; Aanderud et al. 2019; Vega-Cofre et al. 2023; Zhang et al. 2025), where Dothideomycetes like *Preussia lignicola* often increased in abundance, with one study after a natural desert wildfire in Mexico focusing only on AMF, which decreased in richness post-fire (Chimal-Sánchez et al. 2015). As desert wildfires burn more acreage, understanding how symbiotic fungi are affected and if pyrophilous fungi proliferate post-fire is essential for identifying successional trajectories and predicting ecosystem recovery.

Desert fires may also impact archaea and bacteria, which are overrepresented in desert chemical cycling pathways compared to other ecosystems (Makhalanyane et al. 2015). Abundant bacterial phyla in deserts include Actinobacteriota, Chloroflexota, Proteobacteria, and Planctomycetota. Archaea, particularly the phylum Crenarchaeota, are more abundant in deserts than other ecosystems (Ramond and Cowan 2022). Wildfires in forested ecosystems broadly depress the phyla Acidobacteriota, Bacteriodota, and Verrucomicrobiota (Rodríguez et al. 2018; Nelson et al. 2024), but bacteria can also be pyrophilous. For example, members of Actinobacteriota like *Conexibacter* and Proteobacteria like *Massilia* and *Noviherbaspirillum* increased in abundance after a wildfire in chaparral shrublands (Pulido-Chavez et al. 2023) and forests (Soria et al. 2023). Firmicutes also grow in dominance post-fire (Pérez-Valera et al. 2017; Sáenz de Miera et al. 2020; Enright et al. 2022; Pulido-Chavez et al. 2023). Bacteria such

as *Arthrobacter* and *Massilia* persisted in post-fire forests for up to 9 years and may be considered biomarkers of altered communities post-fire (Fernández-González et al. 2023). Rapid-responding prokaryotes are activated by rain pulses in the desert, allowing them to wait through periods of drought (Collins et al. 2014; Cowan et al. 2020). Yet, an increasingly variable precipitation regime may further hamper microbial communities, as decadal succession timelines in plants can disconnect nutrient cycling processes, leading to drainage of essential nutrients deep belowground (Wang et al. 2022a). Thus, long-term sampling is critical to link plant and microbial responses to fires in the desert, where lag effects are common due to delayed plant mortality, slow nutrient turnover, and rain-pulse nature of microbial activity (Vamstad and Rotenberry 2010; Muñoz-Rojas et al. 2016; Maestre et al. 2021).

Fires can affect microbes directly via heat-induced mortality, or indirectly by changes in vegetation or soil chemical properties post-fire (Hart et al. 2005; Certini et al. 2021). Fire intensity refers to heat transfer of fire whereas fire severity refers to either above or belowground mortality (Keeley 2009). Fires affecting areas with lower or less dense aboveground biomass like annual grasslands and deserts are typically fast moving and low intensity with low soil burn severity causing minimal impacts on associated soil microbes (Allen et al. 2011; Glassman et al. 2023). In contrast, fires affecting areas with dense aboveground vegetation like shrublands and forests are typically slower moving, higher intensity, with higher soil burn severity with large reductions in soil microbial biomass and richness (Dooley and Treseder 2012; Nelson et al. 2022a). Beyond heat-induced mortality, a permanent shift in aboveground plants may result in loss of

important plant symbionts like AMF (Stinson et al. 2006; Mummey and Rillig 2006). In August 2020, the Dome Fire burned 175 km^2 (43,273 acres) of the Mojave Desert, burning roughly 1 million *Y. jaegeriana* trees (NPS. 2020). Although this fire was fueled by grasses and spread rapidly at low intensity, it was unusual in that it had high severity impacts on aboveground vegetation killing large tracts of long-lived perennial *Y. jaegeriana* trees and surrounding shrubland, causing concern over the long-term persistence of the species (Smith et al. 2023). This leads to a large knowledge gap, i.e. will microbial impacts be minimal like other fast moving low intensity fires, or large due to the indirect effects of widespread plant mortality?

Here, we investigate the short- and longer-term direct and indirect effects of the 2020 Dome Fire on above and belowground communities across five timepoints at 17 days, 1 and 8 months, and 1- and 3-years post-fire. We asked, 1) how did plant community composition and *Y. jaegeriana* survivorship change? 2) did archaeal, bacterial, and fungal richness and biomass decline? 3) were changes in bacterial and fungal community composition driven by direct or indirect effects? and 4) did pyrophilous microbes commonly seen in other fire-prone ecosystems proliferate? We hypothesized that the atypical severity of the fire on the long-lived perennial plant community would have a more deleterious impact on microbial communities despite being a fast-moving low-intensity fire, and that there would be lag effects in the response due to the delayed impacts of plant mortality and the rain-pulse driven nature of microbial responses in the desert. This would drive decreases in richness of bacteria, fungi, and AMF in particular, with minimal impact on the highly resistant archaeal taxa

but might lead to increases in pyrophilous microbes like fungal Dothideomycetes, which were common after prescribed burns in deserts, and bacterial phyla Firmicutes and Proteobacteria, which are common after fire in many ecosystems.

3.3 Methods

Site description: We sampled in Mojave National Preserve, California, USA, around the Cima Dome (35.264777°, -115.516038°), home to the densest *Y. jaegeriana* stand, where the Dome Fire burned 175km^2 from August 15-24 2020 (Fig. 1a). Our study area had a mean elevation of 1361m, in a region with bimodal summer and winter rains for at least the last century (Tagestad et al. 2016). Vegetation in the nearby unburned area consisted of *Y. jaegeriana* shrublands, including *Y. baccata*, *Y. schidigera* and annual and perennial grasses like *Bouteloua spp.*, *Bromus spp.,* and *Hilaria jamesii*. Shrubs included *Ambrosia salsola, Coleogyne ramosissima, Ephedra nevadensis,* and *Lycium spp.*

Experimental design and soil collection: In September 2020, 17-days after the fire was extinguished, we established nine plots (6 burned and 3 unburned; Fig. 1a), each centered around a singular live or dead *Y. jaegeriana* tree (Fig. 1b). Many trees were highly colonized by the fungus *Neurospora discreta* underneath exposed bark (Fig. 1c), which we identified by culturing and sequencing the genome (Sari et al. 2025). Within each plot, we established four 1m^2 subplots 5m from the focal tree in each of the cardinal directions for a total of 36 subplots (Fig. 1d). During the first sampling timepoint, we

estimated soil burn severity by averaging three ash depth measurements from within each $1m^2$ subplot and estimating percent char at each subplot as previously established (Glassman et al. 2023). We collected soil from the top 10 cm beneath the ash or organic layer with a releasable bulb planter cleaned between subplots with 70% ethanol to reduce contamination and homogenized 2 soil cores from each sub-plot. We collected soils at five time-points: September 10 and 24 2020, April 15 2021, September 9 2021, and September 19 2023 corresponding to 17-days, 1-month, 8-months, and 1 and 3-years post-fire. Our 3-year sampling occurred one month after Tropical Storm Hilary brought the largest 1-day precipitation event in our study period, registering at 61mm of rain on August 20, 2023 (Fig. 1E). We collected soils from all 9 plots at all time points except for the second timepoint at 1-month post-fire where we were only able to collect soils from 7/9 plots including 1 unburned plot (plot #8). Soils were collected and stored on ice and transported to the University of California, Riverside (UCR), where we homogenized and sieved (2mm) within 24hrs of collection. We immediately analyzed soils for gravimetric soil moisture content and stored a portion at -80°C for molecular analysis for all time points. For 3 time points (17 days, 8 months and 3 years post-fire), we performed the KCl extraction method on fresh soil (Carter and Gregorich 2007) and assessed ammonium, phosphate, and NO_x^- at the UCR Environmental Science Research Lab. We measured pH on air-dried soil by making a slurry of 10g of soil and 20mL of distilled water and measuring with a VisionPlus pH6175 meter (Jenco Instruments Inc., San Diego, CA) after one minute of shaking to mix.

Plant communities: We surveyed plant species and *Y. jaegeriana* mortality at 17-days, 1-year, and 3-years post-fire at each plot. We used a point centered quarter survey method (PCQM), which is designed to capture density in a random sample of plants (Cottam et al. 1953). For each plot, we located the nearest *Y. jaegeriana* to the center point of the sampling area. At this sentinel tree we performed a Rapid Assessment (CNPS-CDFW) survey of the surrounding 20-meter radius, which included perennial plant richness and ocular estimates of cover, center point coordinates in UTMs center point coordinates in UTMs (Zone 11, WGS 84) and cardinal photos. From the sentinel, we identified each cardinal direction and found the nearest tree in each quadrant. Each site had a minimum of five trees (sentinel, NE, NW, SE, & SW). During the first sampling, we noted pre-fire mortality of trees by the sole presence of ash on the ground (biomass consumed), fire-related mortality via presence of char on the trees and absence of green leaves, and at subsequent samplings, noted resprouting or persisting green leaves as signs of survival. Then at each tree we took note of living and dead terminal ends of the tree, height of the tallest leaf blade, herbivory, and char.

DNA Extraction and Sequencing: We extracted DNA from 0.25g of frozen soil with Qiagen DNeasy Power Soil Pro Kits, which were modified by replacing 100 µL of the initial C1 solution with 100 µL ATL and incubating overnight at 4°C to improve yields. We PCR amplified DNA with the primer pair 515F-806R targeting the V4 region of the 16S rRNA gene of bacteria and archaea (Caporaso et al. 2011) and the 5.8S-ITS4 primer pair to amplify the ITS2 region (Taylor et al. 2016) of the Internal Transcribed Spacer,

which is the internationally recognized barcode for fungi (Schoch et al. 2012). We attached dual-index primers (DIP) with barcodes and adaptors onto amplicons with a second PCR step (Kozich et al. 2013). To amplify ITS2, we mixed 5μL DNA with 0.5 μL of the 5.8S and ITS4 primers (10 μM), to amplify 16S, we mixed 1 μL DNA with 0.5 μL of the 515F and 806R primers (10 μM), then added 12.5μL AccuStart II PCR Tough Mix (Quantabio, Beverly MA, USA), and added Ultra-Pure Sterile Molecular Biology Grade water (Genesee Scientific, San Diego, CA, USA) up to a 25 μL reaction. We cleaned PCR1 amplicons with AMPure XP magnetic beads (Beckman Coulter Inc.) following manufacturer instructions then attached DIP-barcodes in PCR2 with the following mix: 2.5 μL of 10 mM DIP PCR2 primers, 6.5 μL of ultrapure water, 12.5 μL of Accustart II PCR ToughMix and 1 μL PCR1 product. See Table S1 for PCR thermocycler settings. We pooled 16S and ITS2 PCR products separately based on band-strength then cleaned the pools with Ampure XP magnetic beads following established protocols (Pulido-Chavez et al. 2023). We included negative controls for DNA extractions and PCRs and a Microbial Standard II (Zymobiotics, Orange, CA) mock community in 16S and ITS2 pools. We then assessed amplicon pool size and intensity with the Bioanalyzer before pooling at a 2:3 ratio of 16S to ITS2 to account for the short amplicon preference of Illumina sequencing and the typically longer ITS2 amplicons. We sequenced with Illumina MiSeq 2x300bp at the UCR Institute for Integrative Genome Biology across two sequence libraries.

Biomass*:* We estimated sequence copy number as a proxy of microbial biomass with quantitative polymerase chain reaction (qPCR) for either the 16S for archaea and bacteria using the Eub338/Eub518 primer pair (Fierer et al. 2005) or the 18S FungiQuant primers for fungi (Liu et al. 2012) using standards as previously published (Pulido-Chavez et al. 2023). Each 10 µL qPCR reaction contained 1 µL DNA, 5 µL 1X iTaq SYBR mix (Bio-Rad, Hercules, CA), 0.4 µL (10 µM) of each primer, and 3.2 µL ultra-pure water with thermocycler settings in Table S1. We ran samples in triplicate on the CFX Opus 384 Real-Time PCR System (Bio-Rad, Hercules, CA). We used standards with a known concentration in a dilution series to determine sample starting concentration and calculated gene copy numbers per gram of soil with the following equation: Copy number = (Starting concentration (ng/ µL) * (1 µL in reaction) * 6.022 * 10^23 (Avogadro's constant)) / (Length of standard (bp) * 660 ng (average weight of a base pair)* 10^9 (average number of cells per g of soil).

Bioinformatics and statistical analysis: We analyzed Illumina Miseq data using QIIME2 (Bolyen et al. 2019) to produce tables of Amplicon Sequence Variants (ASVs). We removed forward and reverse adaptors using the QIIME2 cutadapt trim-paired plugin (Martin 2011), demultiplexed, and denoised using DADA2 (Callahan et al. 2016) with the denoise-paired plugin based on the quality of forward reads to ensure median quality scores over 30. We assigned taxonomy of ITS2 sequences using the dynamic database in UNITE v.9 (Abarenkov et al. 2010), and 16S sequences using the database SILVA v.138 (Quast et al. 2013). We then exported the ASV table to R ver. 4.1 (R Core Team 2020),

where we normalized the sequencing depth per Kingdom (638 for archaea, 4,256 for bacteria, and 6,874 for fungi) to account for uneven sequencing depth (Schloss 2024), and estimated alpha diversity metrics with the BiodiversityR package (Kindt 2024). We used qiime2R (Bisanz 2018) to analyze QIIME2 outputs in R and phyloseq (McMurdie and Holmes 2013) to generate relative abundance barplots and line graphs from composition data, and "Probable" or "Highly Probable" guild data of fungi from FUNGuild (Nguyen et al. 2016) using FungalTraits (Põlme et al. 2020). We used generalized linear mixed (GLMM) effects models to test the impact of fire and time on microbial richness and biomass with plot as a random effect using lme4 (Bates et al. 2015), or a generalized least squares (gls) model with an exponential correlation structure based on geographic coordinates to test for spatial autocorrelation using nmle (Pinheiro et al. 2017). We checked the best fit distribution of each variable with the “fitdistr” function in the MASS package (Ripley et al. 2024).

To identify shifts in plant communities, we used estimates of plant cover abundance to compare overall relative abundance of plant families between the burned and unburned plots at 17-days, 1-year, and 3-years post-fire. At the same timepoints, we summed total counts of living and dead *Y. jaegeriana* across burned and unburned plots, which included previously felled trees in unburned plots, and plotted the percentage of total surviving trees per treatment. At each individual timepoint where plants were measured, we used ANOVA to test fire effect on plant richness and used the mantel function within the vegan package (Oksanen et al. 2008) to correlate plant and microbial composition.

To identify drivers of microbial community compositional changes, we the vegan functions adonis2, and betadisper to identify when changes were due to increased heterogeneity across a group. To compare the impacts of soil properties or plant richness on microbial communities, we visualized beta diversity using non-metric multi-dimensional scaling (NMDS) plots of Bray-Curtis dissimilarity with the vegan function metaDMS, overlaid continuous variables with the envfit function, and adjusted p-values with the Bonferroni method using p.adjust for repeated measurements across time. We limited comparisons of microbial composition to plant richness to 17-days, 1-year, and 3-years post-fire for fungi while soil chemical composition was limited to 17-days, 8-months, and 3-years post-fire for bacteria and archaea to match datasets of plant richness or soil chemical composition data. We combined samples across time after determining that days post-fire was not a significant driver of community dissimilarity for each subset of samples and timepoints. We separated the effect of spatial autocorrelation with the vegan function "varpart" using a distance matrix, a PCA of environmental variables, and each Bray-Curtis dissimilarity matrix.

To identify pyrophilous microbes, we used the Deseq2 package (Love et al. 2014) to identify genera with significant log2fold changes (alpha of 0.01) in burned relative to unburned plots at each time point (excluding the 1-month timepoint due to the low number of unburned samples).

Sequences are uploaded to the NCBI SRA under accession XYZ and bioinformatics scripts are found at github.com/arik-chou/DF.

3.4 Results

Fire impact on plant mortality, richness, and diversity*:* At 17-days post-fire, burned subplots had a mean ± standard error ash depth of 0.37 ± 0.07 cm (Fig. 2A) and 43.33% ± 4.37 char percentage (Fig. 2B) whereas unburned plots had none. In unburned plots, *Y. jaegeriana* survivorship was stable at roughly 83% across all time points (Fig. 2C). In contrast, in burned plots, *Y. jaegeriana* survivorship decreased across time with percentage of trees having some green leaves reducing from 86% at 17-days to 50% at 1-year to only 20% at 3 years post-fire (Fig. 2C). Fire significantly reduced plant richness from 12.67 ± 0.33 in unburned to 2.32 ± 0.94 in burned plots at 17-days post-fire (Table S2; Fig. 2D). However, arrival of new plant species led to burned plots (8.6 ± 2.7) having similar richness to unburned plots (12 ± 1.5) at 1-year post-fire (Fig. S1). Yet this change was temporary as plant richness was significantly lower in burned (6 ± 0.6) than unburned plots (11.6 ± 2.3) at 3 years post-fire. Fire initially obliterated plant biomass reducing it from 50% ± 2.78 cover in unburned to nearly undetectable at 0.23% ± 0.09 in burned plots at 17 days post-fire (Table S2; Fig. 2E). Across three years, we observed 65 plant species from 47 unique genera across 19 plant families in burned and unburned plots with large changes in composition at 1- and 3-years post-fire with a notable loss of Cactaceae in burned plots (Fig. 2F). Several plants were first detected in burned plots 1-year post-fire, mainly comprised of native annual and perennial grasses and herbs with only one non-native plant *Erodium cicutarium*, which had minimal cover (Table S3).

Fire impact on soil*:* There were significant effects of fire, time, and fire by time interactions on pH such that fire significantly increased soil pH in burned plots overall and at each time point individually except 8 months (Table S4, Fig. S2A). Fire did not significantly affect phosphate but time did, such that overall mean phosphate decreased from 17-days to 8-months and increased from 8-months to 3-years post-fire across burned and unburned plots (Table S4, Fig. S2B). Fire did not have a significant direct effect on ammonium but time did such that ammonium decreased across time in burned and unburned plots (Table S4, Fig. S2C). There was also a significant fire by time interaction such that ammonium was greater in burned than unburned plots at 8-months and 3-years post-fire (Table S4). Both time and its interaction with fire had significant effects on nitrate and nitrite such that they increased over time but nitrate and nitrite were higher in burned than unburned plots at 3-years post-fire (Table S4, Fig. 2D). Because plots across our two treatments were spatially clustered, we tested models with an exponential spatial correlation for geography and found that phosphate showed spatial autocorrelation at 3 years, but was instead significantly increased by fire at 8-months. Similarly, pH differed between models, with the 1-year comparison showing significant differences between burned and unburned plots when considering spatial distance instead of the nestedness of plot.

Fire impacts on microbial richness and biomass*:* We generated 18,338,870 ITS2 and 14,963,273 16S reads across two libraries. After quality filtering and assigning taxonomy, we had 269 archaeal, 25,444 bacterial, and 6,683 fungal ASVs across our 172

samples from 5 timepoints across 3 years. Fire did not have a direct effect on richness of bacteria, fungi, archaea or AMF (Table S6, Fig. 3). Furthermore, soil burn severity also did not significantly correlate with richness of fungi (Table S6, Fig. S3) or bacteria (Table S6, Fig. S4) any timepoint. However, there were significant time by fire interactions such that burned plots showed greater bacterial richness at 3-years (Table S6, Fig. 3A), and AMF richness at 8-months and 3-years (Table S6, Fig. 3D) relative to unburned plots (Table S6). Fire also did not have a significant direct effect on 16S or 18S copy number (Table S7). However, there was a significant fire by time interaction such that burned relative to unburned plots had higher copy numbers of 16S at 3 years (Table S6, Fig. 3E) and 18S at 1 year (Table S7, Fig. 3F), although the effect at 1 year may be due to spatial autocorrelation (Table S8). Finally, there was a significant effect of time on both 16S and 18S such that across burned and unburned plots, bacterial biomass decreased from 1 month to 1-year post-fire but increased at 3 years and fungal biomass decreased at 3 years (Table S7). Precipitation was not a better predictor of bacterial richness or biomass compared to time alone (Table S9), however precipitation in the last 90 days was a better predictor of fungal biomass but not richness when compared to time and soil moisture (Table S10).

Fire and time impacts on community composition*:* Fire had small but significant impacts on fungal and bacterial community composition at all 5 time points and on archaeal composition at 8 months and 3 years (Table S11). Community heterogeneity (beta-dispersion) temporarily increased for archaea, bacteria, and fungi for up to 1-month,

but homogenized afterwards, such that burned plots became alike while remaining distinct from unburned plots (Table S11).

Drivers of microbial community composition over time and links to plants and soil properties*:* Char percentage was a significant driver of bacterial (Fig. 4A), archaeal (Fig. 4B), and fungal composition (Fig. 4C). Bacterial community dissimilarity was driven primarily by pH, followed by soil moisture, char percentage, nitrate and nitrite, and ammonium (Fig. 4D). Archaeal community dissimilarity was driven primarily by soil moisture, followed by pH, char percentage, and nitrate and nitrite. Fungal community dissimilarity was driven primarily by char percentage, followed by pH, and plant richness. While plant richness was a significant driver of fungal community composition, plant community composition did not correlate to shifts in archaeal ($r = 0.02$, $p = 0.42$), bacterial ($r = 0.03$, $p = 0.48$), or fungal ($r = 0.03$, $p = 0.33$) communities. Although plots across our two treatments were spatially clustered, we note that environmental signals do not appear to be artefacts of spatial autocorrelation for any timepoints except for 17-days in bacteria and archaea but not fungi (Table S12).

Impact of fire on specific prokaryotic taxa and emergence of pyrophilous microbes*:* Bacterial communities were dominated by the phyla Actinobacteriota, followed by Proteobacteria and Acidobacteriota (Fig. S5A). Actinobacteriota increased in burned plots at 1 month and 3 years, while Proteobacteria was consistently higher in burned plots, with a near 7% shift at 1-year (Fig. S5A). Bacteriodota and Firmicutes were more

abundant in unburned plots, whereas Acidobacteriota were more abundant in burned plots. Archaea (6-9% of 16S reads) were more abundant in burned plots (Fig. S5A) primarily represented by the Crenarchaeota genera *Candidatus Nitrocosmicus* and *Can. Nitrososphaera* (Fig. 5B). Cyanobacteria were more abundant in unburned plots during the first month post-fire with *Tychonema* dominating abundance (Fig. S5B). The most abundant genera in burned and unburned plots alike were *Rubrobacter* (Actinobacteriota*)*, *RB41* (Acidobacteriota), and *Can. Nitrososphaera* (Crenarchaeota) (Fig. S5B).

There were 2 archaeal and 17 bacterial genera that responded positively to fire including known pyrophilous microbes like *Massilia* and *Noviherbaspirillum*, with 1 ASV at 17-days, 2 at 8-months, 9 at 1-year, and 7 at 3-years post-fire (Fig. 5A; Table S13). The phyla with the most ASVs showing increased differential log2fold abundance in burned relative to unburned plots were Actinobacteriota with 12 ASVs, Proteobacteriota with 7 ASVs, and Firmicutes with 4 ASVs despite the overall lower relative abundance of the phylum Firmicutes in burned plots. Most bacterial ASVs showing positive differential log2fold abundance in burned plots were undetectable in unburned plots at that same timepoint (Fig. 5A). In contrast, only 7 ASVs from 5 genera negatively responded to fire (Table S14).

Impact of fire on specific fungal taxa and emergence of pyrophilous microbes: Fungi were dominated by phylum Ascomycota, ranging from 81-88% of reads in burned plots and 84-94% of reads in unburned plots (Fig. S6A). Basidiomycota were slightly more abundant (9-16%) in burned than in unburned plots (5-14%; Fig. S6A).

Basidiomycota were dominated by the mushroom-forming genera Lepiota, Montagnea, Disciceda, and Geastrum, and the basidiomycete yeast Naganishia (Fig. S6B). The overall most abundant fungal genus in both burned and unburned plots was Alternaria (Fig. S6B). Glomeromycotina composed < 1% of the reads, except for 3-years post-fire where they in relative abundance in burned plots (Fig. S7). There were 88 fungal genera that responded positively to fire including established pyrophilous taxa Naganishia, Coniochaeta, and Aspergillus and 21 ASVs at 17-days, 12 ASVs at 1-month, 13 ASVs at 8-months, 24 ASVs at 1-year, and 49 ASVs at 3-years (Fig. 5B; Table S15). The fungal classes with the most ASVs showing positive log2fold differential abundance in burned relative to unburned plots were Dothideomycetes (23 ASVs), Sordariomycetes (21 ASVs) and Eurotiomycetes (13 ASVs) within Ascomycota and Tremellomycetes (7 ASVs) and Agaricomycetes (4 ASVs) within Basidiomycota. In contrast, only 42 ASVs from 18 genera negatively responded to fire (Table S15).

3.5 Discussion

Here, we present the first comprehensive examination of direct and indirect effects of a large desert wildfire on above and belowground communities including the iconic *Y. jaegeriana*, surrounding desert plants, Archaea, Bacteria, and Fungi. Despite ~80% *Y. jaegeriana* mortality, archaeal, bacterial and fungal biomass and richness were highly resistant to wildfire at all time points ranging from 2 weeks to 3 years post-fire. Interestingly, by 3 years post-fire, AMF and bacterial richness and 16S biomass were

elevated in burned relative to unburned plots. There were minor but significant impacts of fire on microbiome composition that persisted across the 3 years across the 3 domains, leading to the emergence of several pyrophilous microbes typically seen after high severity wildfires in shrublands and forests such as *Massilia* and *Noviherbaspirillum* for bacteria and *Penicillium, Coniochaeta,* and *Naganishia* for fungi. Microbial communities were explained by various environmental factors including char percentage, but only fungal composition could be linked to plant richness. Together, these findings reveal high resistance and resilience in microbial richness and biomass but small fire-induced shifts in community composition reflecting domain-specific environmental drivers and links between plant and fungal community dynamics.

Dome Fire impacts on plants*:* The Dome Fire led to persistent and widespread mortality of *Y. jaegeriana*, which did not recover but rather became surrounded by herbs, forbs, and grasses. Similar patterns have been documented in the Mojave, with little recovery of some plant communities to unburned plant species composition after decades (Abella 2009) and in some cases, turnover into new and persistent community types (Abella et al. 2021). *Yucca jaegeriana* mortality was severe, increasing from 14% to 80% over the three-year span, similar to findings for *Y. brevifolia* (DeFalco et al. 2010). The delayed mortality of this species emphasizes the long-term vulnerability of Mojave plant communities to additional stressors such as post-fire drought (DeFalco et al. 2010). Annual plant community dynamics in deserts are influenced by the amount and timing of precipitation, including the abundance of exotic annual grasses that fluctuates year-to-

year (Brooks and Berry 2006), and post-fire plant communities are no exception. At 1-year post-fire, the rise in plant richness was driven by an abundance of annual grasses. While small patches of exotic grasses such as *Bromus madritensis* at 17-days post-fire and *Erodium cicutarium* at 1-year post-fire were present, native annual herbs and grasses led to increased plant richness in burned plots at 1-year. However, most annual herbs were ephemeral in their site occupancy, not persisting to 3-years post-fire, leading to the reestablishment of native perennial herbs, grasses, and shrubs and reduced plant richness in burned compared to unburned plots at 3 years post-fire. While deserts are vulnerable to exotic grasses increasing wildfire risks, *Bromus madritensis* was the only exotic annual grass present in unburned plots in 2020. Unburned plots saw an increase in perennial rather than annual grasses, and these similarly reduced in cover by 3-years. While shrubs are essential resource islands for water and nutrients in deserts (Titus et al. 2002a), it remains unclear whether the reemergence of shrubs as the dominant cover in burned plots will drive convergence between burned and unburned plant communities.

Dome Fire impacts on plant associated fungi and AMF: While there were no direct effects of fire on AMF richness, changes in plant richness and composition were correlated with both AMF richness and overall fungal composition. In contrast to a different desert wildfire in Mexico, where AMF richness declined after fire (Chimal-Sanchez 2015), here, AMF richness increased over time in burned relative to unburned plots, with increased pH as a result of the burn potentially driving AMF community changes as it does globally (Davison et al. 2021). The abundance of AMF spores are

heavily reduced in interspaces between Mojave plants (Titus et al. 2002a) so dominance of DSEs like *Alternaria* in these regions is expected, especially with the region's history of cheatgrass invasion which increases colonization of DSEs (Gehring et al. 2016). Plant richness had a strong effect on overall fungal community composition, as one burned plot (#3), consistently ranked higher in plant species richness (Fig. S1) and showed much greater fungal community dissimilarity to other burned samples. This clustering effect was not present in bacterial or archaeal communities (Fig. 4).

Dome Fire impacts on soil chemical properties*:* Fire led to increased soil pH and inorganic nitrogen, aligning with established post-fire trends (Agbeshie et al. 2022). Ash deposition drove soil pH to become more basic in burned plots at nearly all timepoints, despite an ash depth of only <1cm compared to much higher soil burn severity of chaparral shrublands consisting of ~12 cm ash (Pulido-Chavez et al. 2023). Similar to the chaparral shrublands that burned at higher soil burn severity (Pulido-Chavez 2023), ammonium was elevated in burned compared to unburned plots at both 8 months and 3 years post-fire, whereas nitrate and nitrite levels were comparable in burned and unburned plots until year 3, when they became elevated in burned compared to unburned plots. Ammonium, which volatilizes in much greater amounts compared to nitrate and nitrite (Benedict et al. 2017), appears to have evenly deposited on burned and unburned plots, yet was depleted in unburned plots over the years, potentially through AMF more readily transferring it to plants (Meng et al. 2015). Meanwhile, heavy rainfall spurring microbial activity may have driven oxidization of this excess ammonium to nitrate in

burned plots at 3-years post-fire (Wang et al. 2020), resulting in several high readings of nitrate and nitrite in burned plots (Fig. S2D). While phosphate only ephemerally increases post-fire (Neary et al. 1999), it exhibited an ephemeral drop at 8 months and a rise at 3-years post-fire due to several outlier samples, potentially in line with nitrates and nitrites similarly showing "hotspots" of activity (Barnes et al. 2024). These trends were largely the same when accounting for spatial correlations between samples, with a stronger effect of burn increasing phosphate at 3 years and pH at 1 year, while the effect of burn on nitrate and nitrite was weaker at 3 years post-fire.

Dome Fire impacts on microbial richness*:* Soil microbial richness was highly resistant to the Dome Fire for all three kingdoms. Low-intensity fires typically have subtle effects on microbes, impacting community connectivity and ecosystem services rather than richness (Aanderud et al. 2019; Soria et al. 2023; Vega-Cofre et al. 2023). Mojave National Preserve becomes primed for fire when high cool- and warm-season precipitation years are followed by a dry warm-season. These rainfall pulses and droughts also drive microbial dormancy and activation (Wang et al. 2014), consistent with our overall increase in biomass at year 3. However, an immediate post-fire dampening of species richness was not seen unlike high-intensity fires in shrublands and boreal systems (Holden et al. 2016; Pulido-Chavez et al. 2023). Frequent low-severity fires can increase soil C and N, and this abundant substrate correlates with slightly increased bacterial richness in grasslands 1-2 months post-fire (Glassman et al. 2023), prairies sampled 1-month after fire (Mino et al. 2021) and pine forests sampled 1-2 years after fire (Fox et al.

2024). In our case, bacterial richness was resistant in burned plots while unburned plots continued to drop at 3-years post-fire. Studies applying controlled burns to deserts varied from a similarly resistant bacterial community (Vega-Cofre et al. 2023) to a poorly resistant but highly resilient biocrust community (Aanderud et al. 2019). Archaeal richness did not differ post-fire, consistent with their greater resistance to fire even when fungal and bacterial richness decrease (Pérez-Valera et al. 2018). Fungal richness in drought-stricken grasslands showed greater resilience to fire than non-drought burned plots (Hacopian et al. 2024), suggesting that deserts, which have lower precipitation than grasslands, may also filter for highly resilient fungi. AMF richness was also greater in burned plots at 8-months and 3-years, decoupled from trends like plant richness and precipitation, perhaps due to fine-scale edaphic properties or plant dynamics not captured by our study. While no recent studies have comprehensively examined microbial richness after a desert wildfire, our results are aligned with low-intensity fires (Vega-Cofre et al. 2023; Glassman et al. 2023; Zhang et al. 2025) in which bacterial and fungal richness rarely shifts post-fire.

Dome Fire impacts on microbial biomass: Microbial biomass was resistant to fire, which is in line with biomass impacts of low intensity grassland and prescribed fires (Docherty et al. 2012; Pressler et al. 2019). Interestingly, archaeal and bacterial biomass increased in both plots by 3 years, after the influx of rain from tropical storm Hilary, but the abundant inorganic N may have contributed to the greater rise in burned compared to unburned plots. Prior to this rainfall, 16S copy numbers were in line with qPCR-based

biomass estimates in desert biocrusts (Aanderud et al. 2019). Fungal biomass did not follow this pulse trend, rather it saw an increase in burned plots at 1-year post-fire potentially reacting to the widespread invasion of native annual and perennial herbs, a trend seen in other grasslands (Hennecke et al. 2025). AMF also show increases in spore abundance following some wildfires (Moura et al. 2022), reflecting a need for dormancy until vegetation recovers.

Direct versus indirect effects of Dome Fire on microbial composition*:* Fire had direct heat induced mortality effects on microbial community composition for all 3 kingdoms, and effects of fire were persistent with burned versus unburned microbial communities significantly differing for archaea for two and for bacteria and fungi at all timepoints. The limited archaeal response may be due to their lipid membrane structure and thick cell walls (Pérez-Valera et al. 2018). Archaeal and fungal communities appeared to trend towards divergence between burned and unburned rather than becoming more similar over the 3-year study, while the bacterial R^2 did not seem to increase over time (Table S11). These divergences may be a result of fire increasing heterogeneity through pyrodiversity (Hopkins et al. 2025), which is reflected in differences in burned plot plant richness (Fig. S1). However, R^2 values remained relatively small, consistent with grassland fires (Dove and Hart 2017; Semenova-Nelsen et al. 2019) and much smaller than high-severity wildfires in forests and shrublands (Enright et al. 2022; Pulido-Chavez et al. 2023).

Drivers of microbial community composition were largely consistent with established global trends across differing kingdoms. Bacterial community composition was driven primarily by pH ($R^2 = 0.38$) and soil moisture ($R^2 = 0.29$), consistent with their overall resiliency to disturbance in dryland communities (Steven et al. 2021), well-known structuring by pH (Fierer and Jackson 2006) and rapid response to precipitation in drylands (Placella et al. 2012; Blazewicz et al. 2014). Bacteria and archaea often show distinct community structuring, with one study showing nitrate driving bacterial but not archaeal communities (Johnson et al. 2017), inverse to our trend of nitrate correlating with both bacterial and archaeal communities while ammonium only linked to bacterial communities. Archaeal communities are often shaped by ammonium availability due to their activity as nitrifiers, oxidizing ammonium into nitrite during nitrification (Angel et al. 2010).

Fungal communities showed weaker correlations to environmental variables, driven by percent char ($R^2 = 0.16$) followed by pH ($R^2 = 0.09$) and plant richness ($R^2 = 0.09$), which was a significant driver of fungal composition but not bacterial or archaeal. The significant influence of plant richness on fungal communities was consistent with studies in temperate grasslands (Prober et al. 2015; Chen et al. 2017) but contrary to studies in desert systems which show soil, climate, and geographic distance driving fungal community composition in the unburned context (Wang et al. 2018, 2021). Archaeal communities were more similar to bacteria, however the influence of soil moisture ($R^2 = 0.30$) was slightly stronger than pH ($R^2 = 0.27$). Studies of wetting desert soils show differential responses between domains, and although Archaea in general did

not strongly respond to water, *Can. Nitrososphaera* did increase in dominance within Archaea after wetting desert soil (Gao et al. 2021) and after a combined drying-wetting event (Wang et al. 2022b). However, precipitation (considered as total from prior 1-month or 3-month) alone did not result in better models for prokaryotic richness or biomass, suggesting further temporal dynamics beyond precipitation influencing prokaryotic communities. Meanwhile, soil moisture did not drive fungal community composition and yet fungal richness was best modeled by the 3-month sum of prior precipitation, likely reflecting fungal associations with the plant community. As bacterial and archaeal communities responded more directly to environmental conditions, fungal communities appeared to be impacted by the disappearance of the plants (i.e. char) followed by the resulting rise in plant richness in later years.

Impacts of Dome Fire on pyrophilous bacteria and archaea*:* Despite the relatively small changes in community composition, we identified a surprisingly high number of positive fire responding bacteria and archaea, including both known pyrophilous taxa and poorly described ASVs. More ASVs appeared to be selected for by the fire than suppressed (Table S11), potentially allowing drought-tolerant, metabolically versatile microbes to increase in abundance post-fire. This is consistent with trends in forests immediately post-fire, in which bacteria are predominantly responding positively to fire and gradually even out over the span of a decade (Caiafa et al. 2023). After severe fires in shrublands and forests, Firmicutes typically increase whereas Acidobacteriota decrease (Aponte et al. 2022). In contrast, here, Firmicutes decreased and Acidobacteriota

increased in overall relative abundance (Fig. S5A). The Firmicutes genus *Bacillus* had greater relative abundance in unburned plots at every timepoint (Fig. S5B), however other pyrophilous Firmicutes like *Tumebacillus* and *Paenibacillus* were more abundant in burned plots as they were after other fires (Chungopast et al. 2023; Pulido-Chavez et al. 2023), potentially reflecting more post-fire specialization in relation to the globally abundant *Bacillus* (Earl et al. 2008).

Other microbes responded according to their known metabolic activity. For example, nitrifier archaea like *Can. Nitrososphaera* and *Can. Nitrocosmicus* increased in burned plots, consistent with elevated ammonium (Tourna et al. 2011; Han et al. 2024), post-fire nitrogen pulses (Zhou et al. 2025), and their known drought tolerance (Stark and Firestone 1995). *Can. Nitrososphaera* oxidize ammonia into nitrite (Tourna et al. 2011), and are important keystone species in acidic soils for cycling N and aggregating soil (Jiang et al. 2015; Banerjee et al. 2018). We detected previously identified pyrophilous Proteobacteria including *Massilia* (Soria et al. 2023; Fernández-González et al. 2023; Caiafa et al. 2023) and *Noviherbasperillium* (Woolet and Whitman 2020; Pulido-Chavez et al. 2023). Their increase post-fire suggest conserved roles in post-fire soil recovery, even under the extreme drought and nutrient-limited conditions of the Mojave Desert. Bacteriodota members *Adhaeribacter* (Lucas-Borja et al. 2019) and *Segetibacter*, which we detected over 1-year post-fire, were positive fire responders associated with increased metabolic activity and total inorganic nitrogen in other burned soils as well (Adkins et al. 2022). *Pelobacter*, the only Acidobacteriota that increased at 8-months and 1-year, is an anaerobic fermenter, potentially appearing in microsites created by pockets of

hydrophobic burn products and compacted soil (Jiménez-Morillo et al. 2022). Several Actinobacteriota genera such as *Asanoa*, *Crossiella*, *Cellulomonas*, *Rubrobacter*, and *Solirubrobacter* likely benefit from similar shared traits that allow Actinobacteriota to increase in dominance post-fire (Whitman et al. 2019), such as thicker cell walls, a preference to higher pH, and a general stress tolerant physiology (Norman et al. 2017; Jiang et al. 2023). While we describe many taxa found increasing in other wildfire settings, several taxa remain unknown, highlighting the need for both trait-based and genomic investigations to understand post-fire succession in the desert.

Impact of Dome Fire on pyrophilous fungi*:* The desert mycobiome was dominated by Ascomycota, with a variety of genera from saprotrophic and endophytic classes such as Dothideomycetes, Eurotiomycetes, and Sordariomycetes showing positive responses to burn. However, unlike other wildfires, the Dome Fire caused an increase in the phylum Basidiomycota rather than a decrease (Fox et al. 2022; Pulido-Chavez et al. 2023), driven by mushroom-forming saprotrophic fungi such as *Geastrum* and *Lepiota*. *Alternaria,* a DSE saprobe and potential plant pathogen in the class Dothideomycetes (Thomma 2003), made up 5-19% of all fungal reads across our time series and was increased in burned plots at 8-months and 3-years (Fig. S8). Species in this genus may regulate their melanin content according to drought stress (Zuo et al. 2022), potentially increasing their fire resistance (Hopkins and Bennett 2024). Another Dothideomycete genus, *Preussia*, showed increased abundance in burned plots from 2-weeks to 3-years post-fire which has

been seen in controlled desert burns in China (Zhang et al. 2025). This genus forms hardy spores, which enhances their survival in drought conditions (Hacopian et al. 2024).

Despite small overall changes in community composition, a large number (143 ASVs) of fungal taxa showed positive log2fold increases in burned relative to unburned plots. Typically, negative responders match in magnitude (Revillini et al. 2022; Caiafa et al. 2023), however we only detected 33 fungal ASVs decreasing in burned plots, potentially due to adaptations for surviving in the arid desert pre-fire. *Penicillium*, a positive burn responder, is often dominant in both burned and unburned soils post-fire, and its role as a saprotroph makes it a key post-fire fungus that remains dominant in burned soil long-term, from 1 to 5 years post-fire (Whitman et al. 2019, 2025). *Penicillium* harbor a variety of genes for degrading hydrocarbons (Sari et al. 2025), and some species exhibit thermotolerance (van der Spuy 1975). We identified four yeasts, one basidiomycete desert-dweller *Naganishia* (Prober et al. 2015; Wei et al. 2022; Canini et al. 2023; Lopez et al. 2024), and three ascomycetes *Saitoella, Coniochaeta,* and *Aureobasidium*, which showed positive differential abundance at 3-years in our study and in forest fires (Packard et al. 2023). Notably, *Naganishia* was more abundant in burned plots even 10 years after forest fires (Caiafa et al. 2023). Other yeast-like fungi were common extremophiles such as *Neophaeococcomyces* (Kurbessoian et al. 2024) and *Knufia* (Isola et al. 2022) potentially aided in post-fire survival by their thermotolerance.

Through sequencing, we identified many fungi that are known to produce ascocarps post-fire. Consistent with our prediction, we saw an increase from members of Pyronemataceae such as *Pseudotricharina*, *Scutellinia*, and *Spooneromyces*, which are

commonly found fruiting after high severity wildfires (Fox et al. 2022). *Neurospora discreta*, known for its heat-activated spores (Goddard 1935), was observed growing abundantly on burned *Y. jaegeriana* bark but not *Y. schidigera* or *Y. baccata*. However, soil sequencing only identified aconidial species like *N. terricola*, highlighting different lifestyles in closely related species inhabiting the Mojave Desert.

3.6 Conclusion

We performed the most comprehensive study of above and belowground direct and indirect effects of a desert wildfire to date and found that microbial biomass and richness were highly resistant in the face of roughly 80% mortality of *Y. jaegeriana*. Although *Y. jaegeriana* mortality increased over time, there did not appear to be significant lag effects of microbes and in fact certain groups like bacteria and AMF increased rather than decreased in burned plots over time. The impacts on microbial communities were largely in line with low intensity grassland or prescribed fires, which suggests that the Dome Fire was a unique case in which microbial richness and biomass were largely resistant despite widespread death of long-lived perennial trees and shrubs. Finally, surprisingly, despite subtle changes in the overall community composition, we identified a large number of taxa that positively responded to fire, and some of these were consistent with pyrophilous taxa that respond to high severity wildfires in shrublands and forests like *Massilia* and *Noviherbasperillium* for bacteria, *Nitrososphaera* and *Nitrocosmicus* for archaea, and *Penicillium, Coniochaeta, Aureobasidium, Alternaria, Naganishia,* for fungi, and *Preussia,* which responded in other desert fires. This study

thus provides critical new insights into desert wildfire ecology, filling the significant knowledge gap by illustrating the significant resilience of desert microbes in response to a low intensity but high severity wildfire.

Acknowledgements: We thank Scott Heacox for assistance with plant measurements, and Dylan Enright, Elizah Stephens, Marcos Caiafa Sepulveda, and Esbeiry Cordova-Ortiz for field work assistance. We thank Debra Hughson and Drew Kaiser and the Mojave National Preserve for allowing us to sample. We thank Tasha La Doux and Jim Andre and Sweeney Granite Mountains Desert Research Center for allowing us to stay. Funding was provided by UC Riverside, The Shipley Skinner Conservation Science Award to AJ and SIG, and the United States Department of Agriculture (USDA)-NIFA Award #2022-67014-36675 to SIG.

3.6.1.1 Table 1.

Model-estimated mean and standard error of soil chemical properties. Values in bold are significantly greater between pairwise treatments per timepoint, based on generalized mixed effects models.

pH	Unburned	Burned	z-score	p value
Overall	7.05 ± 0.18	**7.56 ± 0.14**	3.13	0.001
17 Days	6.92 ± 0.06	**7.63 ± 0.1**	-3.1	0.006
8 Months	7.2 ± 0.12	7.58 ± 0.08	-1.89	0.09
1 Year	6.68 ±0.05	**7.46 ± 0.09**	-3.5	0.012
3 Years	7.04 ± 0.03	**7.49 ± 0.06**	-2.3	0.048
Phosphate	Unburned	Burned	z-score	p value
Overall	0.346 ± 0.1	0.46 ± 0.1	0.86	0.38
17 Days	0.47 ± 0.39	0.36 ± 0.07	-1.2	0.24
8 Months	0.09 ± 0.03	0.15 ± 0.04	-1.2	0.22
3 Years	0.62 ± 0.24	0.51 ± 0.14	0.33	0.74
Nitrite and Nitrate	Unburned	Burned	z-score	p value
Overall	0.137 ± 0.04	**0.324 ± 0.07**	2.38	0.018
17 Days	0.2 ± 0.09	0.32 ± 0.05	-1.4	0.16
8 Months	0.2 ± 0.01	0.24 ± 0.03	-0.71	0.47
3 Years	0.01 ± 0.01	**0.41 ± 0.23**	-2.1	0.04
Ammonium	Unburned	Burned	z-score	p value
Overall	0.3 ± 0.05	0.44 ± 0.05	1.6	0.11
17 Days	0.6 ± 0.1	0.6 ± 0.08	-0.043	0.96
8 Months	0.32 ± 0.06	**0.51 ± 0.06**	-2.15	0.03
3 Years	0.13 ± 0.02	**0.27 ± 0.03**	-3.3	0.001

3.7 Figures

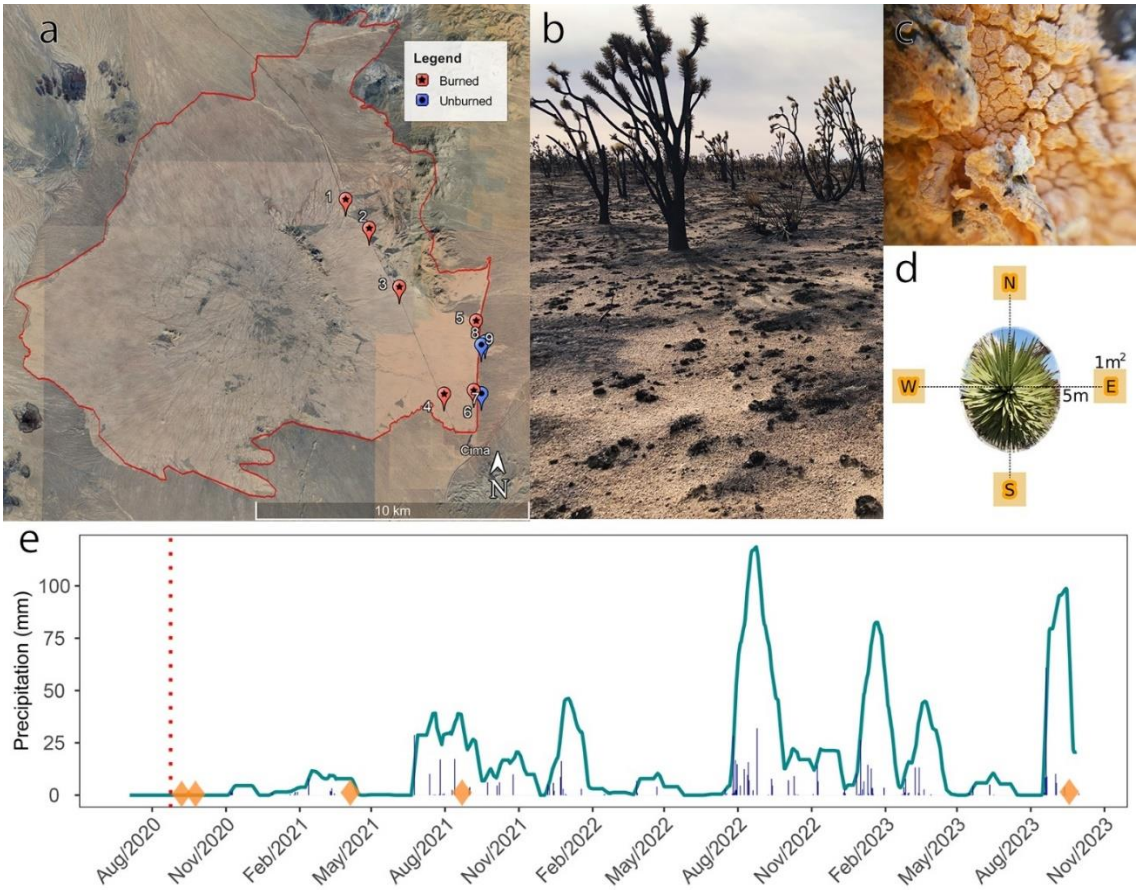

Figure 3.7.1 Cima Dome sampling schematic and precipitation. a) A map of our 9 plots, with the Dome Fire perimeter in red. Unburned plots (7-9) are east of the boundary on Morning Star Mine Rd. b) *Y. jaegeriana* and burnt soil in the Dome Fire burn scar 17 days after the end of the fire. c) *Neurospora discreta* growth on *Y. jaegeriana* bark at 8-months post-fire. d) A schematic demonstrating the 4 1m^2 subplots within the 9 plots. e) Precipitation at the Mojave Mid Hills station. Bars indicate recorded precipitation per month and the blue line indicates a rolling sum of the prior 4-months of precipitation. The red dash marks the Dome Fire, while orange diamonds indicate our 5 sampling dates from 17-days, 1-month, 8-months, 1-year and 3-years post-fire.

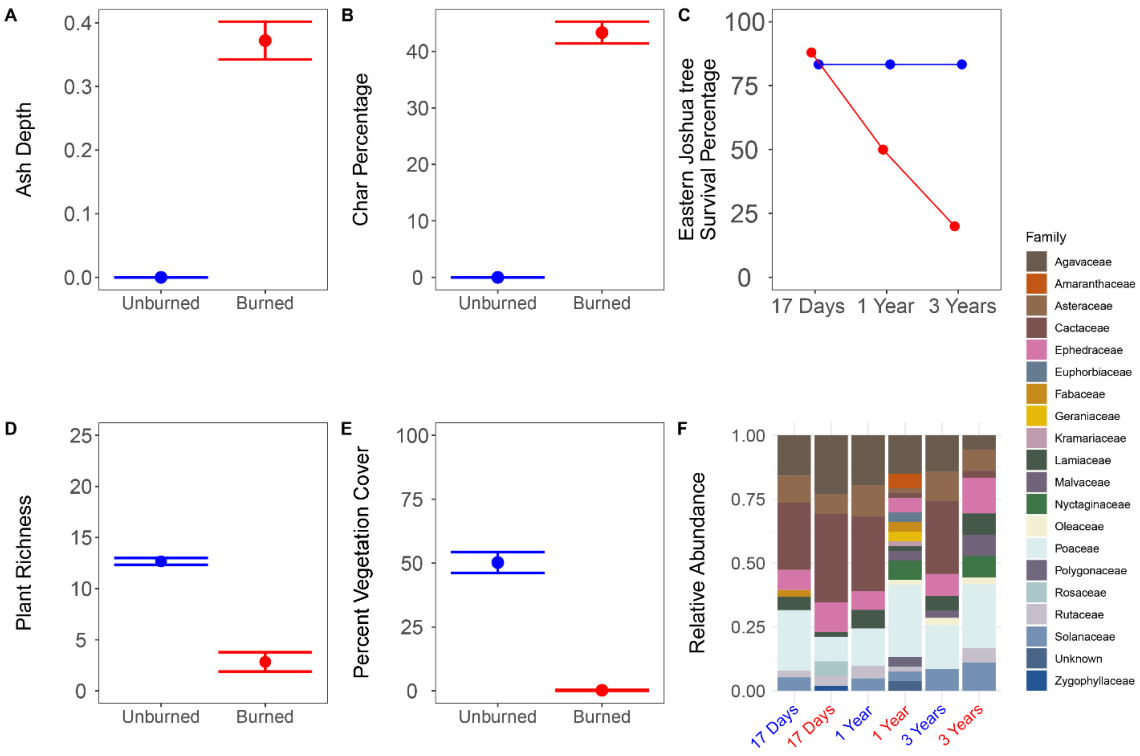

Figure 3.7.2 Plant responses to fire. Mean and standard error bars of: A) Soil burn severity via ash depth in cm. B) Char percentage on the soil surface measured for each subplot at 17-days post-fire. C) Percentage of *Y. jaegeriana* assessed as "living" in 6 burned plots and 3 unburned plots, including previously felled trees. Mean and standard error bars of: D) Plant species richness E) Percent cover of vegetation measured for burned versus unburned plots at 17-days post-fire. F) Plant family relative abundance across unburned (blue) and burned (red) plant families assessed post-fire at 17 days in September 2020, at 1 year in September 2021, and 3 years in September 2023.

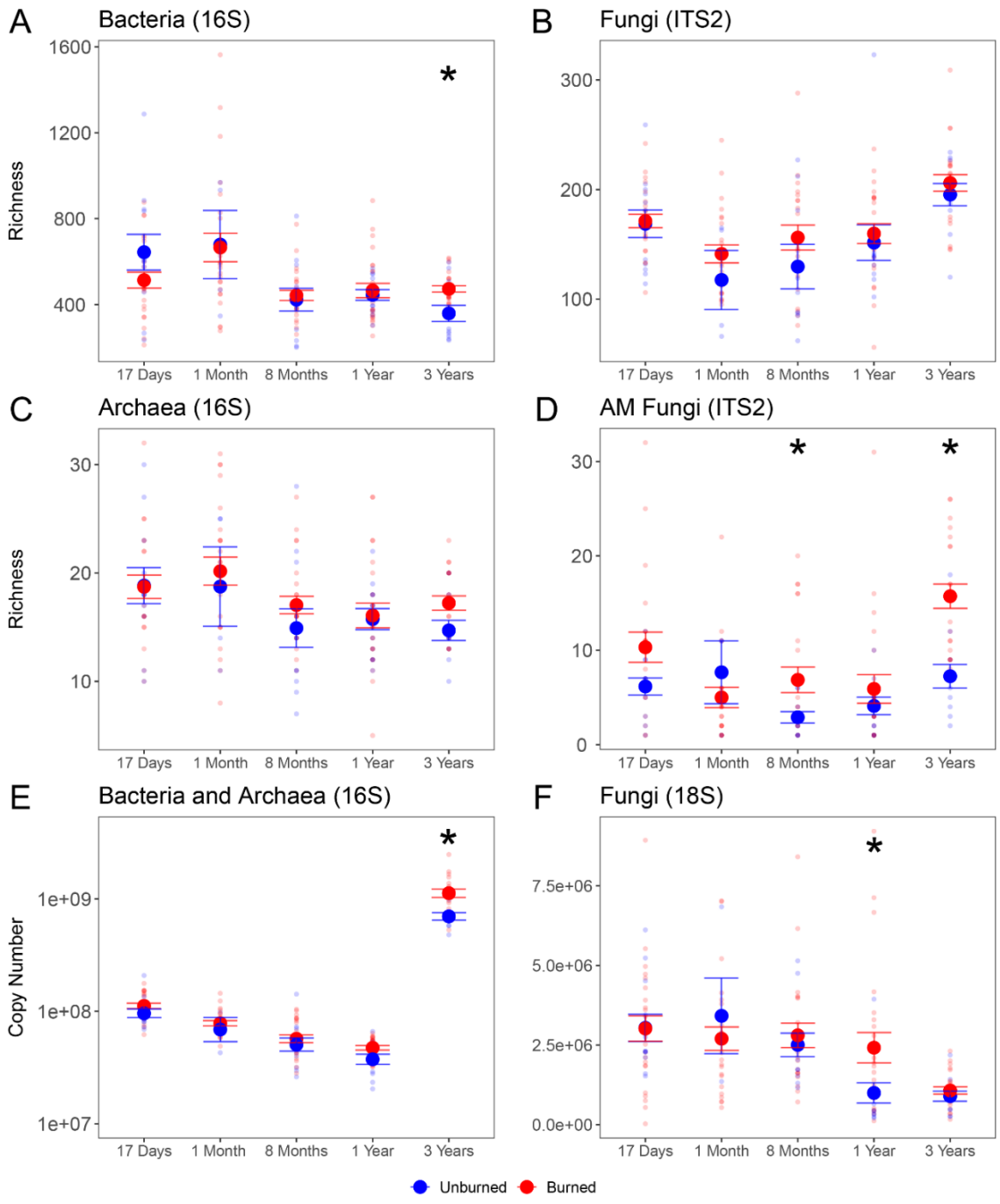

Figure 3.7.3 Microbial ASV richness and copy number. Mean ± standard error of richness and copy number in burned and unburned plots (red and blue, respectively) at each timepoint. Richness of bacteria, fungi, archaea, and arbuscular mycorrhizal fungi are represented by A,B,C, and D respectively. Bacterial and archaeal 16S and fungal 18S are represented by E and F, respectively. Asterisks indicate significant differences between means of burned and unburned plots at a given timepoint. Unburned plots at 1-month only have 4 total samples, causing high variance.

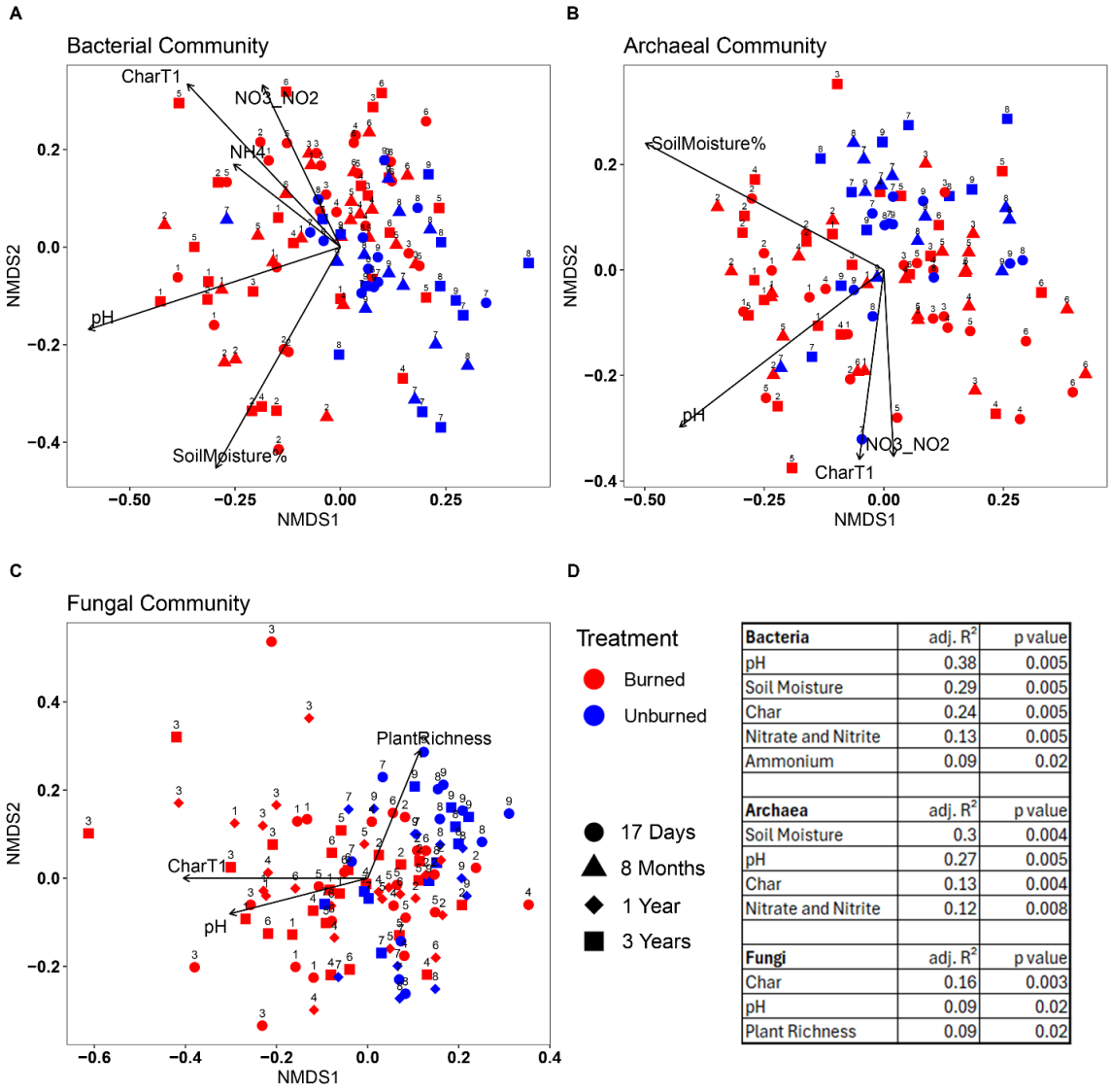

Bacteria	adj. R^2	p value
pH	0.38	0.005
Soil Moisture	0.29	0.005
Char	0.24	0.005
Nitrate and Nitrite	0.13	0.005
Ammonium	0.09	0.02
Archaea	adj. R^2	p value
Soil Moisture	0.3	0.004
pH	0.27	0.005
Char	0.13	0.004
Nitrate and Nitrite	0.12	0.008
Fungi	adj. R^2	p value
Char	0.16	0.003
pH	0.09	0.02
Plant Richness	0.09	0.02

Figure 3.7.4 Microbial community composition shifts. Bray-Curtis dissimilarity plotted by non-metric multidimensional scaling with environmental variables overlaid. CharT1 is the percent char of each subplot as measured at 17-days post-fire. NH4 is Ammonium, and NO3_NO2 is Nitrate and Nitrite. Arrow-length corresponds to the strength of each correlation, independent of the other factors. Bacterial (A) and archaeal (B) communities include samples from 17-days, 8-months, and 3-years post-fire. Fungal (C) communities include samples from 17-days, 1-year, and 3-years post-fire. Each point is labeled with the Plot number it was sampled from (Plot 1-6 are burned, Plot 7-9 are unburned). D) Significant variables ($p < 0.05$) and their adjusted R^2.

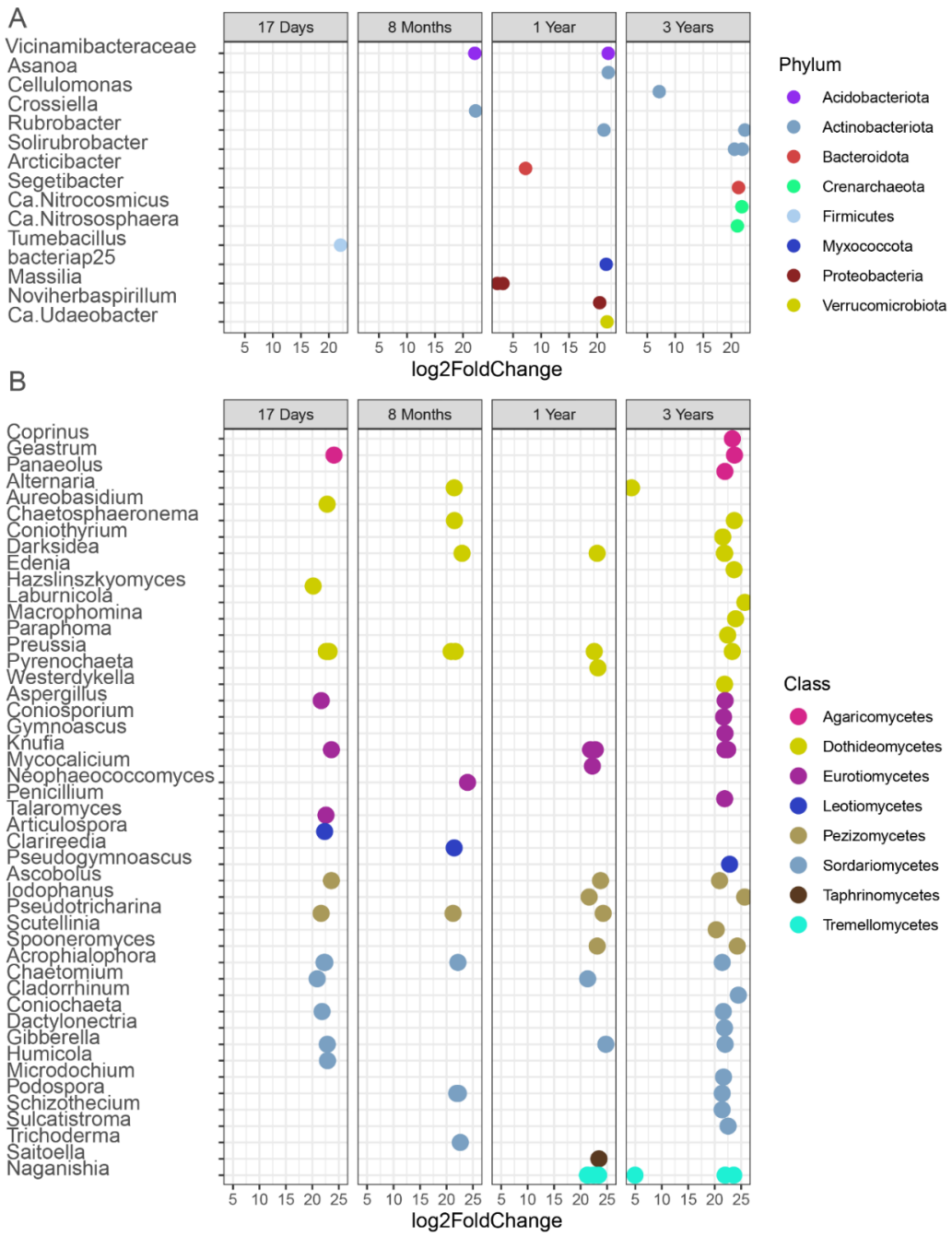

Figure 3.7.5 Pyrophilous microbes over 3 years. Microbial ASVs with increased differential abundance in burned plots at 4 timepoints, sorted by A) phylum for prokaryotes or B) class for fungi. Greater log2fold Change on the x-axis indicates more abundance in burned plots relative to unburned plots. A full list of archaeal, bacterial, and fungal ASVs, including ASVs responding negatively to fire, can be found in the supplemental materials.

3.8 Supplementary Materials

Table S1. PCR thermocycler settings. PCR 1 (initial amplification), PCR 2 (attaching index and barcodes), 16S qPCR (archaeal and bacterial biomass estimation) and FungiQuant 18S qPCR (fungal biomass estimation) listed.

Category	Initial Denaturation	Cycles	Denaturation	Annealing	Extension	Final Extension
PCR1 (16S & ITS2)	94°C for 2 min	30	94°C for 20 sec	55°C for 20 sec	68°C for 1 min	68°C for 2 min
PCR2 (DIP Primers)	94°C for 2 min	10	94°C for 30 sec	60°C for 30 sec	72°C for 1 min	NA
16S qPCR	94°C for 5 min	40	94°C for 20 sec	52°C for 30 sec	72°C for 30 sec	NA
18S FungiQuant qPCR	94°C for 5 min	40	94°C for 20 sec	50°C for 30 sec	72°C for 30 sec	NA

Table S2. Pairwise ANOVA between burned and unburned plots of plant richness and ash cover at each timepoint.

	Plant Richness			**Ash Cover at 17 Days**		
	Pairwise ANOVA			Pairwise ANOVA		
	$F_{1,7}$	t value	p.value	$F_{1,34}$	t value	p.value
17 Days	**49.2**	**11.1**	**0.001**	**144**	**-12**	**8.9e-14**
1 Year	0.66	-0.8	0.44			
3 Years	**9.63**	**-3.1**	**0.02**			

Table S3. Plant species appearing in our 3 field surveys in September 2020, 2021, and 2023. Strata is represented by S = "shrub", T = "Tree", AH = "annual herb", PH = "perennial herb", H = "herb", AG = "annual grass", PG = "perennial grass". Status is either N = "native", N_R = "native, rare" or E = "exotic". First Appearance indicates the sampling year in which a plant species was first observed. The Burned Plot Only column indicates if a plant species was only detected in a burned plot, with orange cells labeled "YES" and green cells labeled "NO". Taxa not identified to genus or species are due to lack of identifiable material in the field.

Strata	Family	Scientific name	Status	First Found	Burned Plot Only
S	Asteraceae	*Ambrosia salsola*	N	2020	NO
AG	Poaceae	*Bromus madritensis*	E	2020	NO
S	Rosaceae	*Coleogyne ramosissima*	N	2020	YES
S	Cactaceae	*Coryphantha alversonii*	N_R	2020	NO
S	Cactaceae	*Cylindropuntia acanthacarpa*	N	2020	NO
S	Cactaceae	*Cylindropuntia echinocarpa*	N	2020	NO
S	Cactaceae	*Cylindropuntia ramosisima*	N	2020	NO
PG	Poaceae	*Dasyochloa pulchella*	N	2020	NO
S	Ephedraceae	*Ephedra viridis*	N	2020	NO
S	Asteraceae	*Ericameria linearifolia*	N	2020	NO
S	Asteraceae	*Gutierrezia microcephala*	N	2020	YES
PH	Poaceae	*Hilaria rigida*	N	2020	NO
S	Solanaceae	*Lycium cooperi*	N	2020	NO
S	Lamiaceae	*Scutellaria mexicana*	N	2020	NO
S	Fabaceae	*Senna armata*	N	2020	NO
PH	Poaceae	*Stipa speciosa*	N	2020	NO
PH	Poaceae	*Stipa hymenoides*	N	2020	NO
S	Rutaceae	*Thamnosma montanta*	N	2020	NO
T	Agavaceae	*Yucca baccata*	N	2020	NO
T	Agavaceae	*Yucca jaegeriana*	N	2020	NO
T	Agavaceae	*Yucca schidigera*	N	2020	NO
S	Asteraceae	*Acamptopappus sphaerocephalus*	N	2021	NO
AH	Amaranthaceae	*Amaranthus fimbriatus*	N	2021	YES
PH	Fabaceae	*Astragalus sp.*	N	2021	YES
H	Nyctaginaceae	*Boerhavia sp.*	N	2021	YES

AG	Poaceae	*Bouteloua sp.*	N	2021	YES
AH	Polygonaceae	*Calyptridium monandrum*	N	2021	YES
S	Cactaceae	*Excobaria vivipara var. rosea*	N_R	2021	NO
S	Cactaceae	*Echinocereus engelmannii*	N	2021	NO
S	Cactaceae	*Echinocereus mojavensis*	N	2021	NO
S	Ephedraceae	*Ephedra nevadensis*	N	2021	NO
AH	Geraniaceae	*Erodium cicutarium*	E	2021	YES
AH	Euphorbiaceae	*Euphorbia albomarginata*	N	2021	YES
AH	Euphorbiaceae	*Euphorbia sp.*	N	2021	YES
S	Poaceae	*Hilaria jamesii*	N	2021	YES
S	Kramariaceae	*Krameria sp.*	N	2021	YES
S	Solanaceae	*Lycium andersonii*	N	2021	NO
S	Cactaceae	*Mammillaria tetrancistra*	N	2021	NO
S	Oleaceae	*Menodora spinescens*	N	2021	YES
PH	Nyctaginaceae	*Mirabilis laevis*	N	2021	YES
H	Asteraceae	*Pectis papposa*	N	2021	YES
AH	Poaceae	*Poaceae sp. (Annual)*	N	2021	YES
H	Malvaceae	*Sphaeralcea ambigua*	N	2021	YES
PH	Malvaceae	*Sphaeralcea sp.*	N	2021	YES
PH	Poaceae	*Stipa sp.*	N	2021	YES
AH	Unknown	*Annual herb/forb sp.*	N	2021	YES
S	Asteraceae	*Ambrosia dumosa*	N	2023	NO
AG	Poaceae	*Aristida purpurea*	N	2023	YES
PG	Poaceae	*Bouteloua eriopoda*	N	2023	YES
S	Asteraceae	*Ericameria cooperi*	N	2023	NO
PH	Nyctaginaceae	*Mirabilis multiflora*	N	2023	YES
S	Poaceae	*Muhlenbergia porteri*	N	2023	NO
PH	Malvaceae	*Sphaeralcea rusbyi var. eremicola*	N_R	2023	YES
PH	Poaceae	*Poaceae sp (Perennial)*	N	2023	NO

Table S4. Generalized mixed effect model statistics for soil chemical properties. Timepoints indicate comparisons across the unburned reference level. Time and fire interactions are listed below the overall treatment effect "Burned". Marginal R^2 reports model effect size after removing random effects.

	pH			**PO_4^{3-}**		
	Marginal R^2 =0.33			Marginal R^2 =0.29		
	estimate	z value	p.value	estimate	z value	p.value
(Intercept)	**1.93**	**87.30**	**<0.01**	**-1.91**	**-4.52**	**<0.01**
Burned	**0.10**	**3.54**	**0.01**	0.59	1.18	0.24
8 Months	**0.04**	**2.99**	**<0.01**	-0.56	-1.20	0.23
3 Years	0.02	1.32	0.19	**1.44**	**3.07**	**<0.01**
8 Months:Burned	**-0.04**	**-2.89**	**0.01**	-0.01	-0.02	0.99
3 Years:Burned	**-0.03**	**-2.19**	**0.03**	-0.75	-1.31	0.19

	NH_4^+			**NO_3^- and NO_2^-**		
	Marginal R^2 =0.61			Marginal R^2 =0.46		
	estimate	z value	p.value	estimate	z value	p.value
(Intercept)	**-0.51**	**-2.90**	**<0.01**	**-1.70**	**-2.33**	**0.0002**
Burned	0.01	0.04	0.97	1.29	1.40	0.36
8 Months	**-0.63**	**-4.72**	**<0.01**	0.47	0.85	0.99
3 Years	**-1.51**	**-11.26**	**<0.01**	**-6.63**	**-10.89**	**<0.001**
8 Months:Burned	**0.45**	**2.76**	**0.01**	-0.64	-0.94	0.69
3 Years:Burned	**0.70**	**4.29**	**<0.01**	**1.20**	**0.97**	**<0.001**

Table S5. Generalized least squares model statistics for edaphic soil properties when accounting for spatial autocorrelation through latitude and longitude instead of the random effect of Plot. Timepoints indicate comparisons to the unburned reference level. Rows are in bold when a significant difference is detected between the burned and unburned treatments. Timepoints where the significance of the effect varies between model types have an asterisk.

pH					
TimePoint	Treatment_Est	Treatment_SE	Treatment_p	Residual_SE	DF_residual
17 DAYS	**0.718**	**0.24**	**0.00514**	**0.389**	**34**
8 MONTHS	**0.409**	**0.196**	**0.0447**	**0.373**	**34**
1 YEAR*	**0.782**	**0.205**	**0.00056**	**0.386**	**34**
3 YEARS	**0.458**	**0.128**	**0.00104**	**0.226**	**34**
Nitrate and Nitrite					
TimePoint	Treatment_Est	Treatment_SE	Treatment_p	Residual_SE	DF_residual
17 DAYS	0.123	0.0959	0.208	0.264	34
8 MONTHS	0.0424	0.0439	0.341	0.107	34
3 YEARS*	0.401	0.328	0.23	0.901	34
Phosphate					
TimePoint	Treatment_Est	Treatment_SE	Treatment_p	Residual_SE	DF_residual
17 DAYS	-0.114	0.291	0.697	0.799	34
8 MONTHS*	**0.113**	**0.0535**	**0.0413**	**0.144**	**34**
3 YEARS	0.372	0.53	0.487	1.25	34
Ammonium					
TimePoint	Treatment_Est	Treatment_SE	Treatment_p	Residual_SE	DF_residual
17 DAYS	0.00938	0.107	0.931	0.294	34
8 MONTHS	**0.189**	**0.0527**	**0.00106**	**0.134**	**34**
3 YEARS	**0.155**	**0.0723**	**0.0392**	**0.135**	**34**

Table S6. Generalized mixed effect model statistics for ASV richness. Timepoints indicate comparisons across the unburned reference level. Time and fire interactions are listed below the overall treatment effect "Burned". Marginal R^2 reports model effect size after removing random effects.

	Bacteria			**Fungi**		
ASV Richness	Marginal R^2 = 0.176			Marginal R^2 = 0.194		
	estimate	z value	p.value	estimate	z value	p.value
(Intercept)	**6.37**	**54.83**	**<0.01**	**168.75**	**10.74**	**<0.01**
1 Month	0.11	0.55	0.59	-24.78	-1.01	0.32
8 Months	**-0.41**	**-3.02**	**0.003**	-33.56	-1.87	0.06
1 Year	**-0.29**	**-2.12**	**0.036**	-17.17	-1.04	0.30
3 Years	-0.54	-3.97	0.0001	24.21	1.43	0.16
Burned	-0.19	-1.34	0.19	2.50	0.13	0.90
1 Month:Burned	0.11	0.51	0.61	-5.22	-0.19	0.85
8 Months:Burned	0.29	1.77	0.08	18.62	0.86	0.39
1 Year:Burned	0.20	1.20	0.23	6.33	0.31	0.76
3 Years:Burned	**0.51**	**3.07**	**0.0025**	10.54	0.51	0.61

	Archaea			**AMF**		
ASV Richness	Marginal R^2 =0.11			Marginal R^2 = 0.31		
	estimate	z value	p.value	estimate	z value	p.value
(Intercept)	**2.92**	**28.38**	**<0.01**	**1.79**	**6.62**	**<0.01**
1 MONTH	0.06	0.41	0.69	0.38	0.80	0.43
8 MONTHS	**-0.23**	**-2.10**	**0.04**	**-0.71**	**-2.32**	**0.02**
1 Year	-0.17	-1.54	0.12	-0.34	-1.10	0.27
3 Years	**-0.26**	**-2.27**	**0.02**	0.16	0.56	0.58
Burned	-0.01	-0.04	0.96	0.45	1.33	0.18
1 Month:Burned	0.01	0.03	0.98	**-1.12**	**-2.15**	**0.03**
8 Months:Burned	0.14	1.04	0.30	0.26	0.69	0.49
1 Year:Burned	0.01	0.07	0.94	-0.27	-0.72	0.47
3 Years:Burned	0.17	1.23	0.22	0.44	1.22	0.22

Table S7. Generalized mixed effect model statistics for copy numbers of 16S and 18S. Timepoints indicate comparisons across the unburned reference level. Time and fire interactions are listed below the overall treatment effect "Burned". Marginal R^2 reports model effect size after removing random effects.

	Bacteria (16S)			**Fungi (18S FungiQuant)**		
Biomass (qPCR Copy Number)	Marginal R^2: 0.924			Marginal R^2: 0.353		
	estimate	z value	p value	estimate	z value	p value
(Intercept)	**18.38**	**155.77**	**<0.01**	**14.86**	**94.59**	**<0.01**
1 Month	-0.22	-1.09	0.28	0.18	0.36	0.72
8 Months	**-0.64**	**-5.32**	**<0.01**	-0.22	-1.19	0.23
1 Year	**-0.94**	**-7.81**	**<0.01**	**-1.12**	**-3.06**	**<0.01**
3 Years	**1.97**	**15.61**	**<0.01**	**-1.29**	**-3.05**	**<0.01**
Burned	0.15	1.06	0.30	-0.03	-0.15	0.88
1 Month:Burned	-0.14	-0.66	0.51	-0.39	-0.70	0.48
8 Months:Burned	-0.03	-0.21	0.83	0.16	0.73	0.46
1 Year:Burned	0.08	0.51	0.61	**0.86**	**2.18**	**0.03**
3 Years:Burned	**0.34**	**2.17**	**0.03**	0.14	0.28	0.78

Table S8. Generalized least squares model statistics for ASV richness and 16S or 18S copy number when accounting for spatial autocorrelation through latitude and longitude instead of the random effect of Plot. Timepoints indicate comparisons to the unburned reference level. Comparisons that differed from the GLMM are marked with an asterisk.

Bacteria richness					
TimePoint	Treatment_Est	Treatment_SE	Treatment_p	Residual_SE	DF_residual
17 Days	-136	103	0.196	218	34
1 Month	-13	193	0.947	314	26
8 Months	20.9	50.1	0.679	138	34
1 Year	20.5	50.6	0.688	139	34
3 Years	**114**	**55.3**	**0.0469**	**93.8**	**34**
16S qPCR					
TimePoint	Treatment_Est	Treatment_SE	Treatment_p	Residual_SE	DF_residual
17 Days	15236980	12730437	0.24	32204015	34
1 Month	7649136	14557212	0.604	22174754	24
8 Months	4882158	9367580	0.606	25539544	33
1 Year	9372118	4668323	0.0532	11040886	32
3 Years	**480954063**	**181625044**	**0.0136**	**371735480**	**26**
Fungal richness					
TimePoint	Treatment_Est	Treatment_SE	Treatment_p	Residual_SE	DF_residual
17 Days	3.35	13.2	0.802	34.1	34
1 Month	24.3	24.7	0.333	40.3	26
8 Months	25.2	25.8	0.338	53.6	28
1 Year	9.42	18.8	0.62	46.6	33
3 Years	11.4	13.8	0.414	35	33
FungiQuant qPCR					
TimePoint	Treatment_Est	Treatment_SE	Treatment_p	Residual_SE	DF_residual
17 Days	-20376	642586	0.975	1766301	34
1 Month	-767152	1588947	0.633	1811192	26
8 Months	224440	582982	0.703	1589612	33
1 Year*	1450993	764630	0.0663	1954367	34

3 Years	177524	194898	0.369	535724	34
Archaea Richness					
TimePoint	Treatment_Est	Treatment_SE	Treatment_p	Residual_SE	DF_residual
17 Days	-0.106	1.91	0.956	5.16	32
1 Month	1.53	4.33	0.727	6.21	26
8 Months	2.12	1.69	0.217	4.64	34
1 Year	0.337	1.73	0.847	4.73	33
3 Years	2.59	1.29	0.0529	2.97	30
AMF Richness					
TimePoint	Treatment_Est	Treatment_SE	Treatment_p	Residual_SE	DF_residual
17 Days	4.32	3.39	0.212	6.25	32
1 Month	-2.63	3.19	0.417	4.92	23
8 Months*	3.69	2.32	0.121	5.23	30
1 Year	1.76	2.66	0.513	5.91	30
3 Years	**8.45**	**2.64**	**0.00311**	**5.25**	**32**

Table S9. Bacterial model comparisons of time as categorical (TimePoint), numerical (Days Post-fire), and precipitation as a sum of 3-months prior, 1 month-prior, and soil moisture. Limiting timepoints to include plant richness did not improve model fidelity. Bolded models are the best fit as determined by comparison of Chi squared and AIC.

Model Comparison for Bacterial Biomass (qPCR) and Richness

Model	Biomass AIC	Biomass DeltaAIC	Biomass ChiSq	Biomass p	Richness AIC	Richness DeltaAIC	Richness ChiSq	Richness p
Null model	6450.5	0.0		NA	152.4	0.0		NA
Precip (3mo)	6332.5	118.0	67.54	<2.2e-16	145.1	7.3	11.31	0.0035
Precip (1mo)	6192.3	258.2	140.14	<2.2e-16	149.6	2.9	0	n.s.
Soil Moisture	6400.0	50.5	56.51	3.28e-12	142.9	9.6	8.7	0.0032
Days Post-fire	6227.6	222.9	0	1.00	144.1	8.3	0	n.s.
TimePoint	**5970.8**	**479.7**	**268.79**	**<2.2e-16**	**133.9**	**18.5**	**20.09**	**0.0027**

Table S10. Fungal model comparisons of time as categorical (TimePoint), numerical (Days Post-fire), and precipitation as a sum of 3-months prior, 1 month-prior, and soil moisture. Limiting timepoints to include plant richness did not improve model fidelity. Bolded models are the best fit out of the available model variables as determined by comparison of Chi squared and AIC.

Model Comparison for Fungal Biomass (qPCR) and Richness

Model	Biomass AIC	Biomass Delta AIC	Biomass ChiSq	Biomass p	Richness AIC	Richness Delta AIC	Richness ChiSq	Richness p
Null model	5329.0	0.0		NA	1732.5	0.0		NA
Precip (3mo)	**5292.5**	**36.5**	**31.73**	**<2e-16**	1723.1	9.4	0	n.s.
Precip (1mo)	5289.6	39.4	2.85	<2e-16	1708.3	24.2	14.74	n.s.
Soil Moisture	5324.2	4.8	10.75	0.013	1722.9	9.6	0	n.s.
Days Post-fire	5290.1	38.9	0	1.00	1710.9	21.6	0	n.s.
TimePoint	5290.9	38.1	11.14	0.084	**1707.6**	**24.9**	**27.32**	**0.0001**

Table S11. Community composition differences between burned and unburned plots in Archaea, Bacteria, and Fungi. PERMANOVA and Beta-dispersion are compared at each timepoint and shown in bold when significant. A significant PERMANOVA indicates differing centroid means and suggests differing community composition. A significant beta-dispersion indicates differing distance to centroid and suggests differing levels of heterogeneity. A combination of significant PERMANOVA and betadispersion suggests differing communities due to differences in both composition and heterogeneity.

Domain	Rarefaction Depth	Time	Burn R^2	PERM-ANOVA F	p-value	Betadisper F	p-value
Archaea	638	17 Days	0.058	1.97	0.065	2.84	0.10
		1 Month	0.062	1.74	0.101	**9.51**	**0.004**
		8 Months	**0.069**	**2.55**	**0.021**	3.18	0.083
		1-Year	0.05	1.78	0.072	4.05	0.052
		3-Years	**0.073**	**2.37**	**0.014**	1.57	0.2185
Bacteria	4256	17 Days	**0.056**	**2.01**	**0.001**	**9.06**	**0.004**
		1 Month	**0.052**	**1.42**	**0.032**	**11.95**	**0.0018**
		8 Months	**0.045**	**1.6**	**0.007**	0.49	0.48
		1-Year	**0.063**	**2.32**	**0.001**	3.44	0.072
		3-Years	**0.047**	**1.69**	**0.001**	2.51	0.12
Fungi	6874	17 Days	**0.068**	**2.48**	**0.001**	**12.09**	**0.0014**
		1 Month	**0.059**	**1.65**	**0.003**	**18.76**	**0.00019**
		8 Months	**0.071**	**2.32**	**0.001**	0.89	0.35
		1-Year	**0.063**	**2.24**	**0.001**	3.62	0.065
		3-Years	**0.085**	**3.07**	**0.001**	0.41	0.52

Table S12. Community composition variation partitioning using the environmental variables. Data matches timepoints used in Figure 4, and a distance matrix of sample latitude and longitude, with values indicating the fractions of the effect attributed to environmental variables [a], space [c], overlapping effects [b], and the residual unexplained proportion [d].

Bacteria		**Fraction**	**17 Days**	**8 Months**	**3 Years**
[a]	X1|X2	Pure Environment	-0.024	0.133	0.077
[c]		Pure Space	0.251	0.091	0.123
[b]	X2|X1	Shared (Env ∩ Space)	0.044	0.061	0.042
[d]	Residuals	Unexplained	0.729	0.715	0.758
Archaea		**Fraction**	**17 Days**	**8 Months**	**3 Years**
[a]	X1|X2	Pure Environment	-0.061	0.068	0.081
[c]		Pure Space	0.183	0.086	-0.024
[b]	X2|X1	Shared (Env ∩ Space)	0	0.04	-0.025
[d]	Residuals	Unexplained	0.879	0.806	0.968
Fungi		**Fraction**	**17 Days**	**1 Year**	**3 Years**
[a]	X1|X2	Pure Environment	0.031	0.1	0.065
[c]		Pure Space	0.208	0.278	0.145
[b]	X2|X1	Shared (Env ∩ Space)	0.099	0.081	0.034
[d]	Residuals	Unexplained	0.662	0.54	0.756

Table S13. Prokaryotic genera showing positive differential abundance in burned plots (increase).

log2Fold Change	padj	Kingdom	Phylum	Genus	Species	Timepoint
22.08	2E-11	Bacteria	Firmicutes	Tumebacillus	NA	17 Days
22.24	3E-11	Bacteria	Actinobacteriota	Crossiella	uncultured bacterium	8 Months
22.10	1E-09	Bacteria	Acidobacteriota	Vicinamibacteraceae	NA	8 Months
22.45	2E-20	Bacteria	Actinobacteriota	NA	NA	1 Year
22.00	1E-12	Bacteria	Proteobacteria	NA	NA	1 Year
21.99	1E-12	Bacteria	Actinobacteriota	Asanoa	NA	1 Year
21.97	1E-12	Bacteria	Acidobacteriota	Vicinamibacteraceae	NA	1 Year
21.96	2E-10	Bacteria	Proteobacteria	NA	NA	1 Year
21.76	1E-12	Bacteria	Verrucomicrobiota	Candidatus Udaeobacter	NA	1 Year
21.61	4E-10	Bacteria	Myxococcota	bacteriap25	NA	1 Year
21.58	4E-10	Bacteria	Acidobacteriota	uncultured	uncultured bacterium	1 Year
21.38	5E-10	Bacteria	Proteobacteria	NA	NA	1 Year
21.20	7E-10	Bacteria	Actinobacteriota	Rubrobacter	uncultured actinobacterium	1 Year
20.84	2E-09	Bacteria	Proteobacteria	NA	NA	1 Year
20.45	3E-09	Bacteria	Proteobacteria	Noviherbaspirillum	NA	1 Year
7.23	5E-05	Bacteria	Bacteroidota	Arcticibacter	uncultured bacterium	1 Year
4.34	3E-05	Bacteria	Firmicutes	NA	NA	1 Year
3.18	3E-03	Bacteria	Proteobacteria	Massilia	NA	1 Year
2.19	2E-08	Bacteria	Proteobacteria	Massilia	NA	1 Year
22.42	7E-15	Bacteria	Actinobacteriota	Rubrobacter	uncultured Rubrobacter	3 Years
21.97	1E-09	Bacteria	Actinobacteriota	Solirubrobacter	NA	3 Years
21.88	2E-11	Archaea	Crenarchaeota	Candidatus Nitrocosmicus	NA	3 Years
21.34	3E-09	Bacteria	Firmicutes	NA	NA	3 Years
21.29	3E-09	Bacteria	Bacteroidota	Segetibacter	NA	3 Years
21.09	5E-09	Archaea	Crenarchaeota	Candidatus Nitrososphaera	NA	3 Years
20.57	1E-08	Bacteria	Actinobacteriota	Solirubrobacter	NA	3 Years
7.15	2E-04	Bacteria	Actinobacteriota	Cellulomonas	NA	3 Years

Table S14. Prokaryotic genera showing negative differential abundance in burned plots (decrease).

log2Fold Change	padj	Kingdom	Phylum	Genus	Species	Timepoint
-22.95	2E-10	Bacteria	Actinobacteriota	Gaiella	NA	17 Days
-22.95	2E-10	Bacteria	Actinobacteriota	uncultured	uncultured bacterium	17 Days
-23.40	5E-11	Bacteria	Myxococcota	bacteriap25	metagenome	8 Months
-23.54	5E-11	Bacteria	Actinobacteriota	NA	NA	8 Months
-24.24	1E-12	Bacteria	Cyanobacteria	uncultured	Scytonema hyalinum	1 Year
-24.66	6E-13	Bacteria	Actinobacteriota	Rubrobacter	uncultured Rubrobacter	1 Year
-24.47	3E-12	Bacteria	Firmicutes	Psychrobacillus	NA	3 Years

Table S15. Fungal genera showing positive differential abundance in burned plots (increase).

log2Fold Change	padj	Kingdom	Phylum	Genus	Species	Timepoint
24.12	4E-13	Fungi	Ascomycota	Pezizaceae inc. sed.	Pezizaceae sp	17 Days
24.09	4E-13	Fungi	Basidiomycota	Geastrum	Geastrum sp	17 Days
23.68	2E-25	Fungi	Ascomycota	NA	NA	17 Days
23.59	4E-13	Fungi	Ascomycota	Knufia	NA	17 Days
23.59	1E-12	Fungi	Ascomycota	Ascobolus	NA	17 Days
23.17	1E-23	Fungi	Ascomycota	Preussia	Preussia fleischhakii	17 Days
22.86	5E-12	Fungi	Ascomycota	Humicola	NA	17 Days
22.82	1E-16	Fungi	Ascomycota	Gibberella	Gibberella avenacea	17 Days
22.79	9E-21	Fungi	Ascomycota	Aureobasidium	NA	17 Days
22.63	8E-12	Fungi	Ascomycota	Preussia	Preussia sp	17 Days
22.58	8E-12	Fungi	Ascomycota	Talaromyces	NA	17 Days
22.38	1E-11	Fungi	Ascomycota	Acrophialophora	Acrophialophora sp	17 Days
22.33	3E-17	Fungi	Ascomycota	Articulospora	NA	17 Days
22.20	7E-12	Fungi	Ascomycota	Acrophialophora	Acrophialophora sp	17 Days
22.02	3E-11	Fungi	Ascomycota	NA	NA	17 Days
21.83	4E-11	Fungi	Ascomycota	Coniochaeta	NA	17 Days
21.71	5E-11	Fungi	Ascomycota	Chaetothyriales inc. sed.	Chaetothyriales sp	17 Days
21.67	5E-11	Fungi	Ascomycota	Aspergillus	NA	17 Days
21.65	5E-11	Fungi	Ascomycota	Pseudotricharina	Pseudotricharina sp	17 Days
21.60	6E-11	Fungi	Ascomycota	NA	NA	17 Days
21.29	1E-10	Fungi	Ascomycota	NA	NA	17 Days
20.91	2E-10	Fungi	Ascomycota	Chaetomium	NA	17 Days

20.16	3E-11	Fungi	Ascomycota	Hazslinszkyomyces	Hazslinszkyomyces lycii	17 Days
8.91	1E-05	Fungi	Ascomycota	Fusarium	NA	17 Days
7.23	7E-03	Fungi	Ascomycota	Knufia	Knufia sp	17 Days
6.34	9E-03	Fungi	Ascomycota	NA	NA	17 Days
23.68	6E-11	Fungi	Ascomycota	NA	NA	1 Month
22.73	4E-08	Fungi	Basidiomycota	Geastrum	Geastrum sp	1 Month
22.45	4E-06	Fungi	Ascomycota	NA	NA	1 Month
22.27	2E-09	Fungi	Ascomycota	Neophaeococcomyces	Neophaeococcomyces sp	1 Month
21.90	4E-10	Fungi	Ascomycota	Neophaeococcomyces	Neophaeococcomyces sp	1 Month
21.86	9E-11	Fungi	Ascomycota	NA	NA	1 Month
21.68	4E-08	Fungi	Ascomycota	Knufia	NA	1 Month
21.63	1E-05	Fungi	Ascomycota	Acrophialophora	Acrophialophora sp	1 Month
21.15	2E-08	Fungi	Ascomycota	NA	NA	1 Month
21.01	1E-05	Fungi	Ascomycota	NA	NA	1 Month
20.85	2E-05	Fungi	Ascomycota	Knufia	NA	1 Month
20.77	1E-10	Fungi	Ascomycota	Sporormia	Sporormia sp	1 Month
20.70	2E-05	Fungi	Ascomycota	Gibberella	NA	1 Month
20.62	1E-05	Fungi	Ascomycota	Didymellaceae inc. sed.	Didymellaceae sp	1 Month
20.41	1E-05	Fungi	Ascomycota	NA	NA	1 Month
20.39	3E-05	Fungi	Ascomycota	Chaetosphaeronema	Chaetosphaeronema sp	1 Month
20.16	4E-05	Fungi	Ascomycota	Pyrenochaeta	Pyrenochaeta sp	1 Month
19.86	5E-05	Fungi	Ascomycota	NA	NA	1 Month
18.80	2E-04	Fungi	Ascomycota	NA	NA	1 Month
9.41	2E-04	Fungi	Ascomycota	Chaetosphaeronema	Chaetosphaeronema sp	1 Month
23.97	3E-28	Fungi	Ascomycota	Neophaeococcomyces	Neophaeococcomyces sp	8 Months
23.96	6E-13	Fungi	Ascomycota	NA	NA	8 Months
22.94	8E-13	Fungi	Ascomycota	Darksidea	Darksidea alpha	8 Months
22.61	3E-17	Fungi	Ascomycota	Trichoderma	NA	8 Months
22.52	2E-11	Fungi	Ascomycota	NA	NA	8 Months
22.45	5E-20	Fungi	Ascomycota	NA	NA	8 Months
22.25	6E-13	Fungi	Ascomycota	Podospora	Podospora sp	8 Months
22.16	3E-11	Fungi	Ascomycota	Acrophialophora	Acrophialophora sp	8 Months
21.94	5E-11	Fungi	Ascomycota	Podospora	Podospora intestinacea	8 Months
21.87	5E-11	Fungi	Ascomycota	NA	NA	8 Months
21.67	8E-11	Fungi	Ascomycota	Preussia	Preussia terricola	8 Months
21.59	1E-12	Fungi	Ascomycota	NA	NA	8 Months
21.50	1E-10	Fungi	Ascomycota	Chaetosphaeronema	Chaetosphaeronema sp	8 Months

21.47	1E-10	Fungi	Ascomycota	Alternaria	NA	8 Months
21.45	1E-10	Fungi	Ascomycota	Clarireedia	Clarireedia bennettii	8 Months
21.40	1E-10	Fungi	Ascomycota	NA	NA	8 Months
21.24	2E-10	Fungi	Ascomycota	Pseudotricharina	Pseudotricharina sp	8 Months
21.22	2E-10	Fungi	Ascomycota	NA	NA	8 Months
20.88	3E-10	Fungi	Ascomycota	Preussia	NA	8 Months
8.71	4E-03	Fungi	Ascomycota	Preussia	Preussia polymorpha	8 Months
6.51	2E-11	Fungi	Ascomycota	NA	NA	8 Months
24.86	8E-14	Fungi	Ascomycota	NA	NA	1 Year
24.78	4E-20	Fungi	Ascomycota	Gibberella	NA	1 Year
24.26	2E-13	Fungi	Ascomycota	Pseudotricharina	Pseudotricharina sp	1 Year
23.77	4E-16	Fungi	Ascomycota	Ascobolus	NA	1 Year
23.46	3E-13	Fungi	Ascomycota	Saitoella	Saitoella complicata	1 Year
23.39	4E-24	Fungi	Basidiomycota	Naganishia	Naganishia albida	1 Year
23.28	2E-12	Fungi	Ascomycota	Pyrenochaeta	Pyrenochaeta sp	1 Year
23.13	2E-12	Fungi	Ascomycota	Spooneromyces	Spooneromyces laeticolor	1 Year
23.13	3E-13	Fungi	Ascomycota	Darksidea	Darksidea alpha	1 Year
22.91	4E-12	Fungi	Ascomycota	NA	NA	1 Year
22.78	5E-12	Fungi	Ascomycota	Knufia	NA	1 Year
22.66	1E-13	Fungi	Ascomycota	NA	NA	1 Year
22.58	7E-12	Fungi	Ascomycota	Preussia	NA	1 Year
22.44	1E-11	Fungi	Basidiomycota	Naganishia	NA	1 Year
22.38	1E-13	Fungi	Ascomycota	NA	NA	1 Year
22.37	1E-11	Fungi	Ascomycota	Didymellaceae inc. sed.	Didymellaceae sp	1 Year
22.35	1E-11	Fungi	Ascomycota	NA	NA	1 Year
22.22	1E-11	Fungi	Ascomycota	Mycocalicium	Mycocalicium victoriae	1 Year
21.88	3E-11	Fungi	Ascomycota	Knufia	NA	1 Year
21.73	4E-11	Fungi	Ascomycota	NA	NA	1 Year
21.61	5E-11	Fungi	Ascomycota	Iodophanus	NA	1 Year
21.56	5E-11	Fungi	Ascomycota	NA	NA	1 Year
21.34	8E-11	Fungi	Basidiomycota	Naganishia	Naganishia albida	1 Year
21.33	8E-11	Fungi	Ascomycota	Chaetomium	NA	1 Year
21.29	9E-11	Fungi	Basidiomycota	Naganishia	NA	1 Year
21.12	1E-10	Fungi	Ascomycota	NA	NA	1 Year
9.51	6E-04	Fungi	Ascomycota	Collariella	Collariella anguipilia	1 Year
8.81	4E-03	Fungi	Ascomycota	NA	NA	1 Year
8.55	1E-04	Fungi	Ascomycota	Fusarium	NA	1 Year
8.23	5E-03	Fungi	Ascomycota	Clarireedia	Clarireedia bennettii	1 Year
7.58	7E-03	Fungi	Ascomycota	Preussia	Preussia polymorpha	1 Year

6.76	3E-04	Fungi	Ascomycota	Oedocephalum	NA	1 Year
5.43	3E-04	Fungi	Ascomycota	NA	NA	1 Year
4.93	2E-04	Fungi	Basidiomycota	Naganishia	Naganishia albida	1 Year
26.61	4E-16	Fungi	Ascomycota	NA	NA	3 Years
25.70	4E-15	Fungi	Ascomycota	Laburnicola	Laburnicola sp	3 Years
25.65	3E-15	Fungi	Ascomycota	Iodophanus	Iodophanus sp	3 Years
24.46	5E-19	Fungi	Ascomycota	Cladorrhinum	Cladorrhinum sp	3 Years
24.29	3E-19	Fungi	Ascomycota	NA	NA	3 Years
24.27	1E-13	Fungi	Ascomycota	Spooneromyces	Spooneromyces laeticolor	3 Years
24.24	1E-13	Fungi	Ascomycota	NA	NA	3 Years
24.15	1E-13	Fungi	Ascomycota	NA	NA	3 Years
23.94	2E-13	Fungi	Ascomycota	Macrophomina	NA	3 Years
23.77	3E-13	Fungi	Ascomycota	Capnodiales inc. sed.	Capnodiales sp	3 Years
23.73	3E-13	Fungi	Basidiomycota	Geastrum	Geastrum sp	3 Years
23.69	3E-13	Fungi	Ascomycota	Chaetosphaeronema	Chaetosphaeronema sp	3 Years
23.66	2E-18	Fungi	Ascomycota	Edenia	Edenia gomezpompae	3 Years
23.65	3E-16	Fungi	Ascomycota	NA	NA	3 Years
23.59	4E-13	Fungi	Basidiomycota	Naganishia	NA	3 Years
23.55	4E-13	Fungi	Ascomycota	NA	NA	3 Years
23.32	7E-13	Fungi	Basidiomycota	Coprinus	Coprinus phaeopunctatus	3 Years
23.30	7E-13	Fungi	Ascomycota	Preussia	NA	3 Years
22.92	3E-13	Fungi	NA	NA	NA	3 Years
22.82	1E-20	Fungi	Ascomycota	Pseudogymnoascus	Pseudogymnoascus pannorum	3 Years
22.79	4E-17	Fungi	Ascomycota	NA	NA	3 Years
22.52	3E-15	Fungi	Ascomycota	Sulcatistroma	Sulcatistroma nolinae	3 Years
22.51	4E-12	Fungi	Chytridiomycota	Lobulomycetales inc. sed.	Lobulomycetales sp	3 Years
22.44	1E-16	Fungi	Ascomycota	Paraphoma	Paraphoma sp	3 Years
22.44	5E-12	Fungi	Ascomycota	Knufia	NA	3 Years
22.23	4E-12	Fungi	Ascomycota	NA	NA	3 Years
22.09	1E-19	Fungi	Ascomycota	NA	NA	3 Years
21.97	3E-16	Fungi	Ascomycota	Gibberella	Gibberella avenacea	3 Years
21.97	6E-13	Fungi	Ascomycota	Aspergillus	Aspergillus ruber	3 Years
21.97	1E-11	Fungi	Basidiomycota	Naganishia	Naganishia albida	3 Years
21.95	1E-11	Fungi	Ascomycota	Gymnoascus	Gymnoascus reessii	3 Years
21.94	1E-11	Fungi	Ascomycota	Knufia	NA	3 Years
21.92	1E-11	Fungi	Basidiomycota	Panaeolus	Panaeolus fimicola	3 Years
21.89	2E-11	Fungi	Ascomycota	Darksidea	Darksidea alpha	3 Years
21.88	2E-11	Fungi	Ascomycota	Penicillium	NA	3 Years

21.87	7E-13	Fungi	Ascomycota	Westerdykella	Westerdykella sp	3 Years
21.86	1E-14	Fungi	Ascomycota	Dactylonectria	Dactylonectria macrodidyma	3 Years
21.82	2E-11	Fungi	Ascomycota	Darksidea	Darksidea alpha	3 Years
21.73	2E-11	Fungi	Ascomycota	NA	NA	3 Years
21.67	2E-11	Fungi	Ascomycota	Coniosporium	Coniosporium sp	3 Years
21.66	2E-11	Fungi	Ascomycota	Microdochium	Microdochium sp	3 Years
21.62	2E-11	Fungi	Ascomycota	Coniochaeta	NA	3 Years
21.52	8E-13	Fungi	Ascomycota	Coniothyrium	Coniothyrium sp	3 Years
21.41	4E-11	Fungi	Ascomycota	Acrophialophora	NA	3 Years
21.41	1E-13	Fungi	Ascomycota	Podospora	Podospora minicauda	3 Years
21.39	5E-12	Fungi	Ascomycota	Schizothecium	NA	3 Years
20.91	8E-12	Fungi	Ascomycota	Ascobolus	Ascobolus sp	3 Years
20.60	2E-10	Fungi	Ascomycota	NA	NA	3 Years
20.28	2E-11	Fungi	Ascomycota	Scutellinia	Scutellinia sp	3 Years
11.22	2E-04	Fungi	Ascomycota	Collariella	Collariella anguipilia	3 Years
9.15	2E-03	Fungi	Ascomycota	NA	NA	3 Years
8.99	4E-04	Fungi	Basidiomycota	Geastrum	Geastrum sp	3 Years
8.21	2E-03	Fungi	Mucoromycota	Rhizopus	Rhizopus arrhizus	3 Years
8.06	3E-03	Fungi	Ascomycota	Preussia	Preussia terricola	3 Years
7.22	2E-05	Fungi	Ascomycota	Iodophanus	Iodophanus sp	3 Years
6.84	1E-02	Fungi	Basidiomycota	Naganishia	Naganishia randhawae	3 Years
6.20	1E-04	Fungi	Ascomycota	Aureobasidium	NA	3 Years
4.94	2E-08	Fungi	Basidiomycota	Naganishia	Naganishia albida	3 Years
4.85	3E-07	Fungi	Ascomycota	Sulcatistroma	Sulcatistroma nolinae	3 Years
4.28	1E-11	Fungi	Ascomycota	Alternaria	NA	3 Years
3.43	2E-03	Fungi	Basidiomycota	Naganishia	NA	3 Years
1.46	2E-03	Fungi	Ascomycota	Alternaria	NA	3 Years

Table S16. Fungal genera showing negative differential abundance in burned plots (decrease).

log2Fold Change	padj	Kingdom	Phylum	Genus	Species	Timepoint
-7.58	1E-03	Fungi	Ascomycota	Pezizaceae inc. sed.	Pezizaceae sp	17 Days
-9.20	2E-06	Fungi	Ascomycota	NA	NA	17 Days
-9.78	5E-05	Fungi	Ascomycota	Didymella	NA	17 Days
-23.27	1E-12	Fungi	Ascomycota	Coniozyma	Coniozyma leucospermi	17 Days
-23.29	1E-12	Fungi	Ascomycota	Capnodiales inc. sed.	Capnodiales sp	17 Days
-23.80	4E-13	Fungi	Basidiomycota	NA	NA	17 Days
-24.82	4E-14	Fungi	Ascomycota	Pezizaceae inc. sed.	Pezizaceae sp	17 Days
-25.14	5E-19	Fungi	Ascomycota	Knufia	NA	17 Days
-25.67	3E-08	Fungi	Ascomycota	Arthoniomycetes inc. sed.	Arthoniomycetes sp	1 Month
-25.88	2E-08	Fungi	Ascomycota	Pezizaceae inc. sed.	Pezizaceae sp	1 Month
-6.57	3E-03	Fungi	Ascomycota	Pezizaceae inc. sed.	Pezizaceae sp	8 Months
-7.32	9E-03	Fungi	Ascomycota	Oedocephalum	Oedocephalum sp	8 Months
-7.51	6E-03	Fungi	Ascomycota	Arthoniomycetes inc. sed.	Arthoniomycetes sp	8 Months
-23.93	5E-13	Fungi	Ascomycota	Phaeococcomyces	Phaeococcomyces sp	8 Months
-24.12	3E-13	Fungi	Ascomycota	NA	NA	8 Months
-24.26	3E-13	Fungi	Ascomycota	Libertasomyces	Libertasomyces myopori	8 Months
-24.89	6E-14	Fungi	Ascomycota	Aureobasidium	Aureobasidium iranianum	8 Months
-25.80	2E-23	Fungi	Ascomycota	Arthoniomycetes inc. sed.	Arthoniomycetes sp	8 Months
-8.14	4E-03	Fungi	Ascomycota	Ramimonilia	Ramimonilia apicalis	1 Year
-21.88	2E-11	Fungi	Basidiomycota	NA	NA	1 Year
-24.18	1E-13	Fungi	Ascomycota	Ascobolus	Ascobolus sp	1 Year
-24.19	1E-13	Fungi	Ascomycota	NA	NA	1 Year
-24.46	1E-13	Fungi	Ascomycota	Pezizaceae inc. sed.	Pezizaceae sp	1 Year
-24.53	1E-13	Fungi	Ascomycota	Ascobolus	Ascobolus sp	1 Year
-24.81	6E-14	Fungi	Ascomycota	Kalmusia	Kalmusia utahensis	1 Year
-25.51	1E-14	Fungi	Ascomycota	NA	NA	1 Year
-8.35	1E-05	Fungi	Ascomycota	Dematiopleospora	Dematiopleospora sp	3 Years
-8.69	2E-04	Fungi	Ascomycota	Pyrenophora	Pyrenophora sieglingiae	3 Years
-23.33	5E-13	Fungi	Ascomycota	NA	NA	3 Years
-23.50	3E-13	Fungi	Ascomycota	Helicoma	Helicoma sp	3 Years
-23.85	2E-13	Fungi	Ascomycota	Pezizaceae inc. sed.	Pezizaceae sp	3 Years
-25.03	1E-14	Fungi	Ascomycota	Helicoma	Helicoma sp	3 Years
-25.41	4E-15	Fungi	Ascomycota	NA	NA	3 Years
-25.59	9E-19	Fungi	Ascomycota	Capnodiales inc. sed.	Capnodiales sp	3 Years
-25.94	1E-15	Fungi	Ascomycota	Chaetomiaceae inc. sed.	Chaetomiaceae sp	3 Years

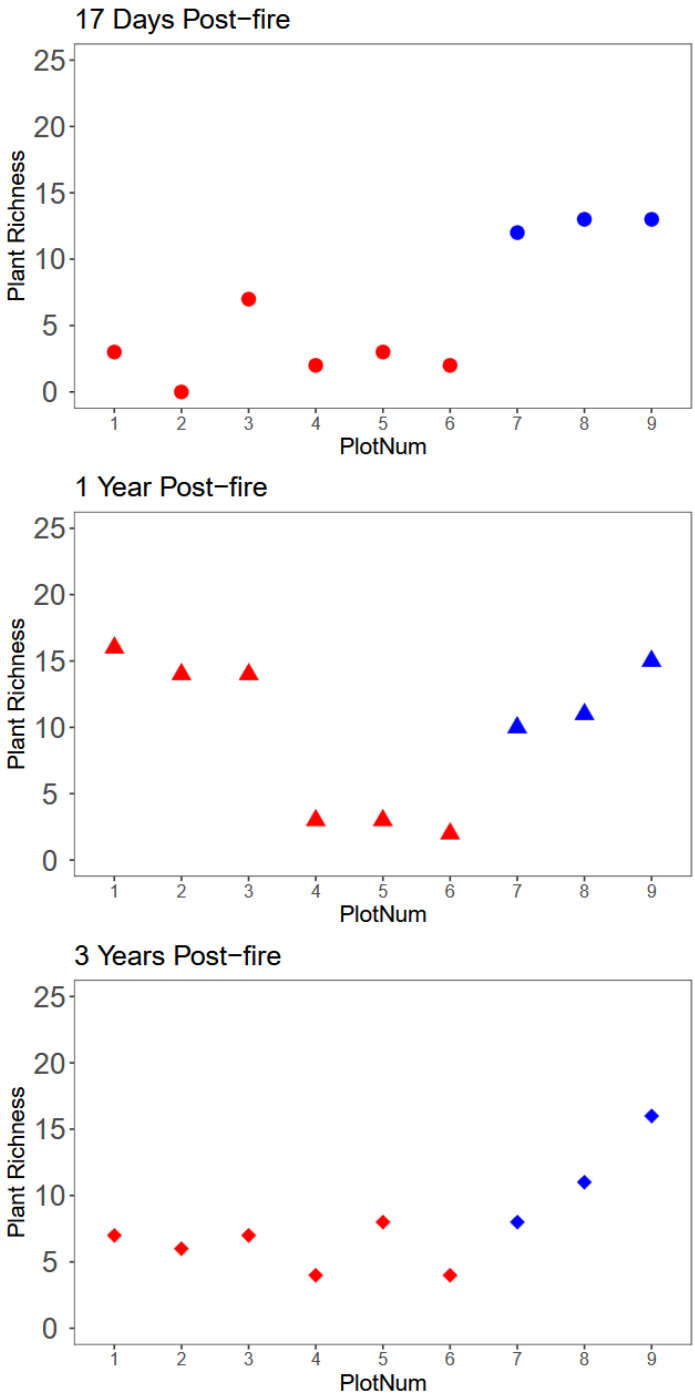

Figure 3.8.1 Plant species richness at each plot in September 2020, 2021, and 2023. Red points indicate burned plots and blue points indicate unburned plots.

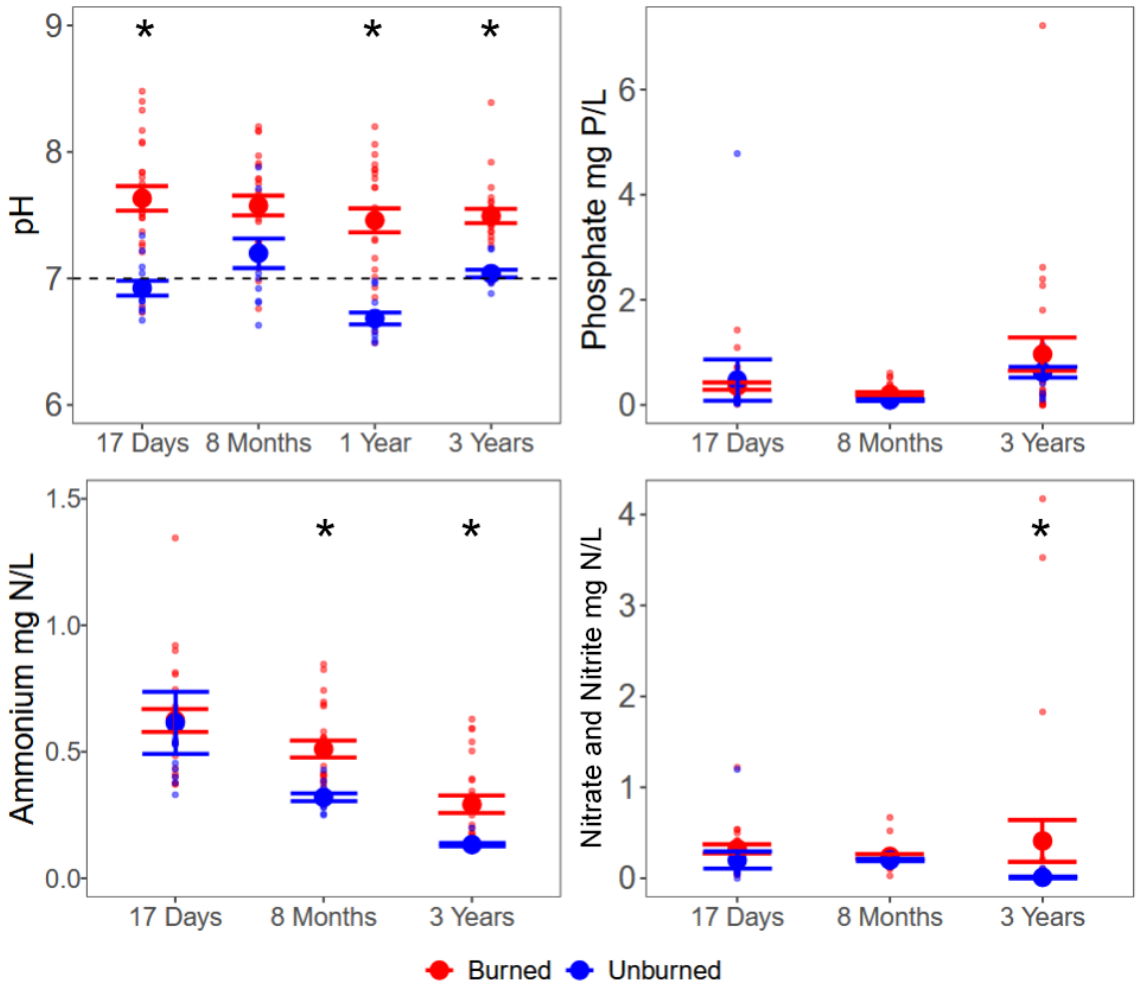

Figure 3.8.2 Soil characteristics at available timepoints. The figure indicates means (center point) and standard error (bars) as well as data points (small points) for A) pH with a dashed line indicating pH 7, B) phosphate levels, C) ammonium levels, and D) nitrate and nitrite levels in unburned and burned plots (blue and red, respectively). Asterisks indicate significant differences between burned and unburned means based on generalized mixed effects models for each variable.

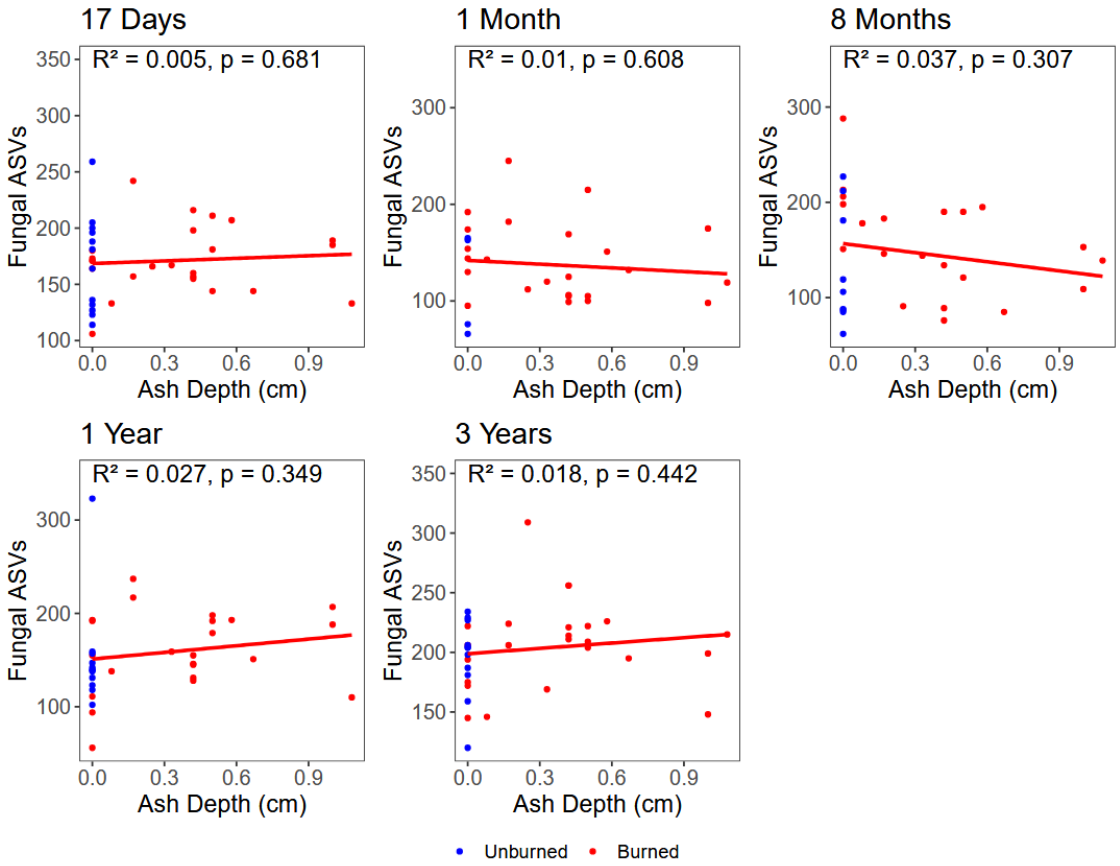

Figure 3.8.3 Fungal richness and ash depth as measured at 17-days post-fire. We tested richness and ash depth as a linear model with R^2 and p-values listed per comparison.

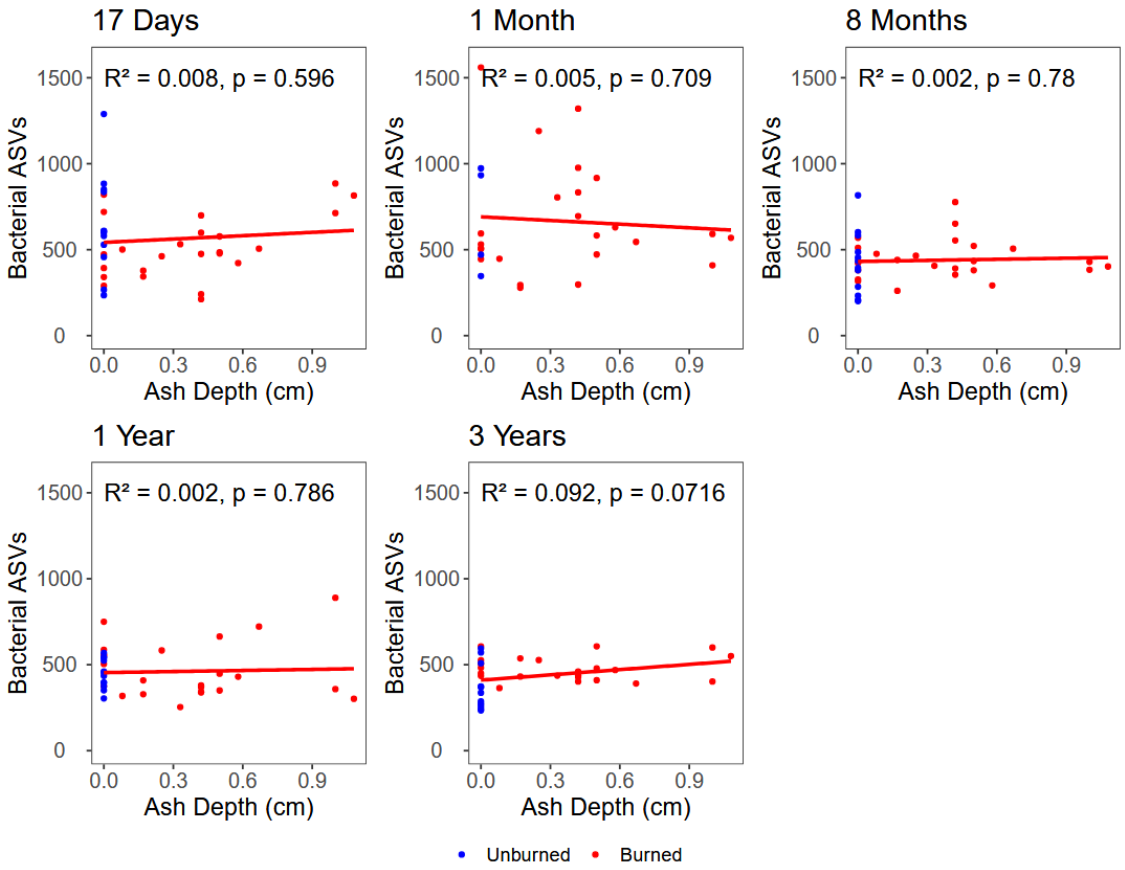

Figure 3.8.4 Figure S3. Bacterial richness and ash depth as measured at 17-days post-fire. We tested richness and ash depth as a linear model with R^2 and p-values listed per comparison.

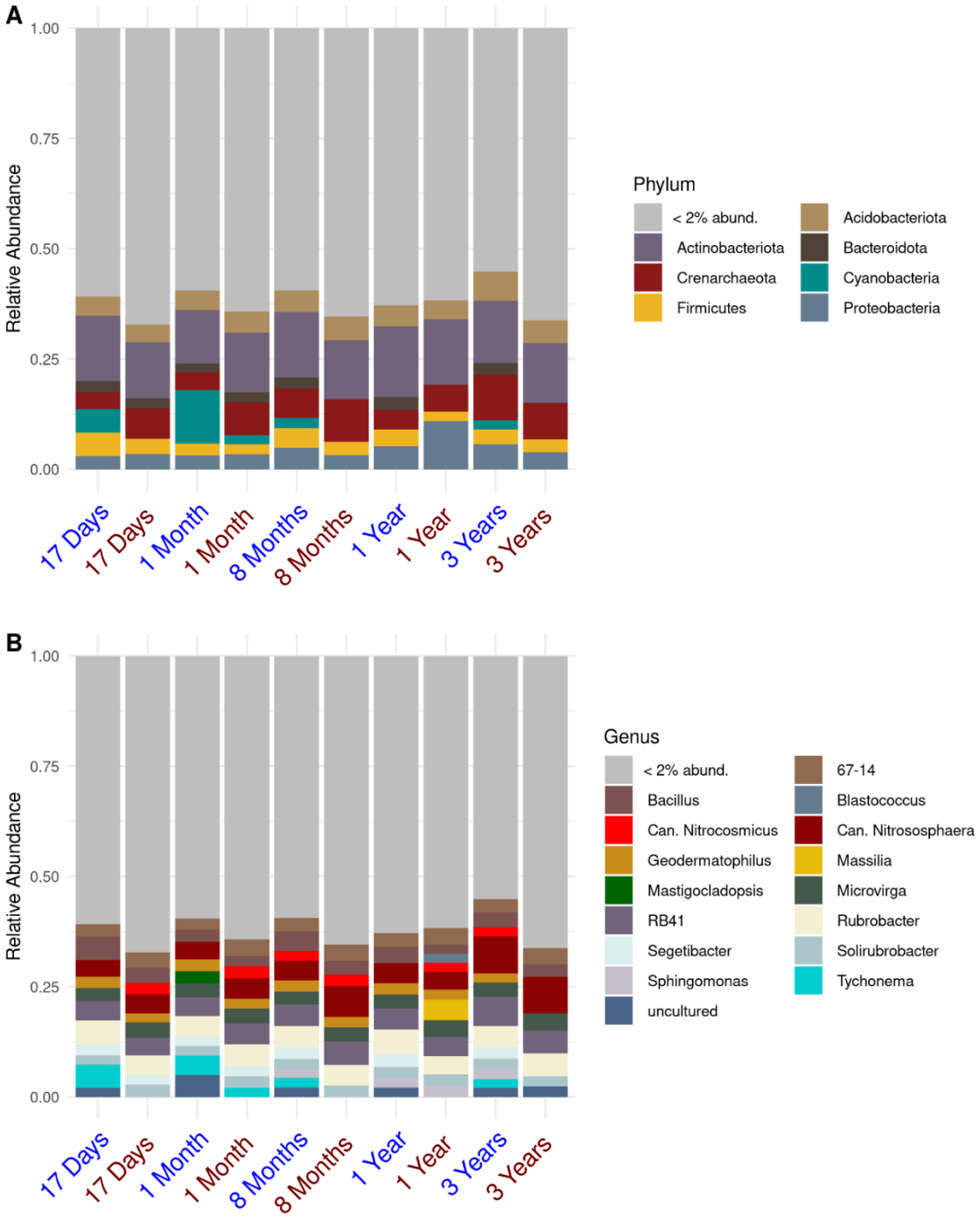

Figure 3.8.5 Relative abundance of archaeal and bacterial A) phyla and B) genera.

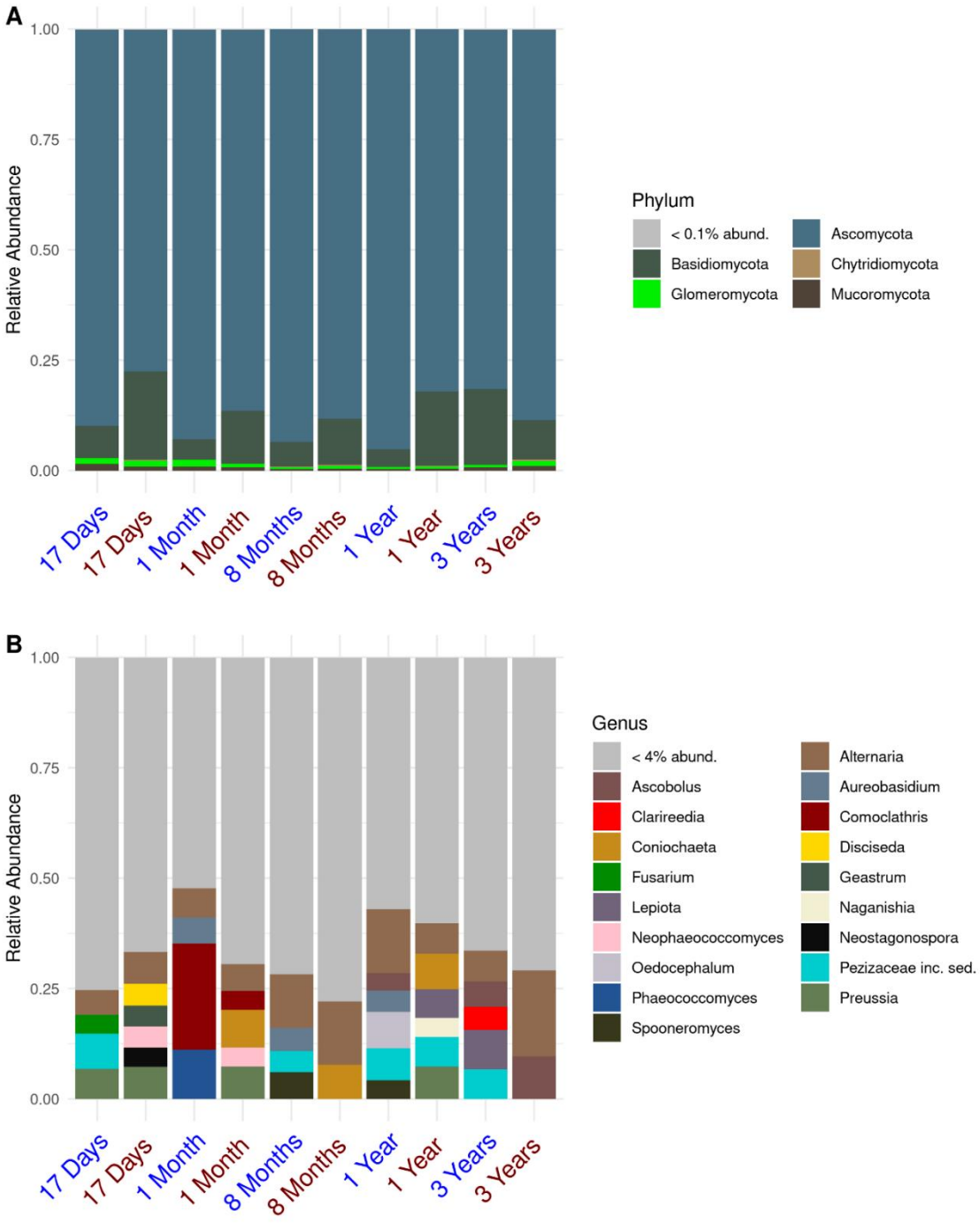

Figure 3.8.6 Relative abundance of fungal A) phyla and B) genera.

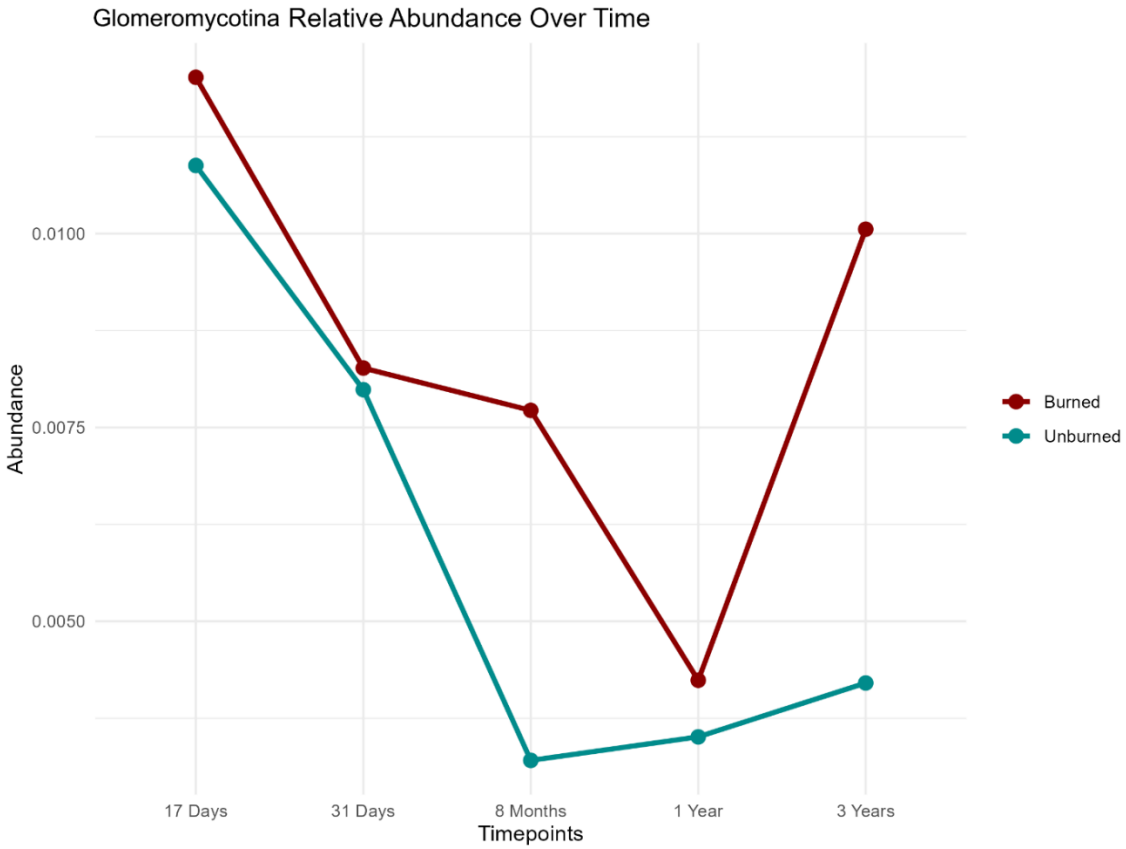

Figure 3.8.7 Glomeromycotina relative abundance in burned and unburned plots.

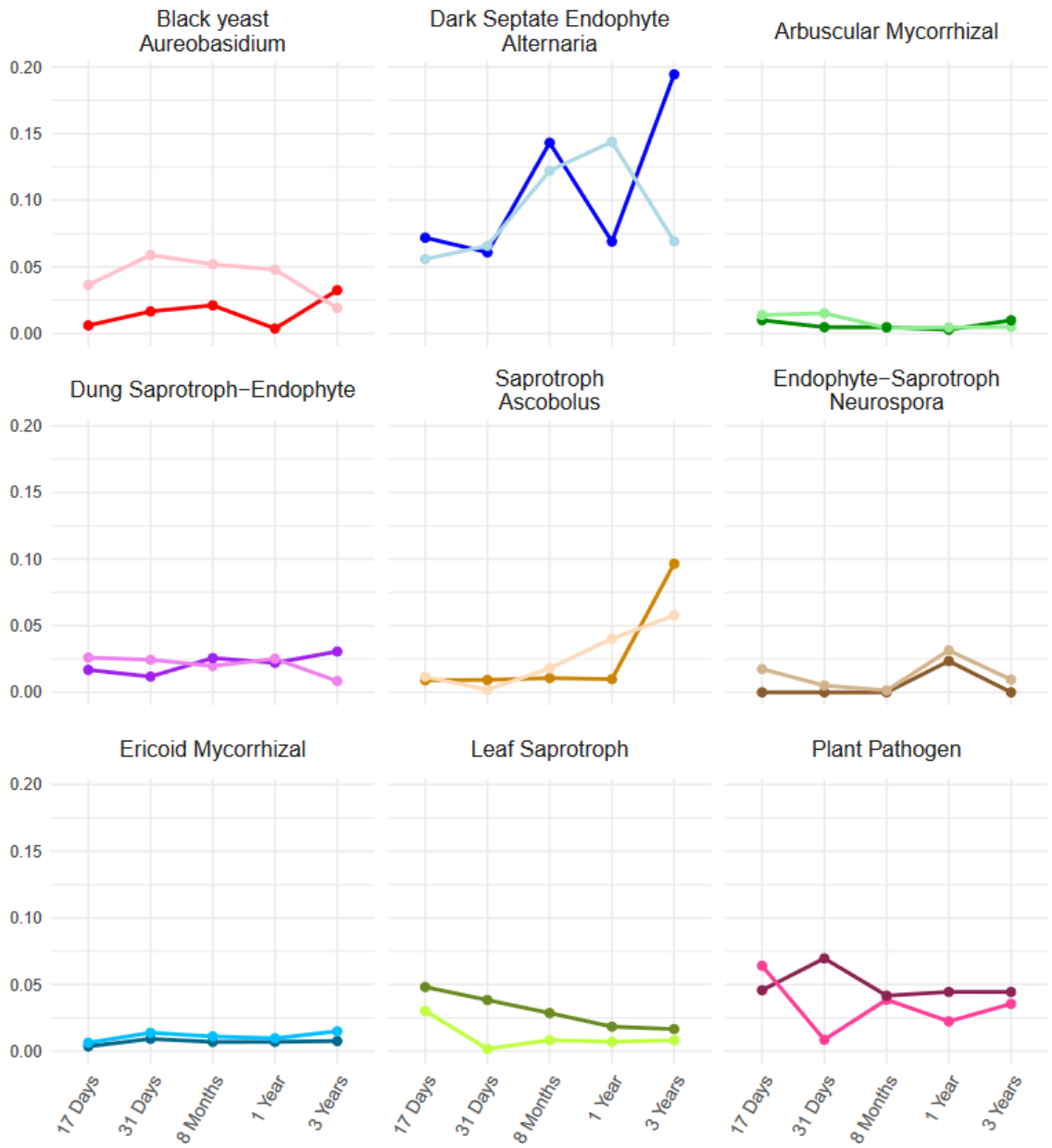

Figure 3.8.8 Fungal guild relative abundance over time. Guilds represented primarily by one genus have the genus listed below the guild name. Darker lines indicate relative abundance in burned plots. Light lines indicate relative abundance in unburned plots.

4 Chapter IV. Microbial cross-kingdom association networks reveal diverging trends of complexity during recovery from low- and high-intensity fires

4.1 Abstract

Drylands, which cover nearly 40% of Earth's surface, are increasingly vulnerable to wildfire, yet post-fire recovery processes in these ecosystems remain poorly understood. Soil microbes are critical to nutrient cycling and ecosystem stability, but their responses to wildfire vary with fire intensity and severity. Here, we used cross-kingdom microbial association networks to investigate post-fire succession in two California drylands which experienced differing levels of fire intensity. Using identical sampling and molecular sequencing techniques, we observed burned and unburned communities around the high-intensity Holy Fire in a chaparral shrubland and the low-intensity Dome Fire in a desert Joshua tree grassland. We combined 16S and ITS2 sequencing across four timepoints (2 weeks to 3 years post-fire) to evaluate changes in bacterial, fungal, and cross-kingdom interactions, focusing on network cohesion, modularity, and keystone taxa.

Chaparral networks exhibited low cohesion and reduced modularity, with partial recovery by 40 months, but remained sensitive to further disturbance. In contrast, desert networks showed higher connectivity and cohesion shortly after fire but revealed delayed reductions in stability after three years. Keystone taxa differed markedly across ecosystems and timepoints: chaparral networks featured low-abundance but highly connected fungi and bacteria, including pyrophilous taxa such as *Massilia* and *Noviherbaspirillum*, while desert networks were structured by generalist bacterial and fungal module hubs such as *Crossiella* and *Pseudotricharina*. No keystone genera were shared across sites, highlighting habitat-specific microbial trajectories across our study. Our results demonstrate that network-based analyses uncover post-fire microbial stress and successional dynamics not detected by traditional diversity metrics. Cross-kingdom network approaches revealed ecosystem-specific vulnerabilities and identified potential keystone taxa that may mediate long-term recovery. These findings highlight several potentially important post-fire microbes and their interactions which have not been explored in studies of pyrophilous microbes, and further support for the application of network metrics for assessing microbial community sensitivity alongside measures of species composition.

4.2 Introduction

Drylands now cover approximately 40% of Earth's surface (Huang et al. 2016), which is expected to rise due to climate change and desertification (Feng and Fu 2013). These landscapes are increasingly prone to wildfires, yet not all arid ecosystems experience fire in the same way (Pausas and Keeley 2021). Fire intensity, or the heat output of a fire, can increase in denser drylands, while fire severity, which reflects the extent of ecological change, can be extreme even without high intensity (Keeley 2009). These differences can alter post-fire recovery trajectories, especially in microbial communities (Nelson et al. 2022b). Soil microbes play critical roles in nutrient cycling (Jacoby et al. 2017), plant regeneration, and overall ecosystem stability , making it essential to understand how fire affects soil microbiomes under varying conditions. Drylands are susceptible to nutrient loss (Schlesinger et al. 1990), so microbial communities may be key to stabilizing nutrients as drylands continue to expand.

The impact of fire on soil microbial communities is strongly influenced by fire intensity and severity. High-intensity fires often lead to substantial reductions in microbial biomass and richness (Dooley and Treseder 2012; Dove and Hart 2017; Pulido-Chavez et al. 2023), while low-intensity fires may leave these metrics largely unchanged (Vega-Cofre et al. 2023; Glassman et al. 2023; Zhang et al. 2025). However, high- and low-intensity fires can still promote the emergence of pyrophilous or fire-loving taxa. Bacteria such as *Noviherbaspirillum*, *Massilia*, and fungi such as *Aspergillus*, *Coniochaeta*, *Pyronema*, and others have been isolated post-fire across the globe (Warcup 1990; Belmok et al. 2019; Enright et al. 2022; Soria et al. 2023; Li et al. 2024).

Pyrophilous microbes are largely defined by their increase in abundance from near-zero to highly dominant post-fire (Fox et al. 2022), and are best described by investigating their traits in post-fire conditions when cultured from burned soil. However, the vast majority of microbes are difficult to culture even with burn-specific media (Woolet and Whitman 2020; Enright et al. 2025), and differential abundance can often detect multiple strains of the same organism indicating greater abundance in both burned and unburned plots (Whitman et al. 2019; Caiafa et al. 2023). Our application of networks to samples from burned soils allows a more efficient exploration of potential interactions between pyrophilous taxa without the exponential cross-plating of microbes. Further, cross-kingdom interactions can be lost when focusing on one microbe at a time, while samples often amplified for prokaryotes and fungi can be combined in cross-kingdom networks.

While metrics like biomass, richness, and composition can inform single-kingdom compositional changes, network analysis identifies taxa-specific associations and broad patterns of sensitivity or resilience to disturbance (Herren and McMahon 2017; Matchado et al. 2021; Hernandez et al. 2021). Association networks allow inference of positive (potential facilitation or co-habitation) (Faust et al. 2015) and negative (potential competition or niche exclusion) interactions between taxa (Hirano and Takemoto 2019). Metrics such as cohesion, a measure of the relative strength of positive versus negative interactions, have been used to assess community stability across ecosystems (Herren and McMahon 2017; Hernandez et al. 2021; Birch et al. 2025). Similarly, modularity quantifies how tightly connected clusters of microbes are within a network, with high modularity often implying higher resilience, as perturbations to network structure remain

compartmentalized within a module, which can provide context to microbial communities across post-disturbance succession and initiate testing of interactions based on network edges (de Vries et al. 2018).

Network analysis may also be useful to identify keystone species (Jordán 2009), which are taxa with a greater impact on the community than their abundance reflects (Power et al. 1996). Organisms essential to the overall community like shrimp in the food chain (Wu et al. 2019), pollinators (Traveset et al. 2017), or mycorrhizal fungi (Timóteo et al. 2023) can drive changes by their interactions. In microbial ecology, keystones are thought of as low-abundance species with a stabilizing effect on the community (Amit and Bashan 2023; Kajihara and Hynson 2024). While the phrase can indicate high importance, in-silico analyses alone cannot identify microbes that maintain the soil community across archaea, bacteria, and fungi. However, these keystone taxa, identified by metrics such as high node degree (connections) and betweenness centrality (shortest path between many nodes) (Kajihara and Hynson 2024) can serve as points for further analysis in post-fire community analysis. Early colonization by keystone taxa can promote more colonization of highly connected taxa, driving microbial succession and creating a more resilient community (Rawstern et al. 2025). While common abundant taxa post-fire can be used as burn indicators or biomarkers for fire history (Fernández-González et al. 2023), keystone taxa could be signs of functioning microbial succession following validation of their associations in networks as interactions. In post-fire communities, previously identified microbes are likely keystone species, as not all taxa dominate the community post-fire but many have shown highly variable enzymatic

activity (Sari et al. 2025), and keystone taxa often exhibit traits of multifunctionality in network analyses (Banerjee et al. 2018; Wang et al. 2023; Luo et al. 2025).

Microbial networks have been applied to studies of succession, disturbance, and soil functioning, often focusing on bacterial or fungal communities separately (Arunrat et al. 2024; Luo et al. 2025). For example, in one study, bacterial correlations were significantly reduced after controlled burns of biocrusts (Aanderud et al. 2019), while in others, bacterial network properties did not shift post-fire (Pérez-Valera et al. 2017; Whitman et al. 2022). However, fewer studies have examined cross-kingdom interactions following fire. One such study identified multiple modules composed of either pyrophilous or fire-suppressed microbes (Whitman et al. 2019), although samples were pooled across a broad severity gradient and geographic range. Another examined cohesion of a cross-kingdom network to show that at 9 years after a forest fire, heavily burned regions had lower cohesion, or an overabundance of positive associations, compared to fire refugia sites (Birch et al. 2025). Despite these insights, the impact of intensity and the long-term recovery of the cross-kingdom community after a high-severity fire is not known. While low-intensity fires often produce little to no change in biomass or diversity metrics, shifts in network properties may reveal an ongoing sensitivity to further disturbance. By generating different networks from different conditions over time, networks can be used to identify opposing responses to stress (de Vries et al. 2018; Hernandez et al. 2021). Most work has yet to explore how network properties shift over time, across fire intensities, while considering cross-kingdom associations.

Time is a crucial variable in post-fire recovery. Microbial responses immediately following a fire can be dramatically different from those observed years later (Pulido-Chavez et al. 2023), even if pyrophilous microbes still remain present long-term (Fernández-González et al. 2023; Caiafa et al. 2023). Closely analyzing wildfires over time therefore allows for a greater understanding of whether microbes have a similar consistent post-fire secondary successional pattern, and how these microbial patterns match the resilience of their respective plant communities. Trends over time can differ between bacteria and fungi in the same wildfire systems (Whitman et al. 2019, 2025; Yang et al. 2024), while other studies show that network complexity drops in both bacteria and fungi compared to decades-old fires (Su et al. 2022). Comparing how burned communities contrast unburned communities can help highlight how microbial secondary succession post-fire can impact taxa through their associations, even if a microbe's overall abundance or dominance does not change. Our study aims to build on this gap by integrating both bacterial and fungal data across time and fire regimes using a network-based approach.

Here, we leverage two longitudinal datasets collected following the same experimental design and both sequencing 16S and ITS2 amplicons from separate high-severity wildfires: the Holy Fire (chaparral; Pulido-Chavez et al. 2023) and the Dome Fire (desert Joshua tree grassland; Joukhajian et al. 2025), both sampled with high temporal resolution ranging from 2 weeks to 3 years post-fire. Previous work identified clear differences in response of microbial biomass, richness, and composition across these fires, while still finding similar responses from the same pyrophilous taxa such as

the bacteria *Noviherbaspirillum*, *Tumebacillus*, *Paenibacillus*, *Massilia*, *RB41*, *Solirubrobacter*, and fungi *Aspergillus*, *Coniochaeta*, *Penicillium*, and *Naganishia* (Whitman et al. 2019; Hopkins et al. 2021; Enright et al. 2022; Pulido-Chavez et al. 2023; Fernández-González et al. 2023; Caiafa et al. 2023). Comparing two California dryland wildfires of low (desert) versus high (chaparral) soil burn severity across 4 timepoints ranging from 2 weeks to 3 years, we ask: 1) how do bacterial, fungal, and bacterial-fungal associations and network metrics such as cohesion and modularity change? 2) can we identify keystone taxa and how do they relate to pyrophilous microbes identified in these systems?

We predict that cohesion will not recover in the Holy Fire over 40 months, but will recover in the Dome Fire which showed overall resilience in the burned plots. However, both fires will result in long-term shifts in modularity, as compositional shifts alter associations. Further, keystone taxa in unburned plots will likely be disturbed in the Holy Fire with minimal associations with pyrophilous taxa, due to the dominance of a few taxa in early successional samplings of the Holy Fire. However, the minor shifts in Dome Fire composition post-fire will show keystone taxa associating with pyrophilous microbes. Using node degree, we will identify microbes important to nutrient cycling in post-fire environments based on their association with multiple cross-kingdom genera in burned networks. Finally, we suspect the combination of cross-kingdom association networks and two similarly sampled fires will reveal important post-fire microbes without any known pyrophilous tendencies identified through single kingdom analyses.

4.3 Methods

Site descriptions: Our chaparral site was in the Cleveland National Forest in California, USA (33.678889, -117.516667). The Holy Fire burned 94 km^2 from August 6 to September 13, 2018, primarily burning chaparral shrubland dominated by manzanita (*Arctostaphylos glandulosa*) and chamise (*Adenostoma fasciculatum*). The fire varied from regions of low to high severity based on rapid post-fire BAER soil burn severity assessments and resulted in several centimeters of ash (Pulido-Chavez et al. 2023) . Our desert site was in Mojave National Preserve in California, USA, centered around the Cima Dome (35.287598, -115.585376). The Dome Fire burned 175km2 around the Cima Dome from August 15 to 24, 2020, killing 1 million Eastern Joshua trees (*Yucca jaegeriana*), and other perennial shrubs and grasses (Kaiser and Hughson 2020). Burned Area Reflectance Classification (BARC) showed low to moderate severity, although these estimates do not account for arid system vegetation loss (Kaiser and Hughson 2020). While pockets of unburned trees remained present within the burn perimeter, plant loss was 80% across our select burned plots.

Sample collection: Soon after each fire was extinguished (~2 weeks), we established 9 plots (6 burned, 3 unburned) with four 1m^2 subplots each in the cardinal directions 5m away from the plot centers (Figure S1). We collected 300-500g of soil using releasable bulb planters cleaned with 70% ethanol from 1m^2 subplots from the top 10cm of soil beneath organic or ash layer at 0.5 months, 8 months, 12 months, and 36 months in the desert, and matched 4 corresponding collections from the chaparral based on successful

sample collection and amplification, limiting analysis to 0.5 months, 6 months, 12 months, and 40 months post-fire out of the total 20 timepoints in the chaparral dataset. We stored soil on ice, and returned samples to the University of California Riverside (UCR) within 24-48 hours. We homogenized samples with ethanol-cleaned sieves (2mm), measured soil gravimetric moisture, and performed the KCl extraction method on fresh soil (Carter and Gregorich 2007) and assessed ammonium, phosphate, and NO_x^- at the UCR Environmental Science Research Lab. We stored a subset of soil at -80°C for future molecular analysis. We air-dried the remainer of soil for biogeochemical analysis, including pH, which we used a VisionPlus pH6175 meter (Jenco Instruments Inc., San Diego, CA) to measure pH after making a slurry of 10g of air-dried soil and 20mL of distilled water and shaking for one minute to mix.

Molecular work: Methods for DNA extraction, PCR amplification, and Illumina Miseq library prep for Holy Fire chaparral samples can be found in (Pulido-Chavez et al. 2023) and for Dome Fire desert samples in (Joukhajian et al.). For Dome Fire Samples, we used Qiagen DNeasy PowerSoil Pro kits, and for Holy Fire samples we used Qiagen DNeasy PowerSoil kits. We amplified DNA in a two-step PCR using the ITS4-fun and 5.8S primer-pair to generate fungal ITS2 amplicons (Taylor et al. 2016), and the 515F and 806R primer-pair for archaeal and bacterial 16S amplicons (Caporaso et al. 2011). Amplicons from 16S and ITS2 pools were combined at a 2:3 ratio to account for preferential sequencing of shorter amplicons, and sequenced together in Illumina Miseq 2x300 runs. We used QIIME2 (Bolyen et al. 2019) to demultiplex and denoise reads, and used de-novo clustering at 97% to create Operational Taxanomic Units (OTUs) for

genus-level comparisons, which are preferable for network analysis because environmental samples often lack species-level designations and intraspecific associations can inflate edge numbers. We performed taxonomic assignment using the Qiime2 Naïve Bayes classifier with the SILVA (v138; (Quast et al. 2013)) and UNITE (v10;(Kõljalg et al. 2005)) databases.

Network construction: We constructed cross-kingdom and individual microbial association networks for archaea, bacteria and fungi using the SpiecEasi R package (Kurtz et al. 2015). For each timepoint, we subset 16S and ITS2 phyloseq objects to matching samples and by treatment prior to constructing networks (burned vs unburned). Since we only had 3 unburned plots (12 samples) compared to 6 burned plots (24 samples), to compare the effect of sample size on network properties, we created a second set of down-sampled burned networks (12 samples) to match the sample size of unburned networks (12 samples). For each kingdom, we collapsed ASVs to genus-level to avoid associations of ASVs matched to the same species, and then removed genera with fewer than 10 reads per treatment per timepoint (Jameson et al. 2023). Further, we only kept genera with a 16% prevalence per network by removing genera appearing in fewer than 2 samples in unburned networks or 4 samples in burned networks according to suggested best practices (Kajihara and Hynson 2024). After filtering, we used the "multi.spiec.easi" function with the Meinshausen–Bühlmann (MB) method (Meinshausen and Bühlmann 2006). We used 999 λ values (from a minimum λ ratio of 1e-3) selected via Stability Approach to Regularization Selection (StARS), with 300 repetitions and a

selection threshold of 0.01. Feature tables used with the SpiecEasi package undergo centered-log ratio transformations to account for uneven sequence depth across samples and primer sets, allowing for cross-kingdom association network construction. This allows for conditional independence while drawing associations between nodes, such that each pair of nodes is evaluated independently from the rest of the network of genera.

Network metrics: We used functions from the igraph package (Csardi 2013) to identify network metrics at each timepoint. To quantify community stability, we calculated abundance weighted mean cohesion per sample in each network. We extracted the signed edge weights from SPIEC-EASI networks by retrieving the adjacency matrix with the SpiecEasi function "getRefit" and corresponding edge weight matrices with "symBeta". We constructed undirected igraph objects from the adjacency matrix and assigned each edge its signed weight from the symmetrized beta matrix. We defined abundance-weighted cohesion as the ratio of summed negative edge weights to summed positive edge weights based on taxa present in each sample (Herren and McMahon 2017). We subsetted all edges connected to each present node (taxon) and summed edge weights for negative and positive separately, which we then used to generate a ratio per sample. We plotted mean cohesion per sample and tested significance of means using a linear model and showed pairwise significance between burned and unburned networks at each timepoint. We calculated modularity using the igraph package "modularity" after finding community structure with the function "cluster_louvain". Higher modularity indicates

that more edges connect nodes that are within the same module rather than across different modules (Csardi 2013).

Keystones: We identified potential keystone taxa using two methods. First, we identified taxa with high betweenness centrality (Kajihara and Hynson 2024), indicative of nodes that frequently occur on the shortest path between other nodes. We labeled any node with >2 standard deviations of the mean betweenness per network, as well as those exhibiting >2 node degree, or connections to other nodes. Second, we calculated within-module connectivity (Zi) and among-module connectivity (Pi) adapted from (Deng et al. 2012) to classify genera into four categories: peripheral taxa with few connections ($Zi < 2.5$ and $Pi < 0.62$), module hubs with in-module connectivity or many edges ($Zi > 2.5$, $Pi < 0.62$), connector nodes with many edges across modules ($Zi < 2.5$, $Pi > 0.62$), and network hubs which are highly connected both within and across modules ($Zi > 2.5$, $Pi > 0.62$). We used igraph to cluster modules from each network, which were subsets of treatment and timepoint, and used ggplot2 to combine results from all networks per site. We identified modules in which non-peripheral nodes appeared and plotted their positive and negative associations using the beta matrix based on weighted adjacency matrices per network. Although we use established methods in graph theory and microbial network analysis (Guimerà and Nunes Amaral 2005; Deng et al. 2012), we cannot confirm these taxa as true keystone species without further testing of their removal and the resulting consequences for the microbial community. However, we refer to these network-identified potential keystones hereafter as “keystones” for brevity.

4.4 Results

Chaparral and desert wildfires varied in soil burn severity with mean ± standard error (SE) ash depth of 4.63 ± 0.6 cm in chaparral and 0.4 cm ± 0.07 in desert (Fig. S1A), which resulted in significantly increased pH for both sites but with deserts being more basic than chaparral (Fig. S1B). Wildfires significantly affected ammonium and nitrate such that ammonium initially increased in chaparral but decreased to unburned levels over time whereas ammonium levels remained elevated in burned plots in desert (Fig. S1C), and nitrate/nitrite increased in burned plots over time in both sites (Fig. 1D). Desert microbial species richness was not reduced by fire while chaparral microbial species richness was heavily reduced in burned plots (Fig. S2).

Desert cross-kingdom network metrics*:* Cross-kingdom microbial networks from the desert displayed marked divergences in early and late post-fire comparisons. At 17-days post-fire, burned networks had a higher number of total edges (170) and greater density (0.00193) than unburned networks (117 edges; density = 0.00127). Yet, modularity of burned networks (0.90) was lower than the modularity of unburned networks (0.97; Fig. 1B). Unburned networks showed high modularity throughout our timepoints (0.96-0.97), compared to burned networks despite a reduction in edge numbers by 36 months post-fire (66). In contrast, burned plots still had more total edges at 36 months post-fire (166).

Cross-kingdom cohesion after fire: Across 40 months of post-fire sampling, both the chaparral (Fig. 1C) and desert (Fig. 1D) burned plots displayed much lower cohesion, as

a result of having a high number of positive associations within burned samples. However, initial cohesion (0.5 - 8 months) in desert unburned plots was lower than burned plots, which correspond to periods of continued drought.

Since unburned networks at each timepoint were only made with 12 samples, we sub-sampled burned networks to 12 samples. Trends were identical in the chaparral, with burned networks still showing significantly lower cohesion at each time point (Fig. S3A). However, for desert samples, reduction of sample number made a larger difference and although trends were the same, ¾ of the time points were no longer significantly different (Fig. S3B).

Chaparral cross kingdom network metrics*:* Cross-kingdom microbial networks following the Holy Fire displayed strong temporal divergence between burned and unburned plots during the 3-year post-fire successional period. In unburned plots, the total number of edges peaked at 576 by six-months, while modularity grew from 0.94 at 25-days post-fire to 0.98 at 40 months post-fire, suggesting more compartmentalization of microbial associations. In contrast, burned networks were sparsely connected, with the total edge counts ranging from 76 to 146 across all timepoints. Burned networks had lower modularity, especially at 6-months and 1-year (0.82), though they partially recovered by 40 months (0.90; Fig. 1C). Network density of burned plots was slightly higher than in unburned plots after 6-months.

Comparison of cross-kingdom network metrics across sites*:* Unburned plots from the chaparral were much more interconnected than desert plots. The largest connected component (LCC) from the chaparral at 0.5 months was 178 nodes (Fig. 2), while in desert plots, there were only 9 nodes (Fig. 3). This trend continued, although the LCC from unburned chaparral networks shrank over time, from 274 nodes at 6 months, to 30 at 12 months, and finally 18 nodes at 40 months post-fire. The LCC in unburned desert nodes did not grow, as there were 7 nodes at 8 months, 9 nodes at 12 months, and 5 nodes at 36 months post-fire. Burned networks showed more edges and bigger LCCs, fluctuating from 64 nodes at 0.5 months, 18 at 8 months, 52 at 12 months, and 20 at 36 months. Conversely, burned chaparral samples resulted in smaller LCCs only relative to unburned chaparral, ranging from an LCC of 13 at 0.5 months, 52 at 6 months, 71 at 12 months, and 62 at 40 months.

Chaparral keystone taxa*:* No archaea were identified as keystones from the chaparral, and most keystone genera in unburned plots were fungi. This trend was present throughout 40 months of sampling unburned plots, while the reverse was true for burned plots with bacteria being the only keystones at 0.5 months and only 1 fungal genus in each of the later timepoints (Fig. 4A). For unburned plots, the genera with high betweenness and the highest node degree at each timepoint were *Pezizellaster* at 0.5 months (6 edges, <1% relative abundance), a tie between *Blastococcus*, *Neoconiothrium*, and *Exophiala* at 6 months (6, <2%), *Dendrophoma* at 12 months (6, <1%), and a tie between *Reyranella*, *Rhodanobacter*, *Rhodopila*, and *Polyscytalum* at 40 months (4,

<1%). The genera with high betweenness and the highest node degree at each timepoint in burned plots were *Solirubrobacter* (4, 2% relative abundance) at 0.5 months, the Acidobacteriota taxa in Subgroup 7 at 6 months (6, <1%), *Candidatus Udaeobacter* at 12 months (12, <2%), and *Candidatus Udaeobacter* at 40 months (11, <2%).

When comparing nodes across timepoints to the same standards of within-module connectivity (Zi) and among-module connectivity (Pi), 5 genera from burned plots emerged as keystones as either connectors with high among-module connectivity, or module hubs with high within-module connectivity (Fig. 4A). *Massilia* (connector), *Candidatus Udaeobacter*, and *Inocybe* (module hubs) were keystones at 6 months, *Noviherbaspirillum*, *Candidatus Udaeobacter*, and a bacterium from 67.14 were module hubs at 12 months, and *Candidatus Udaeobacter* (module hub) and *Gelasinospora* (connector) were keystones at 40 months post-fire (Fig. 5). Thirteen genera were keystones in unburned plots from 0.5 months to 12 months post-fire, including *Roseiarcus, Mycobacterium, Jatrophihabitans, Novosphingobium, B12.WMSP1, Lacunisphaera, Myxococcus, Afipia, Bordetella, Exophiala, Ceriporia, Chaetosphaeronema, and Dendrophoma.*

Desert keystone taxa*:* Keystone taxa included archaea, fungi, and bacteria in burned plots while unburned plots had either bacteria and fungi or only fungi with high betweenness (Fig. 4B). The genera with high betweenness and the highest node degree at each timepoint in unburned plots was a genus from Pleosporaceae at 0.5 months (4 edges, <1% relative abundance), *Baia* at 8 months (4, <1%), *Lepiota* and *Papiliotrema* at 12

months (3, <1%), and Teunia at 36 months (3, <1%). The genera with high betweenness and the highest node degree at each timepoint in burned plots was an archaeon in Nitrososphaeraceae at 0.5 months (6, 5%), a tie between *Rubrobacter*, *Candidatus Nitrososphaeraceae*, and *Pseudotricharina* at 8 months (5, <6%), *Gaiella* at 12 months (5, <1%), and a genus from Nitrososphaeraceae at 36 months (5, 6%).

When comparing nodes across timepoints to the same standards of within-module connectivity (Zi) and among-module connectivity (Pi), we only detected hub taxa from burned networks in the desert (Fig. 4B). These included a bacterium from wb1-P19 (module hub) at 0.5 months, *Pseudotricharina* and a bacterium from CCD24 (module hubs) at 8 months, *Rubrobacter* (connector) at 12 months, and *Crossiella* (module hub) at 36 months (Fig. 6).

4.5 Discussion

We used network analysis to highlight long-term impacts of disturbance on cross-kingdom communities, identifying trends that were previously undetectable while focusing on diversity metrics. We classified several low- and high-abundance taxa as keystones which were highly interconnected in modules across time. Keystone taxa in chaparral post-fire networks reflected distinct ecological roles and patterns over time, with fungi dominating unburned plots and bacteria emerging in burned ones. While there was some congruence between keystones identified through ZiPi plots and those with high betweenness centrality, one notable distinction is that not all timepoints were represented with strong keystones in ZiPi plots, while comparing betweenness to mean

betweenness per network always resulted in some nodes having relatively higher betweenness centrality than the rest of the nodes. Since ZiPi plots standardize comparisons rather than guarantee a highest-betweenness node in every network, they provide a more conservative estimate of keystones. Notably, no keystones identified in ZiPi plots were re-occurring across treatments or sites. Identifying these early keystones may be important for understanding post-fire succession, since keystones tend to recruit other keystones moreso than generalist taxa during early successional periods, shaping the future of the community (Rawstern et al. 2025).

Network cohesion across time: Post-fire network cohesion revealed a long-term rise in positive microbial associations, suggesting that microbes may be growing interdependently and thus be more vulnerable to a future disturbance. This trend occurred late in the desert plots, after rainfall spurred activity in unburned microbial communities. This differed from richness trends seen in the desert, as burned and unburned plots had similar microbial richness prior to 12 months post-fire. In the chaparral, bacterial richness was not immediately lower in burned plots at 0.5 months while fungal richness was, and a decrease in cohesion may reflect cross-kingdom associations revealing a whole-community impact. This increase in positive associations potentially destabilizes communities. For example, should a second disturbance like another fire kill highly connected taxa this could lead to loss of associated taxa in the dependent module. In both sites, large wildfires occurred near our study sites, with the 2024 Airport Fire (95 km^2) occurring in the chaparral and the 2023 York Fire (377 km^2) in the desert. While there

was no overlap between the Dome and York fires, large areas burned by the Holy Fire were later reburned by the Airport Fire, potentially setting course for a different microbial successional trajectory following rapid return intervals in the chaparral. These trends have already been seen in boreal forests, in which community composition shifts in reburned areas compared to burned and unburned areas despite similarities in richness (Woolet et al. 2022).

To test the robustness of our results to unequal sample sizes, we compared the cohesion metric with an equal sample size between treatments. We only had 12 unburned reference samples per timepoint, and reducing burned sample numbers to 12 resulted in different observable trends in cohesion within the desert system but not in the chaparral. While methods such as SPIEC EASI attempt to solve the issue which arises when networks are constructed with a much greater number of nodes than samples (as is the case in most microbial communities), network stability is still strengthened by high sample number. Researchers attempting to classify regions as sensitive or recovered following disturbance should be careful to collect a large amount of samples per timepoint.

Network modules across sites: Wildfire altered microbial network structure differently across sites, with desert burns promoting increased connectivity and chaparral burns reducing modularity and stability. In our desert sites, burned networks had higher edge numbers and density than unburned networks across our 3-year study period. This increase in connectivity may reflect an increase in generalist or stress-tolerant taxa which

can facilitate broader associations. Burned plots also consistently had larger LCCs than unburned plots, regardless of initial drought at 0.5-8 months. In deserts, increasing aridity led to reductions in multifunctionality and network complexity of bacteria but not fungi, potentially driven by the deterministic soil properties that drove bacterial communities but not fungi (Dong et al. 2025). Few studies explore cross-kingdom associations, which were sparse in individual kingdom networks and much richer after combining (Fig. 3). The influx of nutrients after fire appeared to create more complex cross-kingdom associations in burned compared to unburned networks in the desert. However, modularity appeared to decrease initially at 0.5 months in burned desert plots, which is associated with environmental stress, as high modularity limits edges between nodes in the same module, preventing cascading effects during disturbance (Hernandez et al. 2021).

Chaparral networks showed the opposite pattern, in which unburned plots had large, complex modules with high numbers of edges and burned networks were more fragmented. Despite burning more plant mass, and causing more significant drops in richness and biomass compared to their local unburned communities, burned chaparral networks were still showing larger LCCs than desert burned plots, potentially reflecting a community more adapted to high-return intervals of fire. At 40 months in the chaparral, burned networks showed larger LCCs than unburned across sites, which suggests that desert wildfires select for transient microbial interactions between generalists, while chaparral wildfires result in richer microbial networks with long-term post-fire organic matter utilization. Burned chaparral networks also showed reduced modularity, to a

greater extent than the desert and for a longer period of time. This decrease in cohesion and modularity suggests more positive associations across modules as a result of shared niche preferences or sustained interdependence (Coyte et al. 2015) as microbes break down the abundant substrate post-fire.

Chaparral keystones: Overall, pyrophilous microbes appeared to be connectors across various modules in the burned chaparral networks, potentially reflecting a common habitat preference among many pyrophilous taxa or associations with distinct functional modules of post-fire substrate degradation. At 6 months, *Massilia* appeared to be a connector across different modules, likely as a result of its dominance within the community at that timepoint. *Inocybe* and *Candidatus Udaeobacter* were not otherwise dominant at 6 months, yet appeared to be important connectors and module hubs respectively. As an ectomycorrhizal fungus following widespread loss of other EMF taxa, *Inocybe* likely connects mycorrhizal plant seedlings and the microbial community, thus bridging different modules across the network, consistent with trends of ectomycorrhizal fungi in particular enhancing connectivity across multi-kingdom networks in forests (Yang et al. 2022). Meanwhile, *Candidatus Udaeobacter*, a genus of highly abundant grassland bacteria from Verrucomicrobiota, may contain species with a shrunken genome which more efficiently focus on key enzymatic pathways in amino acid synthesis (Brewer et al. 2016), while also driving dependence on other microbes. Members of this genus may also use high antibiotic resistance to scavenge critical biomolecules after antibiotic release kills other microbes (Willms et al. 2020), making them highly adapted to high

post-fire mortality of microbes. Further, the genus appears to be highly connected across desert soil networks (Li et al. 2021).

Certain taxa like *Noviherbaspirillum* highlight how dominant microbes can structure early successional networks by associating with low-abundance saprotrophs. While it initially grew in abundance at 3-months post-fire (Pulido-Chavez et al. 2023), *Noviherbaspirillum* emerged as a burn keystone at 12 months, positively associated with *Arsenicitalea*, *Flavitalea*, *Microvirga*, and a genus in Longimicrobiaceae (Fig. 5). Despite *Noviherbaspirillum* increasing in dominance, it mostly associated with low abundance bacteria. These taxa are known degraders, with *Arsenicitalea* reducing nitrate (Mu et al. 2016), *Flavitalea* (family Chitinophagaceae) showing high glycoside hydrolase activity (Kim et al. 2016), the type species in Longimicrobiaceae showing high phosphatase activity (Pascual et al. 2016), and *Microvirga* species displaying high heat and radiation tolerance and phosphatase (Li et al. 2020).

Desert keystones: In contrast to the chaparral, desert microbial keystone taxa in burned plots suggest a shift towards substrate-specializing generalists able to thrive in post-fire environments. The influx of nutrients in the burned plots shifting pH and substrates resulted in one connector and four module hub genera in burned networks across time. A bacterium referred to as wb1-P19 (Fig. 6), also found as a keystone in a cave system with basic soil in China (Li et al. 2021) and in the nearby Lehman Caves in Great Basin Nevada, possesses methanotroph genes including enzymes used to degrade methanol and formaldehyde, as well as a membrane-bound dissimilatory nitrate reductase (NarGHJI)

useful for nitrate reduction (Jones et al. 2024). Formaldehyde is a fire byproduct making wb1-P19 well-suited in post-fire substrate utilization (Liao et al. 2021, p. 202). This bacterium, along with *Crossiella*, another desert burn keystone, was found to be important for yellow biofilm formation in caves across the world (Martin-Pozas et al. 2024). *Crossiella* potentially forms syntrophic associations with nitrifying bacteria in cave systems (Martin-Pozas et al. 2022). *Pseudotricharina*, a member of Pyronemataceae, is poorly described but a likely post-fire saprotroph, or potentially related to orchid mycorrhizae (Healy et al. 2017). Unburned networks did not produce any connector or module hub genera, consistent with prokaryotic networks becoming less complex with increasing aridity (Dong et al. 2025).

Despite the precedence for identified keystone taxa in our study appearing as highly connected in other environments, we found no overlap between keystones in burned networks from chaparral and desert systems. While some taxa such as *Massilia* respond positively to fire in both systems, their overall importance in association networks differ. Additionally, bacterial and fungal keystones differed in their roles. Bacteria were linked to carbon and nitrogen turnover, whereas fungal keystones appeared to drive nutrient exchange or modify soil structure, traits strongly linked to Ascomycota (Lehmann et al. 2020) and ectomycorrhizal fungi (Zheng et al. 2014). Further studies of post-fire microbes across varying habitats may reveal more consistent trends of common keystone taxa within the post-fire microbial succession, but network analysis is not yet a ubiquitous tool applied in studies of microbial ecology. While some taxa we highlight are not known to be pyrophilous, these findings may warrant further investigation into their

roles post-fire to better understand how the post-fire environment changes with their presence. Studies testing post-disturbance inoculation may find greater recruitment of multifunctional taxa by adding the high across-module connected keystones from the burned chaparral networks, or high facilitation following inoculation of the generalist within-module connected desert network keystones.

4.6 Conclusion

We showed that network analysis reveals signals of microbial stress not detected by traditional diversity metrics alone. While richness appeared stable in deserts, networks revealed a lagging decrease in cohesion suggesting microbial sensitivity to further disturbance in deserts. In contrast, chaparral networks were initially fragmented post-fire but became highly connected by 12 months, potentially showing signs of microbial adaptation to more frequent fire intervals. However, the chaparral networks still showed signs of sensitivity to further disturbance at 40 months, indicating that reburns like the 2024 Airport Fire may be degrading association networks moreso than a single burn would.

Keystone taxa, which are often low-abundance yet highly connected, were abundant in chaparral yet sparse in desert networks. Genera did not re-occur as keystones across timepoints, potentially matching successional patterns of post-fire plant communities with distinct stages, and were distinct across habitats corresponding to fire-adapted microbes in the chaparral and more broadly found saprotrophs in the desert. These findings highlight that assessing ecosystem recovery after disturbance can be

enhanced by network-based metrics. However, these studies should include robust sampling regimes to ensure network stability and reproducibility. Further insights can be found in sampling specific microsites such as biocrusts and rhizosphere soil to better understand what interactions are occurring when microbes are in close proximity.

Taken together, our results mostly aligned with our initial predictions, such that cohesion did not recover at 3-years following the high-intensity chaparral fire. However, we expected an initial reduction in post-fire cohesion in the low-intensity desert fire and instead saw high post-fire cohesion up to 8-months post-fire and a longer term reduction at 3-years rather than a recovery. Our analysis of two similarly sampled wildfires showed that cross-kingdom network approaches uncovered novel post-fire keystone taxa, either as known pyrophilous microbes or associated with a variety of pyrophilous taxa within modules, which can be used to explore both direct interactions as well as key post-fire successional shifts following wildfires.

4.7 Figures

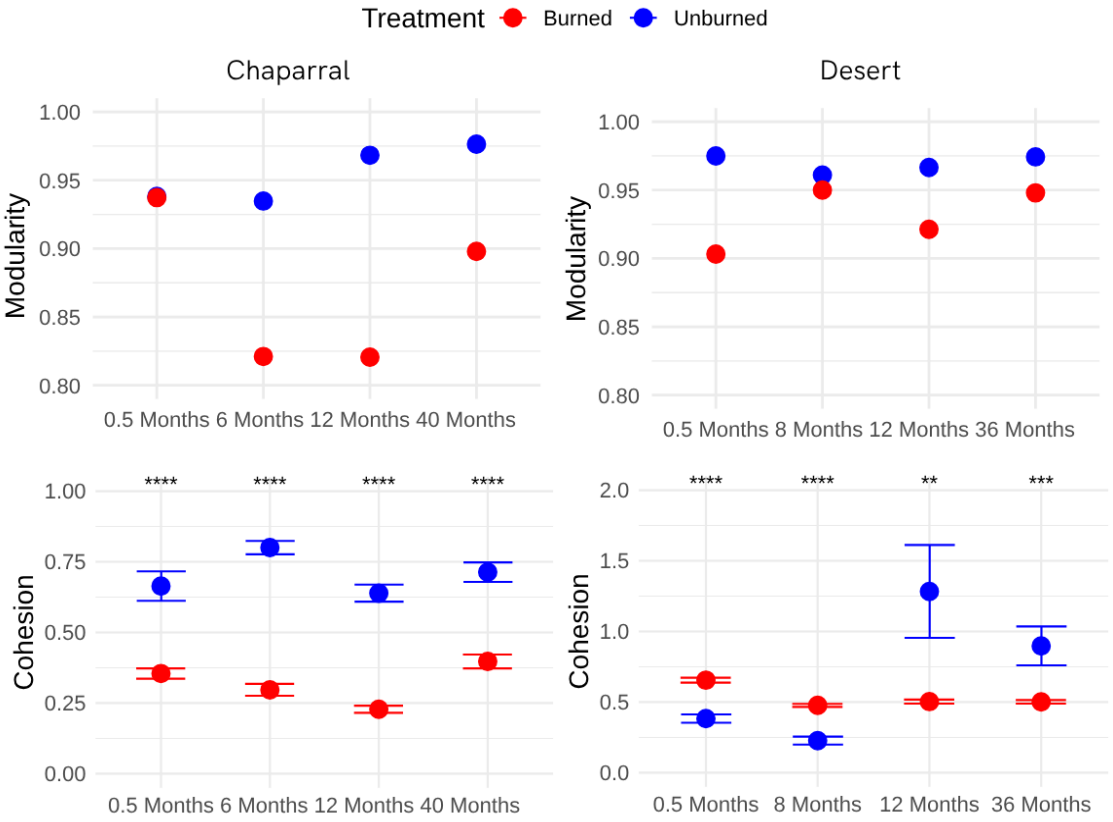

Figure 4.7.1 Network metrics from the chaparral and desert. Modularity is a measure of how often edges connect nodes within modules rather than across different modules. Cohesion is a measure of the ratio of negative to positive edges, weighted by abundance of the nodes between the edges.

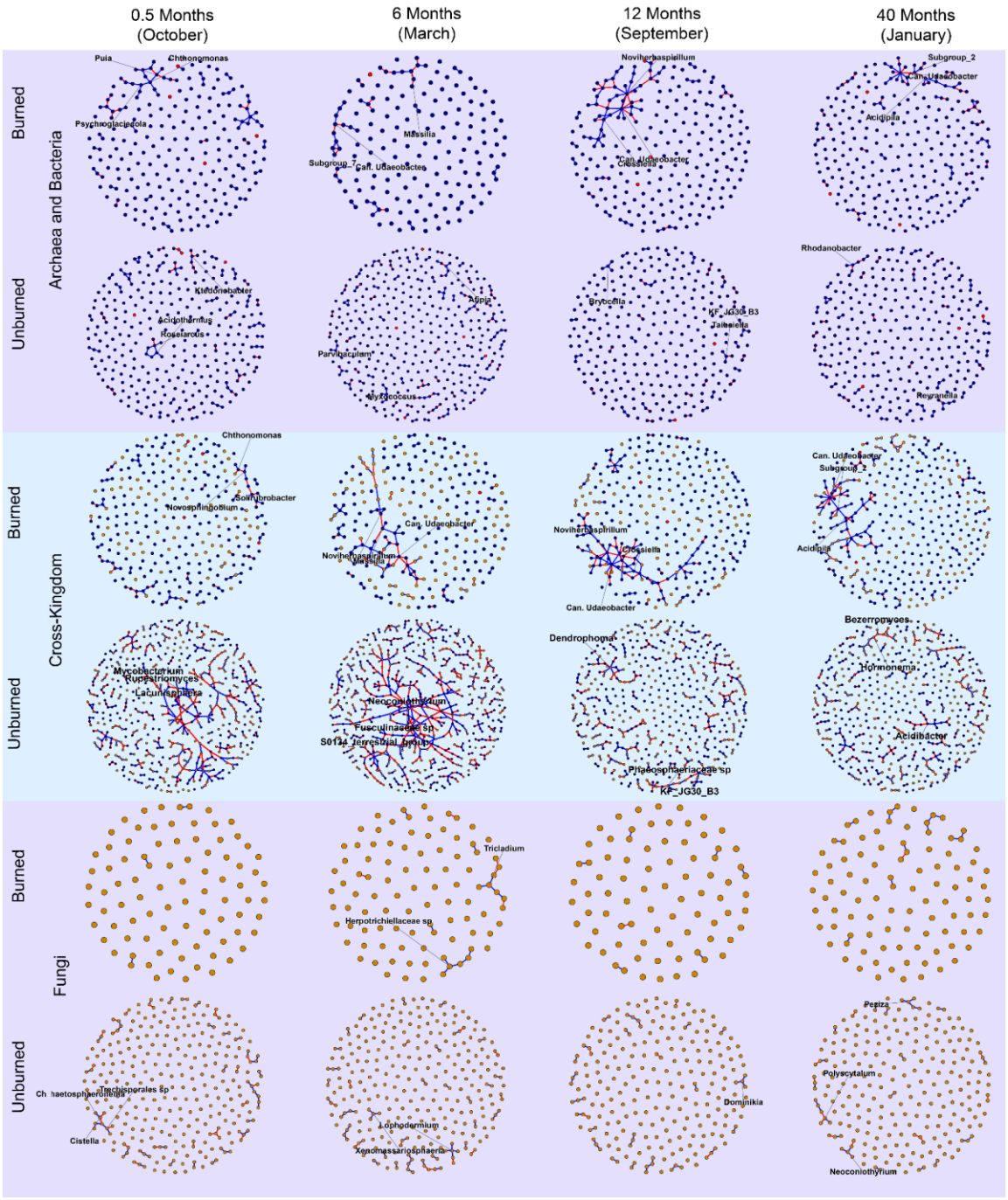

Figure 4.7.2 Networks from chaparral 16S and ITS2 sequence data in purple respectively. Cross-kingdom networks displayed in blue. Blue edges are positive associations and red edges are negative. Node colors correspond to kingdoms, with red being archaea, blue being bacteria, and orange being fungi.

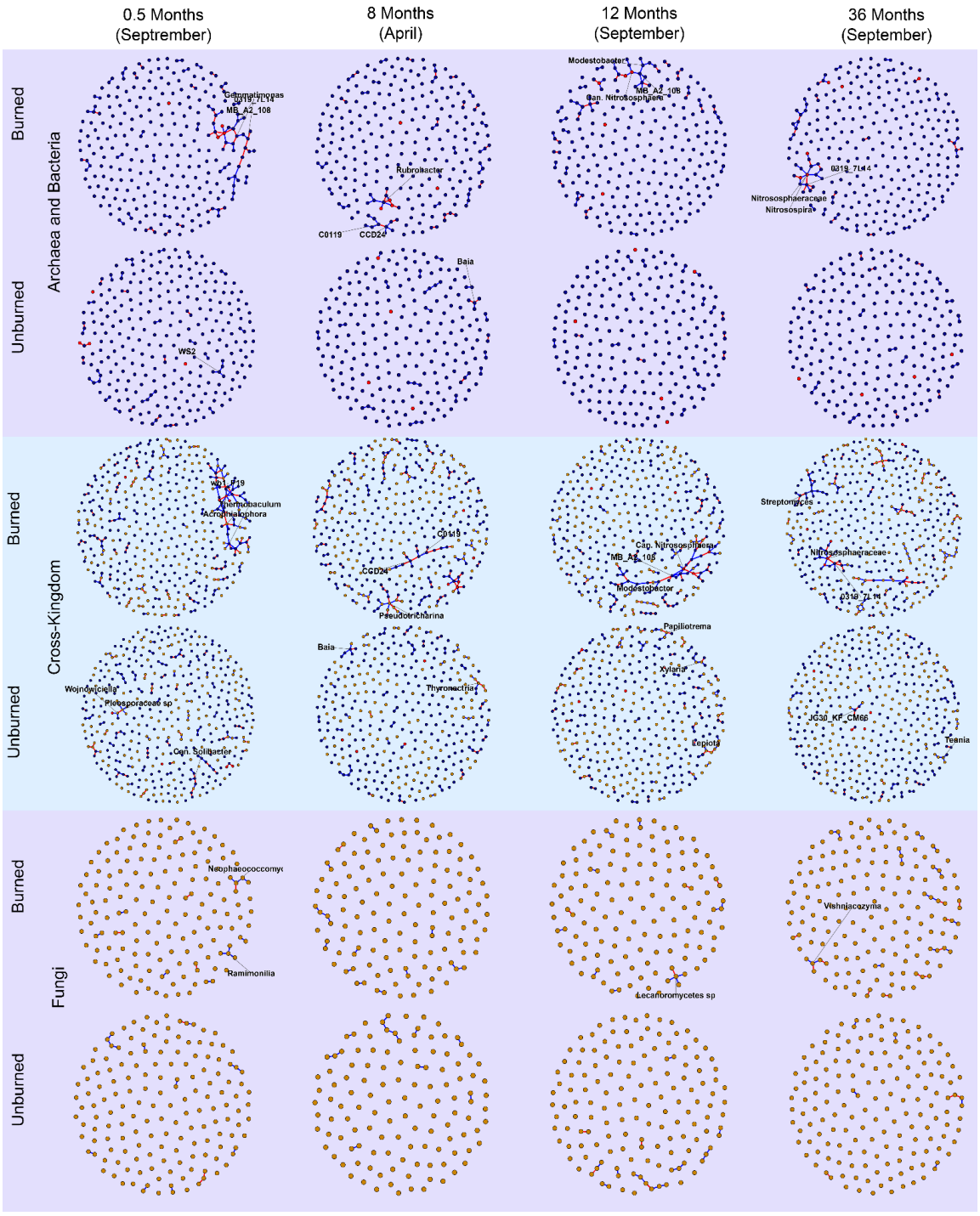

Figure 4.7.3 Networks from desert 16S and ITS2 sequence data in purple respectively. Cross-kingdom networks displayed in blue. Blue edges are positive associations and red edges are negative. Node colors correspond to kingdoms, with red being archaea, blue being bacteria, and orange being fungi.

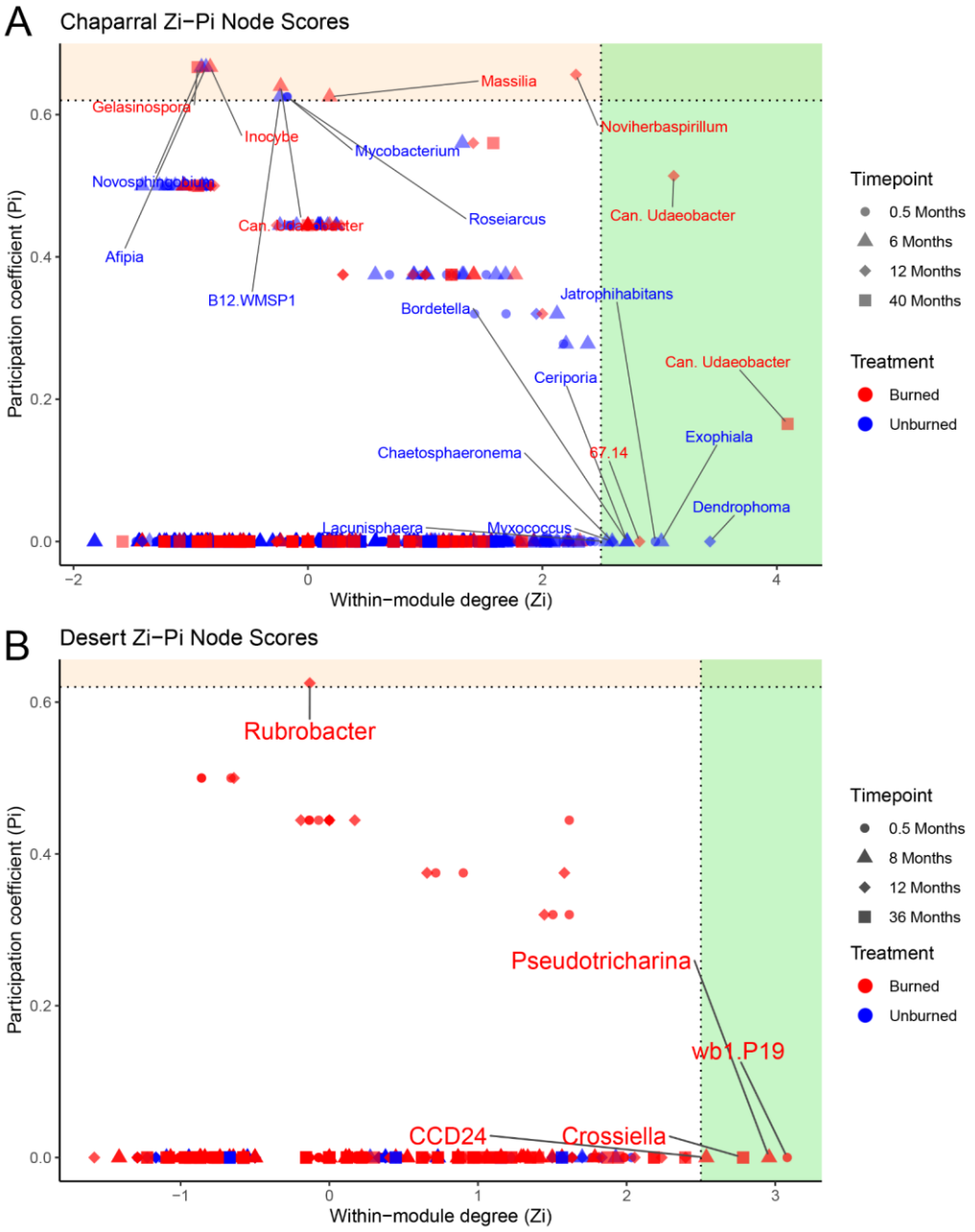

Figure 4.7.4 Zi-Pi plots of cross-kingdom networks from A) chaparral and B) desert systems. Shapes indicate timepoints, and colors indicate treatment (red and blue are burned and unburned respectively). Peripheral taxa with few connections (Zi < 2.5 and Pi < 0.62), module hubs with in-module connectivity or many edges (Zi > 2.5, Pi < 0.62), connector nodes with many edges across modules (Zi < 2.5, Pi > 0.62), and network hubs which are highly connected both within and across modules (Zi >2.5, Pi > 0.62).

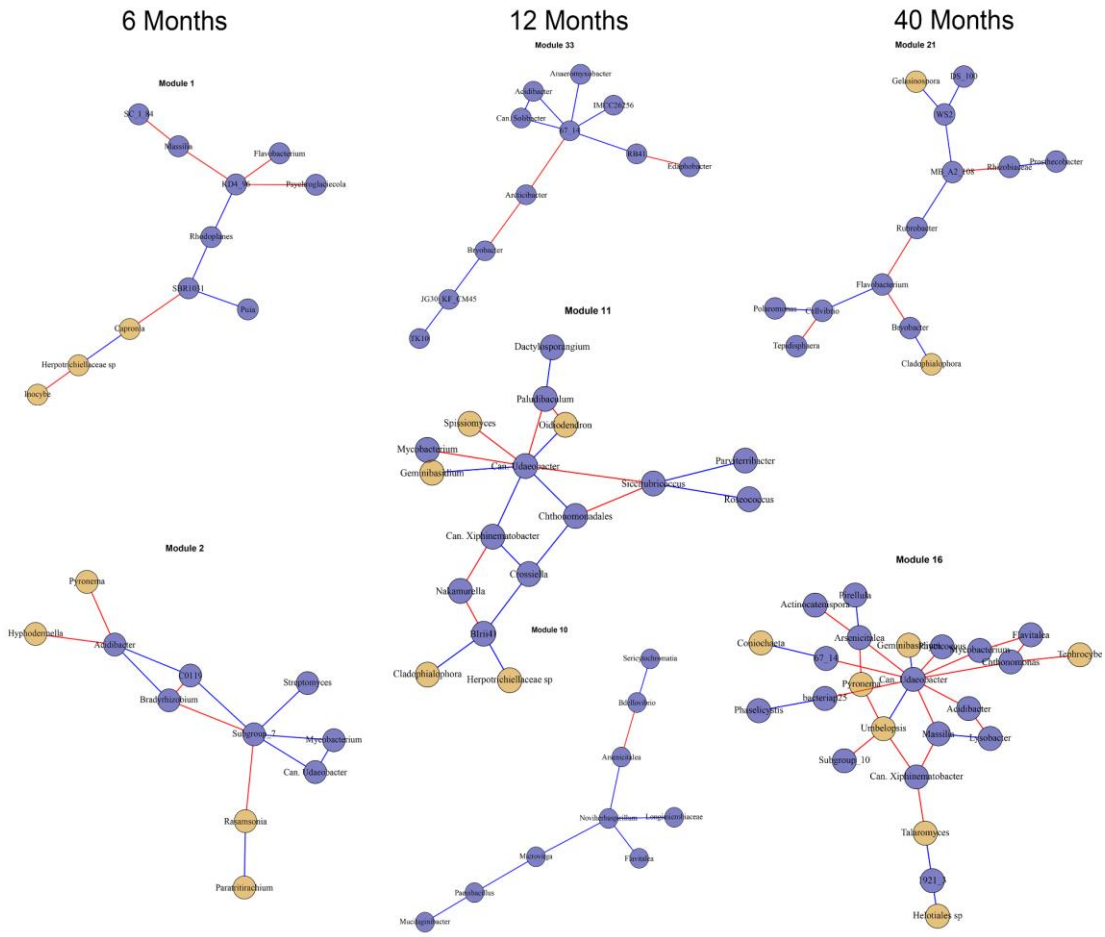

Figure 4.7.5 Modules of burned network hubs in the chaparral site. Blue edges are positive associations and red edges are negative. Node colors correspond to kingdoms, with red being archaea, blue being bacteria, and orange being fungi.

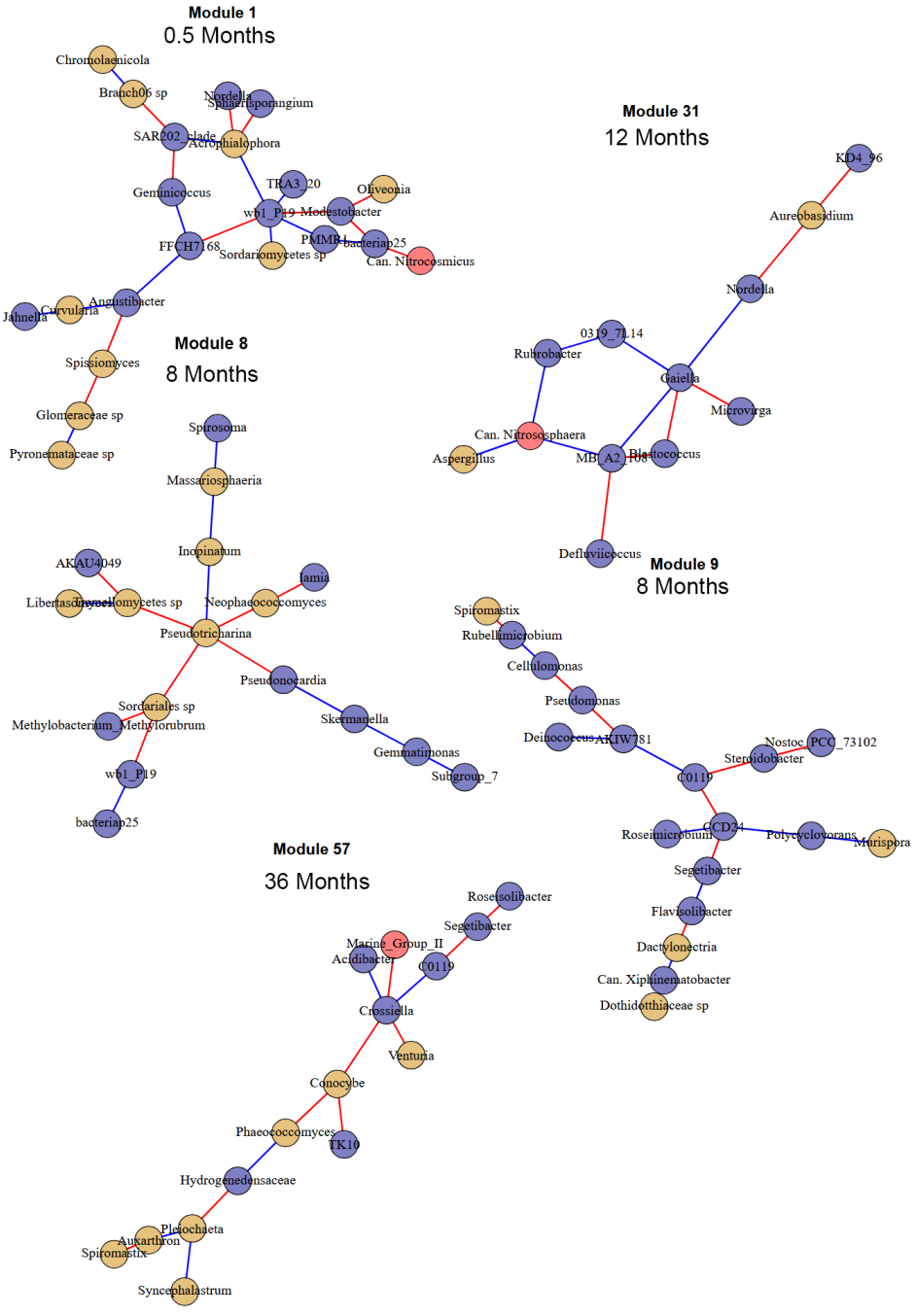

Figure 4.7.6 Modules of burned network hubs of all timepoints from the desert site. Blue edges are positive associations and red edges are negative. Node colors correspond to kingdoms, with red being archaea, blue being bacteria, and orange being fungi.

4.8 Supplemental Figures

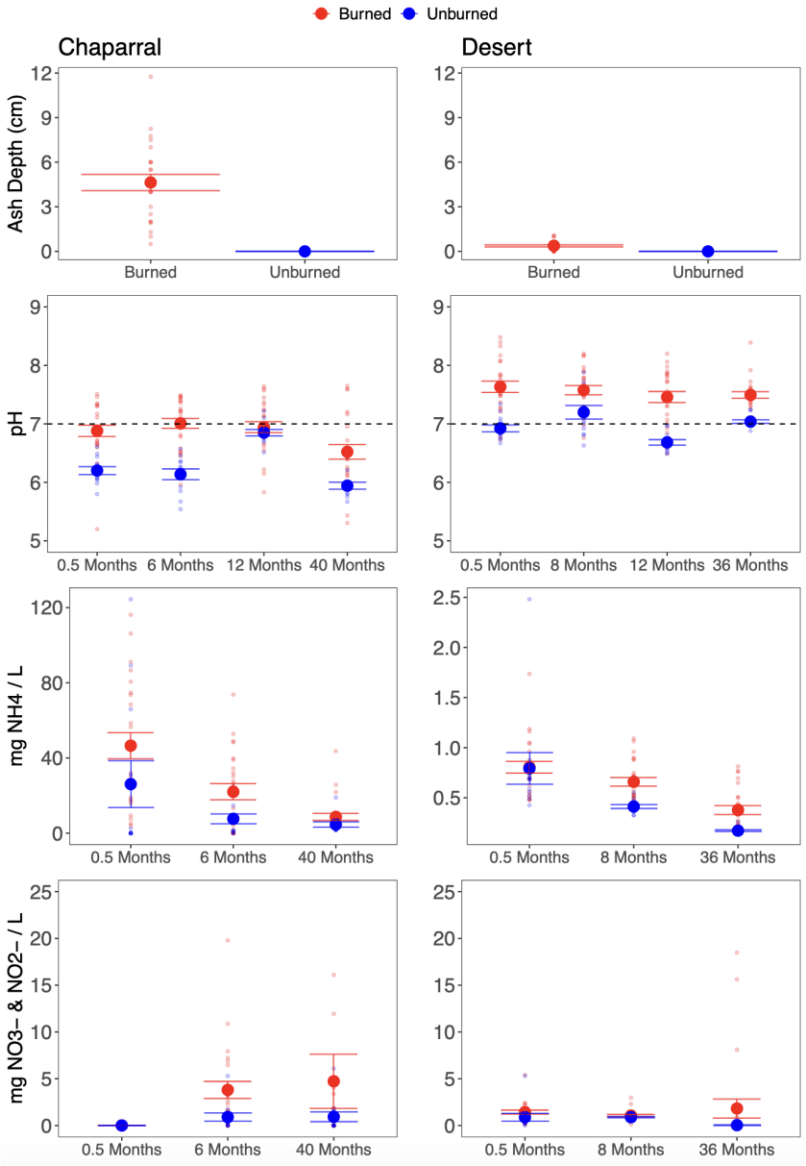

Figure 4.8.1 Fire impacts on soil in chaparral and desert. Red and blue points indicate means of burned and unburned plots with standard error bars. We measured ash depth at the first timepoint post-fire, pH at every timepoint, and measured ammonium, nitrate, and nitrite through KCl extractions at select timepoints.

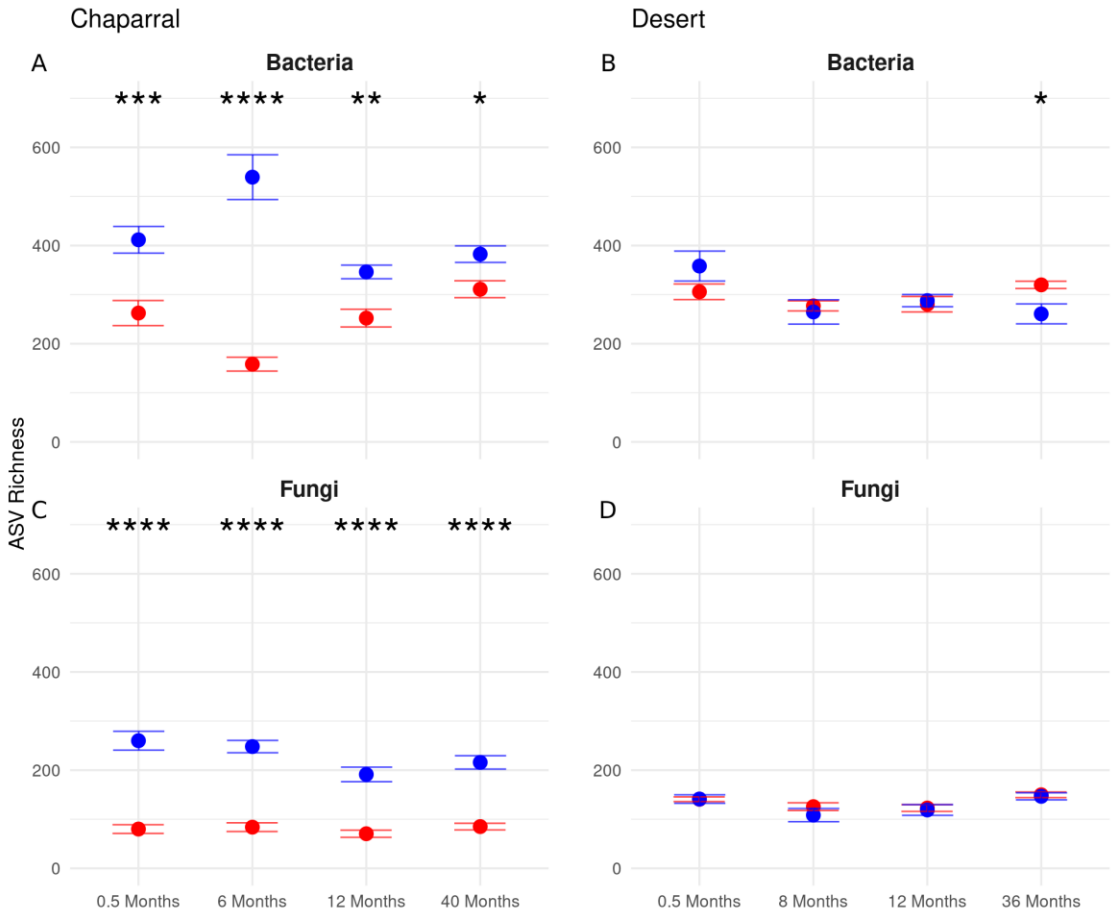

Figure 4.8.2 ASV richness in bacteria as determined by 16S sequencing from A) the chaparral and B) desert. ASV richness in fungi as determined by ITS2 sequencing from C) the chaparral and D) desert.

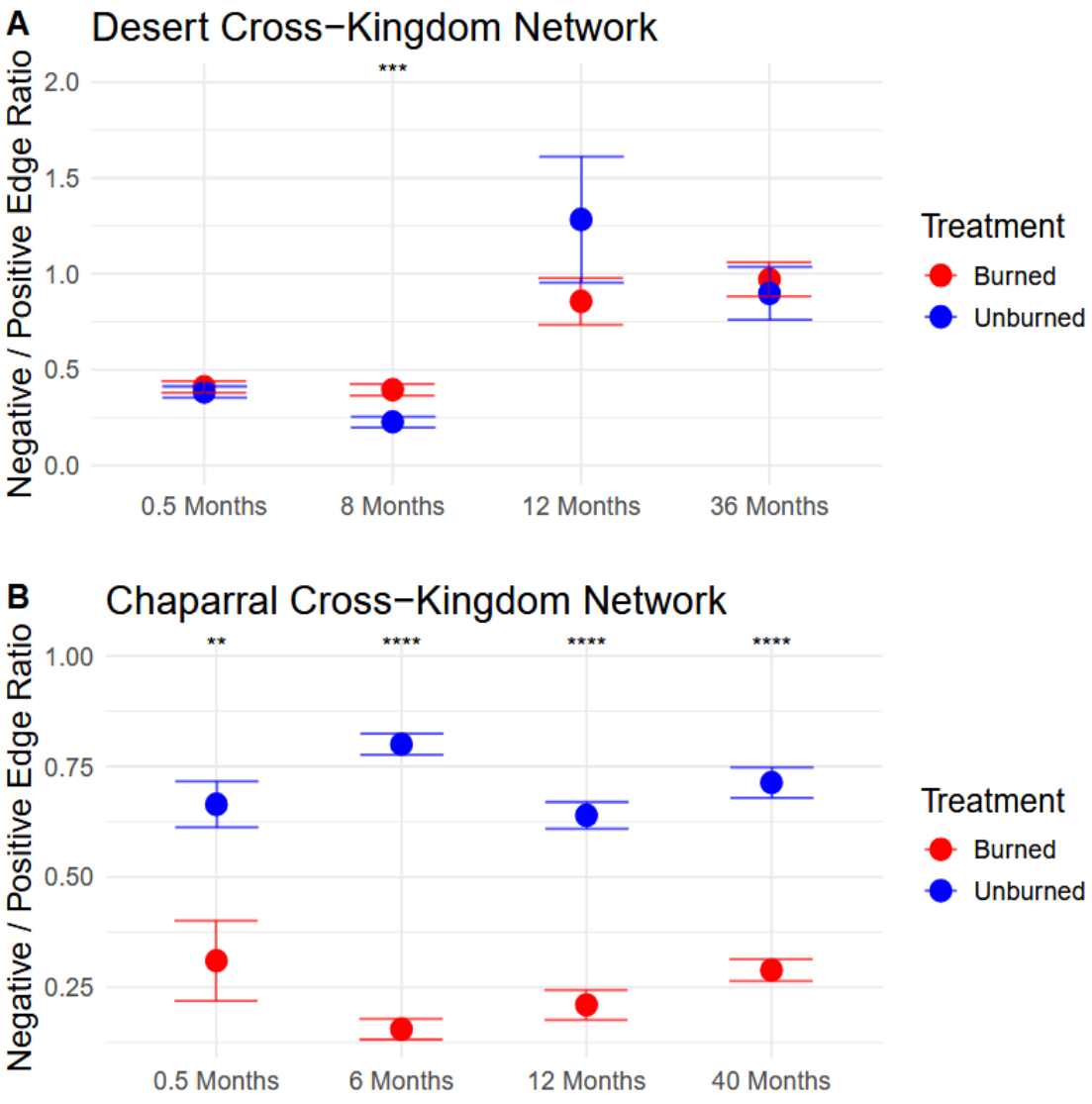

Figure 4.8.3 Cross-kingdom cohesion results after subsampling burned networks to match the number of unburned samples. Networks constructed with n = 12 samples, randomly selected from a pool of 24 burned samples per timepoint.

5 Chapter V.
Conclusion to the Dissertation

This dissertation provides the first broad-scale, long-term, and network-based assessment of desert microbial communities following seasonal changes and post-fire shifts, revealing a diverse community of AMF, resiliency in community composition, and network sensitivity. Notably, *Yucca jaegeriana* was dominated by the AMF *Glomus* VTX00294 year-round, a taxon not previously recorded in *Y. brevifolia* (Harrower and Gilbert 2021), despite the presence of *Glomus* VTX00294 in other continents (Davison et al. 2015), suggesting greater host specificity than is commonly assumed. Microbial abundance and diversity remained stable following the Dome Fire, and the broader microbial community showed compositional shifts without losses in richness or biomass. Network analysis revealed hidden sensitivity in burned soils despite stable or even rising microbial diversity post-fire, with the rarely studied bacterium *Crossiella* emerging as a potential post-fire keystone microbe, consistent with its assignment as a keystone in other systems (Cheng et al. 2023). Together, these findings challenge assumptions about post-fire trends of microbial communities in arid ecosystems, enhance methods of identifying important post-fire microbes and their associations, and lend further support to observing cohesion post-fire as an assessment of fire impacts on microbes, informing land management in an era of increasing wildfire frequency.

In my first research chapter, I showed that the AMF associated with *Yucca jaegeriana* are diverse, distinct from the closely related *Y. brevifolia*, more diverse when

sampled from soils than roots, stable across seasons but reduced in summer, and largely unaffected by fire. The AMF community was most rich in the Fall and Winter, consistent with the Yucca growth habits. Since Joshua tree seedlings are more likely to die when sprouting in the Spring and facing Summer heat (DeFalco et al. 2010), and also show preferential uptake of warmer Summer rains compared to cooler Winter rains (Ehleringer et al. 1991), there appears to be parity in the increasing abundance of AMF species associating with *Y. jaegeriana* in Fall and Winter months. Further, the AMF community was largely distinct from the AMF associating with *Y. brevifolia* some ~100km southwest in Joshua Tree National Park, despite similar edaphic properties. This may lend further evidence that AMF are not as broadly generalist in their host associations as previously thought.

In my second research chapter, I showed that the Dome Fire had limited impacts on archaeal, bacterial, and fungal biomass and richness despite widespread mortality of *Y. jaegeriana*, but community composition was affected such that pyrophilous microbes were stimulated. Burned soil did not significantly decrease in microbial richness or biomass, and in fact grew in richness and biomass at certain timepoints because of excess nutrients available in the soil, or potentially due to pH which remained increased 3 years post-fire. While richness is a good estimate for functional diversity in an environment, it can easily be masked by increases and decreases in different groups of taxa, and beta-diversity comparisons may miss shifts in critically important taxa if the overall communities still appear to be similar. However, there appeared to be overall resilience by the microbial community in response to a high-severity wildfire that had dramatic

impacts on the aboveground plant community. Several pyrophilous microbes emerged, with a large number of fungi increasing 3-years post-fire, and a select few archaea and bacteria. Many of the microbes found positively responding to fire overlapped with those increasing in forest fires (Whitman et al. 2019; Caiafa et al. 2023) and chaparral fires (Pulido-Chavez et al. 2023), prompting further inquiries into their importance in post-fire desert nutrient cycling and community recovery.

In my third research chapter, I further compared burned and unburned desert samples to a chaparral wildfire to determine differing network properties across fires of varying intensity. The low-intensity desert fire matched signs of sensitivity found in the high-intensity chaparral fire even at 3-years post-fire, suggesting greater impacts on the cross-kingdom microbial community than the diversity metrics would suggest. While pyrophilous microbes were important to network structure in the chaparral, they did not overlap with potential keystones identified in the desert burn networks, which instead overlapped with network-identified keystone taxa found in other low-nutrient environments like caves. In either case, keystone taxa from the unburned communities did not appear to be important to burned community networks, highlighting the broader shift in post-fire communities.

While pyrophilous microbes emerged in the desert post-fire, these taxa did not appear as important to network architecture. Understanding their ecological roles may require inoculum manipulations, in which only a few microbes are placed in experimental burn systems shortly after burning soil to disentangle actual pyrophilous microbe interactions in situ. While trends of association in bulk soil mixes may reveal overall

community sensitivity, there may also be microsites in which specific interactions occur such as on root surfaces, in soil pores, or directly on degrading litter surfaces. As sequencing costs continue to decline, large-scale sampling of such sites may greatly increase our understanding of which microbes appear to associate under certain environments, allowing us to initially bypass the difficulties associated with culture-based pairwise testing of direct microbial interactions. Our work showcases a diverse desert microbiome that reflects trends found in pyrophilous microbes globally, while highlighting an innate resilience to extreme heat. In the face of a shifting climate, these findings can initiate testing on mycorrhizal consortia which are already adapted to the conditions found in the ever-expanding drylands, and appear to show hubs of microbes with important post-fire activity occurring across environments.

5.1 References

Aanderud ZT, Bahr J, Robinson DM, et al (2019) The Burning of Biocrusts Facilitates the Emergence of a Bare Soil Community of Poorly-Connected Chemoheterotrophic Bacteria With Depressed Ecosystem Services. Front Ecol Evol 7:. https://doi.org/10.3389/fevo.2019.00467

Aanderud ZT, Smart TB, Wu N, et al (2018) Fungal loop transfer of nitrogen depends on biocrust constituents and nitrogen form. Biogeosciences 15:3831–3840. https://doi.org/10.5194/bg-15-3831-2018

Abarenkov K, Nilsson RH, Larsson K-H, et al (2010) The UNITE database for molecular identification of fungi – recent updates and future perspectives. New Phytologist 186:281–285. https://doi.org/10.1111/j.1469-8137.2009.03160.x

Abella SR (2009) Post-fire plant recovery in the Mojave and Sonoran Deserts of western North America. Journal of Arid Environments 73:699–707. https://doi.org/10.1016/j.jaridenv.2009.03.003

Abella SR (2010) Disturbance and Plant Succession in the Mojave and Sonoran Deserts of the American Southwest. International Journal of Environmental Research and Public Health 7:1248–1284. https://doi.org/10.3390/ijerph7041248

Abella SR, Gentilcore DM, Chiquoine LP (2021) Resilience and alternative stable states after desert wildfires. Ecological Monographs 91:e01432. https://doi.org/10.1002/ecm.1432

Adkins J, Docherty KM, Miesel JR (2022) Copiotrophic Bacterial Traits Increase With Burn Severity One Year After a Wildfire. Front For Glob Change 5:. https://doi.org/10.3389/ffgc.2022.873527

Agbeshie AA, Abugre S, Atta-Darkwa T, Awuah R (2022) A review of the effects of forest fire on soil properties. J For Res 33:1419–1441. https://doi.org/10.1007/s11676-022-01475-4

Aguilar-Fernández M, Jaramillo VJ, Varela-Fregoso L, Gavito ME (2009) Short-term consequences of slash-and-burn practices on the arbuscular mycorrhizal fungi of a tropical dry forest. Mycorrhiza 19:179–186. https://doi.org/10.1007/s00572-009-0229-2

Alguacil M del M, Torres MP, Montesinos-Navarro A, Roldán A (2016) Soil Characteristics Driving Arbuscular Mycorrhizal Fungal Communities in Semiarid Mediterranean Soils. Applied and Environmental Microbiology 82:3348–3356. https://doi.org/10.1128/AEM.03982-15

Allen EB, Steers RJ, Dickens SJ (2011) Impacts of Fire and Invasive Species on Desert Soil Ecology. Rangeland Ecology & Management 64:450–462. https://doi.org/10.2111/REM-D-09-00159.1

Allen M (1992) Mycorrhizal Functioning: An Integrative Plant-Fungal Process. Springer Science & Business Media

Allen MF (1989) Mycorrhizae and rehabilitation of disturbed arid soils: Processes and practices. Arid Soil Research and Rehabilitation 3:229–241. https://doi.org/10.1080/15324988909381201

Amit G, Bashan A (2023) Top-down identification of keystone taxa in the microbiome. Nat Commun 14:3951. https://doi.org/10.1038/s41467-023-39459-5

Angel R, Soares MIM, Ungar ED, Gillor O (2010) Biogeography of soil archaea and bacteria along a steep precipitation gradient. The ISME Journal 4:553–563. https://doi.org/10.1038/ismej.2009.136

Aponte H, Galindo-Castañeda T, Yáñez C, et al (2022) Microbial Community-Level Physiological Profiles and Genetic Prokaryotic Structure of Burned Soils Under Mediterranean Sclerophyll Forests in Central Chile. Front Microbiol 13:. https://doi.org/10.3389/fmicb.2022.824813

Apple M, Thee C, Smith-Becker V, et al (2005) Arbuscular mycorrhizal colonization of Larrea tridentata and Ambrosia dumosa roots varies with precipitation and season in the Mojave Desert. SYMBIOSIS 39:

Arel-Bundock V, Gassen J, Eastwood N, et al (2022) modelsummary: Summary Tables and Plots for Statistical Models and Data: Beautiful, Customizable, and Publication-Ready

Arunrat N, Sansupa C, Sereenonchai S, Hatano R (2024) Short-term response of soil bacterial and fungal communities to fire in rotational shifting cultivation, northern Thailand. Applied Soil Ecology 196:105303. https://doi.org/10.1016/j.apsoil.2024.105303

Augé RM (2001) Water relations, drought and vesicular-arbuscular mycorrhizal symbiosis. Mycorrhiza 11:3–42. https://doi.org/10.1007/s005720100097

Augé RM, Toler HD, Saxton AM (2015) Arbuscular mycorrhizal symbiosis alters stomatal conductance of host plants more under drought than under amply watered conditions: a meta-analysis. Mycorrhiza 25:13–24. https://doi.org/10.1007/s00572-014-0585-4

Banerjee S, Schlaeppi K, van der Heijden MGA (2018) Keystone taxa as drivers of microbiome structure and functioning. Nat Rev Microbiol 16:567–576. https://doi.org/10.1038/s41579-018-0024-1

Barnes ME, Johnson DW, Hart SC (2024) The Median Isn't the Message: soil nutrient hot spots have a disproportionate influence on biogeochemical structure across years, seasons, and depths. Biogeochemistry 167:75–95. https://doi.org/10.1007/s10533-023-01107-x

Bates D, Maechler M, Bolker B, et al (2024) lme4: Linear Mixed-Effects Models using "Eigen" and S4

Bates D, Maechler M, Bolker B, et al (2015) Package 'lme4.' convergence 12:2

Bellgard SE, Whelan RJ, Muston RM (1994) The impact of wildfire on vesicular-arbuscular mycorrhizal fungi and their potential to influence the re-establishment of post-fire plant communities. Mycorrhiza 4:139–146. https://doi.org/10.1007/BF00203532

Belmok A, Rodrigues-Oliveira T, Lopes FAC, et al (2019) Long-Term Effects of Periodical Fires on Archaeal Communities from Brazilian Cerrado Soils. Archaea 2019:6957210. https://doi.org/10.1155/2019/6957210

Bencherif K, Boutekrabt A, Dalpé Y, Lounès-Hadj Sahraoui A (2016) Soil and seasons affect arbuscular mycorrhizal fungi associated with *Tamarix* rhizosphere in arid and semi-arid steppes. Applied Soil Ecology 107:182–190. https://doi.org/10.1016/j.apsoil.2016.06.003

Benedict KB, Prenni AJ, Carrico CM, et al (2017) Enhanced concentrations of reactive nitrogen species in wildfire smoke. Atmospheric Environment 148:8–15. https://doi.org/10.1016/j.atmosenv.2016.10.030

Bever JD, Schultz PA, Pringle A, Morton JB (2001) Arbuscular Mycorrhizal Fungi: More Diverse than Meets the Eye, and the Ecological Tale of Why: The high diversity of ecologically distinct species of arbuscular mycorrhizal fungi within a single community has broad implications for plant ecology. BioScience 51:923–931. https://doi.org/10.1641/0006-3568(2001)051%255B0923:AMFMDT%255D2.0.CO;2

Birch JD, Lutz JA, Dickinson MB, et al (2025) Small-scale fire refugia increase soil bacterial and fungal richness and increase community cohesion nine years after fire. Science of The Total Environment 966:178677. https://doi.org/10.1016/j.scitotenv.2025.178677

Bisanz JE (2018) qiime2R: Importing QIIME2 artifacts and associated data into R sessions. https://github.com/jbisanz/qiime2R. Accessed 9 Feb 2025

Błaszkowski J (2012) Glomeromycota. W. Szafer Institute of Botany, Polish Academy of Sciences

Blazewicz SJ, Schwartz E, Firestone MK (2014) Growth and death of bacteria and fungi underlie rainfall-induced carbon dioxide pulses from seasonally dried soil. Ecology 95:1162–1172. https://doi.org/10.1890/13-1031.1

Bolyen E, Rideout JR, Dillon MR, et al (2019) Reproducible, interactive, scalable and extensible microbiome data science using QIIME 2. Nature Biotechnology 37:852–857. https://doi.org/10.1038/s41587-019-0209-9

Brewer TE, Handley KM, Carini P, et al (2016) Genome reduction in an abundant and ubiquitous soil bacterium 'Candidatus Udaeobacter copiosus.' Nat Microbiol 2:16198. https://doi.org/10.1038/nmicrobiol.2016.198

Brianne P, Rebecca H, David L (2020) The fate of biological soil crusts after fire: A meta-analysis. Global Ecology and Conservation 24:e01380. https://doi.org/10.1016/j.gecco.2020.e01380

Brooks ML, Berry KH (2006) Dominance and environmental correlates of alien annual plants in the Mojave Desert, USA. Journal of Arid Environments 67:100–124. https://doi.org/10.1016/j.jaridenv.2006.09.021

Brooks ML, Matchett JR (2006) Spatial and temporal patterns of wildfires in the Mojave Desert, 1980–2004. Journal of Arid Environments 67:148–164. https://doi.org/10.1016/j.jaridenv.2006.09.027

Brundrett MC, Tedersoo L (2018) Evolutionary history of mycorrhizal symbioses and global host plant diversity. New Phytol 220:1108–1115. https://doi.org/10.1111/nph.14976

Bruns TD, Chung JA, Carver AA, Glassman SI (2020) A simple pyrocosm for studying soil microbial response to fire reveals a rapid, massive response by Pyronema species. PLOS ONE 15:e0222691. https://doi.org/10.1371/journal.pone.0222691

Caiafa MV, Nelson AR, Borch T, et al (2023) Distinct fungal and bacterial responses to fire severity and soil depth across a ten-year wildfire chronosequence in beetle-killed lodgepole pine forests. Forest Ecology and Management 544:121160. https://doi.org/10.1016/j.foreco.2023.121160

Callahan BJ, McMurdie PJ, Rosen MJ, et al (2016) DADA2: High-resolution sample inference from Illumina amplicon data. Nat Methods 13:581–583. https://doi.org/10.1038/nmeth.3869

Camenzind T, Aguilar-Trigueros CA, Heuck MK, et al (2024) Progressing beyond colonization strategies to understand arbuscular mycorrhizal fungal life history. New Phytologist 244:752–759. https://doi.org/10.1111/nph.20090

Canini F, Borruso L, Newsham KK, et al (2023) Wide divergence of fungal communities inhabiting rocks and soils in a hyper-arid Antarctic desert. Environmental Microbiology 25:3671–3682. https://doi.org/10.1111/1462-2920.16534

Caporaso JG, Lauber CL, Walters WA, et al (2011) Global patterns of 16S rRNA diversity at a depth of millions of sequences per sample. PNAS 108:4516–4522. https://doi.org/10.1073/pnas.1000080107

Carpenter SE, Trappe JM (1985) Phoenicoid fungi: a proposed term for fungi that fruit after heat treatment of substrates. Mycotaxon 23:203–206

Carter MR, Gregorich EG (eds) (2007) Soil Sampling and Methods of Analysis, 2nd edn. CRC Press, Boca Raton

Certini G, Moya D, Lucas-Borja ME, Mastrolonardo G (2021) The impact of fire on soil-dwelling biota: A review. Forest Ecology and Management 488:118989. https://doi.org/10.1016/j.foreco.2021.118989

Chaudhary VB, Nokes LF, González JB, et al (2025) TraitAM, a global spore trait database for arbuscular mycorrhizal fungi. Sci Data 12:588. https://doi.org/10.1038/s41597-025-04940-x

Chaudhary VB, Nolimal S, Sosa-Hernández MA, et al (2020) Trait-based aerial dispersal of arbuscular mycorrhizal fungi. New Phytologist 228:238–252. https://doi.org/10.1111/nph.16667

Chaudhary VB, O'Dell TE, Rillig MC, Johnson NC (2014) Multiscale patterns of arbuscular mycorrhizal fungal abundance and diversity in semiarid shrublands. Fungal Ecology 12:32–43. https://doi.org/10.1016/j.funeco.2014.06.003

Chávez-González JD, Flores-Núñez VM, Merino-Espinoza IU, Partida-Martínez LP (2024) Desert plants, arbuscular mycorrhizal fungi and associated bacteria: Exploring the diversity and role of symbiosis under drought. Environmental Microbiology Reports 16:e13300. https://doi.org/10.1111/1758-2229.13300

Chen H (2022) VennDiagram: Generate High-Resolution Venn and Euler Plots

Chen Y-L, Xu T-L, Veresoglou SD, et al (2017) Plant diversity represents the prevalent determinant of soil fungal community structure across temperate grasslands in northern China. Soil Biology and Biochemistry 110:12–21. https://doi.org/10.1016/j.soilbio.2017.02.015

Cheng X, Xiang X, Yun Y, et al (2023) Archaea and their interactions with bacteria in a karst ecosystem. Front Microbiol 14:. https://doi.org/10.3389/fmicb.2023.1068595

Cherlet M, Hutchinson C, Reynolds J, et al (2018) World Atlas of Desertification. In: JRC Publications Repository. https://publications.jrc.ec.europa.eu/repository/handle/JRC111155. Accessed 14 Nov 2024

Chimal-Sánchez E, Araiza-Jacinto ML, Román-Cárdenas VJ (2015) Fire effect on arbuscular mycorrhizal fungi species richness associated with plants of desert scrubland in the Eco Park "Cubitos." TIP 18:107–115. https://doi.org/10.1016/j.recqb.2015.09.002

Chungopast S, Phankamolsil N, Thaymuang W, et al (2023) Correlation of Soil Physiochemical Properties, Microorganism Numbers, and Bacterial Communities Following Unburned and Burned Sugarcane Harvest. Applied and Environmental Soil Science 2023:9618349. https://doi.org/10.1155/2023/9618349

Clark NM, Rillig MC, Nowak RS (2009) Arbuscular mycorrhizal fungal abundance in the Mojave Desert: Seasonal dynamics and impacts of elevated CO2. Journal of Arid Environments 73:834–843. https://doi.org/10.1016/j.jaridenv.2009.03.004

Collins SL, Belnap J, Grimm NB, et al (2014) A Multiscale, Hierarchical Model of Pulse Dynamics in Arid-Land Ecosystems. Annual Review of Ecology, Evolution, and Systematics 45:397–419. https://doi.org/10.1146/annurev-ecolsys-120213-091650

Cottam G, Curtis JT, Hale BW (1953) Some Sampling Characteristics of a Population of Randomly Dispersed Individuals. Ecology 34:741–757. https://doi.org/10.2307/1931337

Cowan DA, Hopkins DW, Jones BE, et al (2020) Microbiomics of Namib Desert habitats. Extremophiles 24:17–29. https://doi.org/10.1007/s00792-019-01122-7

Coyte KZ, Schluter J, Foster KR (2015) The ecology of the microbiome: Networks, competition, and stability. Science 350:663–666. https://doi.org/10.1126/science.aad2602

Csardi MG (2013) Package 'igraph.' Last accessed 3:2013

d'Entremont TW, Kivlin SN (2023) Specificity in plant-mycorrhizal fungal relationships: prevalence, parameterization, and prospects. Front Plant Sci 14:. https://doi.org/10.3389/fpls.2023.1260286

Da Costa CRG, Coelho Moura D, De Lima Marques A, et al (2021) Biological rhythms of Arbuscular Mycorrhizal Fungi under influence of seasonality in semiarid region in Brazil. Biological Rhythm Research 52:1432–1437. https://doi.org/10.1080/09291016.2019.1646506

Davison J, Moora M, Öpik M, et al (2015) Global assessment of arbuscular mycorrhizal fungus diversity reveals very low endemism. Science 349:970–973. https://doi.org/10.1126/science.aab1161

Davison J, Moora M, Semchenko M, et al (2021) Temperature and pH define the realised niche space of arbuscular mycorrhizal fungi. New Phytol 231:763–776. https://doi.org/10.1111/nph.17240

Davison J, Öpik M, Zobel M, et al (2012) Communities of Arbuscular Mycorrhizal Fungi Detected in Forest Soil Are Spatially Heterogeneous but Do Not Vary throughout the Growing Season. PLoS ONE 7:e41938. https://doi.org/10.1371/journal.pone.0041938

de Vries FT, Griffiths RI, Bailey M, et al (2018) Soil bacterial networks are less stable under drought than fungal networks. Nat Commun 9:3033. https://doi.org/10.1038/s41467-018-05516-7

DeFalco LA, Esque TC, Scoles-Sciulla SJ, Rodgers J (2010) Desert wildfire and severe drought diminish survivorship of the long-lived Joshua tree (Yucca brevifolia; Agavaceae). American Journal of Botany 97:243–250. https://doi.org/10.3732/ajb.0900032

Deng Y, Jiang Y-H, Yang Y, et al (2012) Molecular ecological network analyses. BMC Bioinformatics 13:113. https://doi.org/10.1186/1471-2105-13-113

Djotan AKG, Matsushita N, Fukuda K (2024) Year-round dynamics of arbuscular mycorrhizal fungi communities in the roots and surrounding soils of Cryptomeria japonica. Mycorrhiza 34:119–130. https://doi.org/10.1007/s00572-024-01143-x

Docherty KM, Balser TC, Bohannan BJM, Gutknecht JLM (2012) Soil microbial responses to fire and interacting global change factors in a California annual grassland. Biogeochemistry 109:63–83. https://doi.org/10.1007/s10533-011-9654-3

Dong L, Bai X, Yu X, et al (2025) Aridity simplified the bacterial network and thus reduced soil multifunctionality in arid and semiarid regions. Plant Soil. https://doi.org/10.1007/s11104-025-07573-6

Dooley SR, Treseder KK (2012) The effect of fire on microbial biomass: a meta-analysis of field studies. Biogeochemistry 109:49–61. https://doi.org/10.1007/s10533-011-9633-8

Dove NC, Hart SC (2017) Fire Reduces Fungal Species Richness and In Situ Mycorrhizal Colonization: A Meta-Analysis. fire ecol 13:37–65. https://doi.org/10.4996/fireecology.130237746

Dumbrell AJ, Ashton PD, Aziz N, et al (2011) Distinct seasonal assemblages of arbuscular mycorrhizal fungi revealed by massively parallel pyrosequencing. New Phytologist 190:794–804. https://doi.org/10.1111/j.1469-8137.2010.03636.x

Earl AM, Losick R, Kolter R (2008) Ecology and genomics of Bacillus subtilis. Trends Microbiol 16:269. https://doi.org/10.1016/j.tim.2008.03.004

Ehleringer JR, Phillips SL, Schuster WSF, Sandquist DR (1991) Differential utilization of summer rains by desert plants. Oecologia 88:430–434. https://doi.org/10.1007/BF00317589

Ellouze W, Hamel C, Singh AK, et al (2018) Abundance of the arbuscular mycorrhizal fungal taxa associated with the roots and rhizosphere soil of different durum wheat cultivars in the Canadian prairies. Can J Microbiol 64:527–536. https://doi.org/10.1139/cjm-2017-0637

Enright DJ, Frangioso KM, Isobe K, et al (2022) Mega-fire in redwood tanoak forest reduces bacterial and fungal richness and selects for pyrophilous taxa that are phylogenetically conserved. Molecular Ecology 31:2475–2493. https://doi.org/10.1111/mec.16399

Enright DJ, Veerabahu A, Quaal RJ, et al (2025) Evaluating Best Practices for Isolating Pyrophilous Bacteria and Fungi from Burned Soil. In: bioRxiv. https://www.biorxiv.org/content/10.1101/2024.09.16.612975v2.abstract. Accessed 16 June 2025

Espinosa J, Dejene T, Guijarro M, et al (2023) Fungal diversity and community composition responses to the reintroduction of fire in a non-managed Mediterranean shrubland ecosystem. Forest Ecosystems 10:100110. https://doi.org/10.1016/j.fecs.2023.100110

Esque TC, Shryock DF, Berry GA, et al (2023) Unprecedented distribution data for Joshua trees (Yucca brevifolia and Y. jaegeriana) reveal contemporary climate

associations of a Mojave Desert icon. Front Ecol Evol 11:. https://doi.org/10.3389/fevo.2023.1266892

Faust K, Lima-Mendez G, Lerat J-S, et al (2015) Cross-biome comparison of microbial association networks. Front Microbiol 6:. https://doi.org/10.3389/fmicb.2015.01200

Feng S, Fu Q (2013) Expansion of global drylands under a warming climate. Atmospheric Chemistry and Physics 13:10081–10094

Fernández-González AJ, Lasa AV, Cobo-Díaz JF, et al (2023) Long-Term Persistence of Three Microbial Wildfire Biomarkers in Forest Soils. Forests 14:1383. https://doi.org/10.3390/f14071383

Fierer N, Jackson JA, Vilgalys R, Jackson RB (2005) Assessment of Soil Microbial Community Structure by Use of Taxon-Specific Quantitative PCR Assays. Applied and Environmental Microbiology 71:4117–4120. https://doi.org/10.1128/AEM.71.7.4117-4120.2005

Fierer N, Jackson RB (2006) The diversity and biogeography of soil bacterial communities. Proceedings of the National Academy of Sciences 103:626–631. https://doi.org/10.1073/pnas.0507535103

Fox J, Weisberg S, Price B, et al (2023) car: Companion to Applied Regression

Fox S, Sikes BA, Brown SP, et al (2022) Fire as a driver of fungal diversity — A synthesis of current knowledge. Mycologia 114:215–241. https://doi.org/10.1080/00275514.2021.2024422

Fox S, Taylor MK, Callaham M, Jumpponen A (2024) Fire-excluded and frequently burned longleaf pine forests have contrasting soil microbial communities. Forest Ecology and Management 551:121519. https://doi.org/10.1016/j.foreco.2023.121519

Gao C, Montoya L, Xu L, et al (2019) Strong succession in arbuscular mycorrhizal fungal communities. The ISME Journal 13:214–226. https://doi.org/10.1038/s41396-018-0264-0

Gao C, Montoya L, Xu L, et al (2020) Fungal community assembly in drought-stressed sorghum shows stochasticity, selection, and universal ecological dynamics. Nat Commun 11:34. https://doi.org/10.1038/s41467-019-13913-9

Gao Y, Xu X, Ding J, et al (2021) The Responses to Long-Term Water Addition of Soil Bacterial, Archaeal, and Fungal Communities in a Desert Ecosystem. Microorganisms 9:981. https://doi.org/10.3390/microorganisms9050981

Garnier S, Ross N, Rudis B, et al (2024) viridis: Colorblind-Friendly Color Maps for R

Gehring CA, Hayer M, Flores-Rentería L, et al (2016) Cheatgrass invasion alters the abundance and composition of dark septate fungal communities in sagebrush steppe. Botany 94:481–491. https://doi.org/10.1139/cjb-2015-0237

Gemma JN, Koske RE, Carreiro M (1989) Seasonal dynamics of selected species of V-A mycorrhizal fungi in a sand dune. Mycological Research 92:317–321. https://doi.org/10.1016/S0953-7562(89)80072-3

Glassman SI, Levine CR, DiRocco AM, et al (2016) Ectomycorrhizal fungal spore bank recovery after a severe forest fire: some like it hot. The ISME Journal 10:1228–1239. https://doi.org/10.1038/ismej.2015.182

Glassman SI, Peay KG, Talbot JM, et al (2015) A continental view of pine-associated ectomycorrhizal fungal spore banks: a quiescent functional guild with a strong biogeographic pattern. New Phytologist 205:1619–1631. https://doi.org/10.1111/nph.13240

Glassman SI, Randolph JWJ, Saroa SS, et al (2023) Prescribed versus wildfire impacts on exotic plants and soil microbes in California grasslands. Applied Soil Ecology 185:104795. https://doi.org/10.1016/j.apsoil.2022.104795

Goddard DR (1935) THE REVERSIBLE HEAT ACTIVATION INDUCING GERMINATION AND INCREASED RESPIRATION IN THE ASCOSPORES OF NEUROSPORA TETRASPERMA. Journal of General Physiology 19:45–60. https://doi.org/10.1085/jgp.19.1.45

Guida RJ, Abella SR, Smith Jr. WJ, et al (2014) Climatic Change and Desert Vegetation Distribution: Assessing Thirty Years of Change in Southern Nevada's Mojave Desert. The Professional Geographer 66:311–322. https://doi.org/10.1080/00330124.2013.787007

Guimerà R, Nunes Amaral LA (2005) Functional cartography of complex metabolic networks. Nature 433:895–900. https://doi.org/10.1038/nature03288

Habeck JR, Mutch RW (1973) Fire-dependent forests in the Northern Rocky Mountains. Quaternary Research 3:408–424. https://doi.org/10.1016/0033-5894(73)90006-9

Hacopian MT, Finks SS, Treseder KK (2024) Drought mediates the response of soil fungal communities post-wildfire in a Californian grassland and coastal sage scrubland. Soil Biology and Biochemistry 196:109511. https://doi.org/10.1016/j.soilbio.2024.109511

Han S, Kim S, Sedlacek CJ, et al (2024) Adaptive traits of Nitrosocosmicus clade ammonia-oxidizing archaea. mBio 15:e02169-24. https://doi.org/10.1128/mbio.02169-24

Hanes TL (1971) Succession after Fire in the Chaparral of Southern California. Ecological Monographs 41:27–52. https://doi.org/10.2307/1942434

Harrower JT, Gilbert GS (2021) Parasitism to mutualism continuum for Joshua trees inoculated with different communities of arbuscular mycorrhizal fungi from a desert elevation gradient. PLOS ONE 16:e0256068. https://doi.org/10.1371/journal.pone.0256068

Hart MM, Reader RJ (2005) The role of the external mycelium in early colonization for three arbuscular mycorrhizal fungal species with different colonization strategies. Pedobiologia 49:269–279. https://doi.org/10.1016/j.pedobi.2004.12.001

Hart SC, DeLuca TH, Newman GS, et al (2005) Post-fire vegetative dynamics as drivers of microbial community structure and function in forest soils. Forest Ecology and Management 220:166–184. https://doi.org/10.1016/j.foreco.2005.08.012

Healy R, Pfister D, Mujic A, et al (2017) Pseudotricharina lanigera (Pezizales), a new species from the Patagonian region of Argentina

Hempel S, Renker C, Buscot F (2007) Differences in the species composition of arbuscular mycorrhizal fungi in spore, root and soil communities in a grassland ecosystem. Environmental Microbiology 9:1930–1938. https://doi.org/10.1111/j.1462-2920.2007.01309.x

Hennecke J, Bassi L, Albracht C, et al (2025) Plant Species Richness and the Root Economics Space Drive Soil Fungal Communities. Ecology Letters 28:e70032. https://doi.org/10.1111/ele.70032

Hernandez DJ, David AS, Menges ES, et al (2021) Environmental stress destabilizes microbial networks. The ISME Journal 15:1722–1734. https://doi.org/10.1038/s41396-020-00882-x

Herren CM, McMahon KD (2017) Cohesion: a method for quantifying the connectivity of microbial communities. The ISME Journal 11:2426–2438. https://doi.org/10.1038/ismej.2017.91

Hirano H, Takemoto K (2019) Difficulty in inferring microbial community structure based on co-occurrence network approaches. BMC Bioinformatics 20:329. https://doi.org/10.1186/s12859-019-2915-1

Holden SR, Rogers BM, Treseder KK, Randerson JT (2016) Fire severity influences the response of soil microbes to a boreal forest fire. Environ Res Lett 11:035004. https://doi.org/10.1088/1748-9326/11/3/035004

Homyak PM, Blankinship JC, Marchus K, et al (2016) Aridity and plant uptake interact to make dryland soils hotspots for nitric oxide (NO) emissions. PNAS 113:E2608–E2616. https://doi.org/10.1073/pnas.1520496113

Hopkins JR, Bennett AE (2023) Spore traits mediate disturbance effects on arbuscular mycorrhizal fungal community composition and mutualisms. Ecology 104:e4016. https://doi.org/10.1002/ecy.4016

Hopkins JR, Bennett AE (2024) Leveraging traits for insight into the fungal ecology of burned ecosystems. Ecosphere 15:e70008. https://doi.org/10.1002/ecs2.70008

Hopkins JR, Bennett AE, McKenna TP (2025) Fire Frequency Driven Increases in Burn Heterogeneity Promote Microbial Beta Diversity: A Test of the Pyrodiversity-Biodiversity Hypothesis. Molecular Ecology 34:e17756. https://doi.org/10.1111/mec.17756

Hopkins JR, Bever JD (2024) Arbuscular mycorrhizal fungal spore communities and co-occurrence networks demonstrate host-specific variation throughout the growing season. Mycorrhiza 34:463–475. https://doi.org/10.1007/s00572-024-01168-2

Hopkins JR, McKenna TP, Bennett AE (2024) Fire season and time since fire determine arbuscular mycorrhizal fungal trait responses to fire. Plant Soil 503:231–245. https://doi.org/10.1007/s11104-024-06500-5

Hopkins JR, Semenova-Nelsen T, Sikes BA (2021) Fungal community structure and seasonal trajectories respond similarly to fire across pyrophilic ecosystems. FEMS Microbiology Ecology 97:fiaa219. https://doi.org/10.1093/femsec/fiaa219

Huang J, Yu H, Guan X, et al (2016) Accelerated dryland expansion under climate change. Nature Clim Change 6:166–171. https://doi.org/10.1038/nclimate2837

Ianson DC, Allen MF (1986) The Effects of Soil Texture on Extraction of Vesicular-Arbuscular Mycorrhizal Fungal Spores from Arid Sites. Mycologia 78:164–168. https://doi.org/10.1080/00275514.1986.12025227

Isola D, Prigione VP, Zucconi L, et al (2022) Knufia obscura sp. nov. and Knufia victoriae sp. nov., two new species from extreme environments. International Journal of Systematic and Evolutionary Microbiology 72:005530. https://doi.org/10.1099/ijsem.0.005530

Jacobson DJ, Powell AJ, Dettman JR, et al (2004) Neurospora in temperate forests of western North America. Mycologia 96:66–74. https://doi.org/10.1080/15572536.2005.11832998

Jacoby R, Peukert M, Succurro A, et al (2017) The Role of Soil Microorganisms in Plant Mineral Nutrition—Current Knowledge and Future Directions. Front Plant Sci 8:. https://doi.org/10.3389/fpls.2017.01617

James TY, Stajich JE, Hittinger CT, Rokas A (2020) Toward a Fully Resolved Fungal Tree of Life. Annu Rev Microbiol 74:291–313. https://doi.org/10.1146/annurev-micro-022020-051835

Jameson BD, Murdock SA, Ji Q, et al (2023) Network analysis of 16S rRNA sequences suggests microbial keystone taxa contribute to marine N2O cycling. Commun Biol 6:212. https://doi.org/10.1038/s42003-023-04597-5

Jiang Y, Sun B, Li H, et al (2015) Aggregate-related changes in network patterns of nematodes and ammonia oxidizers in an acidic soil. Soil Biology and Biochemistry 88:101–109. https://doi.org/10.1016/j.soilbio.2015.05.013

Jiang Z-M, Mou T, Sun Y, et al (2023) Environmental distribution and genomic characteristics of Solirubrobacter, with proposal of two novel species. Front Microbiol 14:. https://doi.org/10.3389/fmicb.2023.1267771

Jiménez-Morillo NT, Almendros G, Miller AZ, et al (2022) Hydrophobicity of soils affected by fires: An assessment using molecular markers from ultra-high resolution mass spectrometry. Sci Total Environ 817:152957. https://doi.org/10.1016/j.scitotenv.2022.152957

Johnson NC (2010) Resource stoichiometry elucidates the structure and function of arbuscular mycorrhizas across scales. New Phytologist 185:631–647. https://doi.org/10.1111/j.1469-8137.2009.03110.x

Johnson RM, Ramond J-B, Gunnigle E, et al (2017) Namib Desert edaphic bacterial, fungal and archaeal communities assemble through deterministic processes but are influenced by different abiotic parameters. Extremophiles 21:381–392. https://doi.org/10.1007/s00792-016-0911-1

Jones DS, Green KM, Brown A, et al (2024) Metagenomic insights into an enigmatic gammaproteobacterium that is important for carbon cycling in cave ecosystems worldwide. 2024.08.23.608578

Jordán F (2009) Keystone species and food webs. Philos Trans R Soc Lond B Biol Sci 364:1733–1741. https://doi.org/10.1098/rstb.2008.0335

Joukhajian A, Glassman SI (2025) Eastern Joshua Tree Arbuscular Mycorrhizal Fungi Largely Consistent Across Roots, Soils, and Seasons. Environmental Microbiology 27:e70138. https://doi.org/10.1111/1462-2920.70138

Joukhajian A, Pulido Barriga MF, Davis MJ, et al Mojave Desert microbial communities show high resistance and resilience over three years despite widespread plant mortality following the Dome Fire. in prep

Kaiser D, Hughson D (2020) The Dome Fire. Sweeney Granite Mountains Desert Research Center Science Newsletter 20

Kajihara KT, Egan CP, Swift SOI, et al (2022) Core arbuscular mycorrhizal fungi are predicted by their high abundance–occupancy relationship while host-specific taxa are rare and geographically structured. New Phytologist 234:1464–1476. https://doi.org/10.1111/nph.18058

Kajihara KT, Hynson NA (2024) Networks as tools for defining emergent properties of microbiomes and their stability. Microbiome 12:184. https://doi.org/10.1186/s40168-024-01868-z

Kakouridis A, Hagen JA, Kan MP, et al (2020) Routes to Roots: Direct Evidence of Water Transport by Arbuscular Mycorrhizal Fungi to Host Plants

Keeley JE (2009) Fire intensity, fire severity and burn severity: a brief review and suggested usage. Int J Wildland Fire 18:116–126. https://doi.org/10.1071/WF07049

Keeley JE, Pausas JG, Rundel PW, et al (2011) Fire as an evolutionary pressure shaping plant traits. Trends in Plant Science 16:406–411. https://doi.org/10.1016/j.tplants.2011.04.002

Keeley JE, Syphard AD (2021) Large California wildfires: 2020 fires in historical context. Fire Ecology 17:22. https://doi.org/10.1186/s42408-021-00110-7

Kemmelmeier K, dos Santos DA, Grittz GS, Stürmer SL (2022) Composition and seasonal variation of the arbuscular mycorrhizal fungi spore community in litter, root mat, and soil from a subtropical rain forest. Mycorrhiza 32:409–423. https://doi.org/10.1007/s00572-022-01084-3

Kennedy LJ, Tiller RL, Stutz JC (2002) Associations between arbuscular mycorrhizal fungi and Sporobolus wrightii in riparian habitats in arid South-western North America. Journal of Arid Environments 50:459–475. https://doi.org/10.1006/jare.2001.0899

Kim S-J, Ahn J-H, Weon H-Y, et al (2016) Flavitalea soli sp. nov. isolated from soil. International Journal of Systematic and Evolutionary Microbiology 66:562–566. https://doi.org/10.1099/ijsem.0.000754

Kindt R (2024) BiodiversityR: Package for Community Ecology and Suitability Analysis

Klinger R, Underwood EC, McKinley R, Brooks ML (2021) Contrasting Geographic Patterns of Ignition Probability and Burn Severity in the Mojave Desert. Front Ecol Evol 9:. https://doi.org/10.3389/fevo.2021.593167

Kobae Y, Hata S (2010) Dynamics of Periarbuscular Membranes Visualized with a Fluorescent Phosphate Transporter in Arbuscular Mycorrhizal Roots of Rice. Plant and Cell Physiology 51:341–353. https://doi.org/10.1093/pcp/pcq013

Kõljalg U, Larsson K-H, Abarenkov K, et al (2005) UNITE: a database providing web-based methods for the molecular identification of ectomycorrhizal fungi. New Phytologist 166:1063–1068. https://doi.org/10.1111/j.1469-8137.2005.01376.x

Koske RE, Gemma JN (1989) A modified procedure for staining roots to detect VA mycorrhizas. Mycological Research 92:486–488

Kozich JJ, Westcott SL, Baxter NT, et al (2013) Development of a Dual-Index Sequencing Strategy and Curation Pipeline for Analyzing Amplicon Sequence Data on the MiSeq Illumina Sequencing Platform. Applied and Environmental Microbiology 79:5112–5120. https://doi.org/10.1128/AEM.01043-13

Kurbessoian T, Ahmed SA, Quan Y, et al (2024) Description of new micro-colonial fungi species Neophaeococcomyces mojavensis, Coniosporium tulheliwenetii, and Taxawa tesnikishii cultured from biological soil crusts. 2024.06.12.598762

Kurtz ZD, Müller CL, Miraldi ER, et al (2015) Sparse and Compositionally Robust Inference of Microbial Ecological Networks. PLOS Computational Biology 11:e1004226. https://doi.org/10.1371/journal.pcbi.1004226

Lee J, Lee S, Young JPW (2008) Improved PCR primers for the detection and identification of arbuscular mycorrhizal fungi. FEMS Microbiology Ecology 65:339–349. https://doi.org/10.1111/j.1574-6941.2008.00531.x

Lehmann A, Zheng W, Ryo M, et al (2020) Fungal Traits Important for Soil Aggregation. Front Microbiol 10:. https://doi.org/10.3389/fmicb.2019.02904

Lekberg Y, Gibbons SM, Rosendahl S, Ramsey PW (2013) Severe plant invasions can increase mycorrhizal fungal abundance and diversity. ISME J 7:1424–1433. https://doi.org/10.1038/ismej.2013.41

Lenz L (2007) Reassessment of Yucca brevifolia and Recognition of Y. jaegeriana as a Distinct Species. Aliso: A Journal of Systematic and Floristic Botany 24:97–104. https://doi.org/10.5642/aliso.20072401.07

Li J, Gao R, Chen Y, et al (2020) Isolation and Identification of Microvirga thermotolerans HR1, a Novel Thermo-Tolerant Bacterium, and Comparative Genomics among Microvirga Species. Microorganisms 8:101. https://doi.org/10.3390/microorganisms8010101

Li Q, Song A, Yang H, Müller WEG (2021) Impact of Rocky Desertification Control on Soil Bacterial Community in Karst Graben Basin, Southwestern China. Front Microbiol 12:. https://doi.org/10.3389/fmicb.2021.636405

Li X, Kimball S, Ta P, et al (2024) Understanding post-fire vegetation recovery in southern California ecosystems with the aid of pre-fire observations from long-term monitoring. Journal of Vegetation Science 35:e13308. https://doi.org/10.1111/jvs.13308

Liao J, Wolfe GM, Hannun RA, et al (2021) Formaldehyde evolution in US wildfire plumes during the Fire Influence on Regional to Global Environments and Air Quality experiment (FIREX-AQ). Atmospheric Chemistry and Physics 21:18319–18331. https://doi.org/10.5194/acp-21-18319-2021

Liu CM, Kachur S, Dwan MG, et al (2012) FungiQuant: A broad-coverage fungal quantitative real-time PCR assay. BMC Microbiology 12:255. https://doi.org/10.1186/1471-2180-12-255

Liu X, Lindemann WC, Whitford WG, Steiner RL (2000) Microbial diversity and activity of disturbed soil in the northern Chihuahuan Desert. Biol Fertil Soils 32:243–249. https://doi.org/10.1007/s003740000242

Lopez A, Anthony M, Catalan-Dibene J, et al (2024) Dryland fungi are spatially heterogeneous and resistant to global change drivers. Ecosphere 15:e70031. https://doi.org/10.1002/ecs2.70031

Love MI, Huber W, Anders S (2014) Moderated estimation of fold change and dispersion for RNA-seq data with DESeq2. Genome Biol 15:550. https://doi.org/10.1186/s13059-014-0550-8

Lucas-Borja ME, Miralles I, Ortega R, et al (2019) Immediate fire-induced changes in soil microbial community composition in an outdoor experimental controlled system. Science of The Total Environment 696:134033. https://doi.org/10.1016/j.scitotenv.2019.134033

Luo W, Wang P, Liu J, Tao J (2025) Microbial keystone taxa and network complexity, rather than diversity, sustain soil multifunctionality along an elevational gradient in a subtropical karst mountain. CATENA 256:109115. https://doi.org/10.1016/j.catena.2025.109115

Maestre FT, Benito BM, Berdugo M, et al (2021) Biogeography of global drylands. New Phytologist 231:540–558. https://doi.org/10.1111/nph.17395

Maitra P, Zheng Y, Chen L, et al (2019) Effect of drought and season on arbuscular mycorrhizal fungi in a subtropical secondary forest. Fungal Ecology 41:107–115. https://doi.org/10.1016/j.funeco.2019.04.005

Makhalanyane TP, Valverde A, Gunnigle E, et al (2015) Microbial ecology of hot desert edaphic systems. FEMS Microbiology Reviews 39:203–221. https://doi.org/10.1093/femsre/fuu011

Malicka M, Magurno F, Piotrowska-Seget Z (2022) Plant association with dark septate endophytes: When the going gets tough (and stressful), the tough fungi get going. Chemosphere 302:134830. https://doi.org/10.1016/j.chemosphere.2022.134830

Martin M (2011) Cutadapt removes adapter sequences from high-throughput sequencing reads. EMBnet.journal 17:10–12. https://doi.org/10.14806/ej.17.1.200

Martinez DJ, Seraphin B, Marks-Block T, et al (2023) Indigenous Fire Futures: Anticolonial Approaches to Shifting Fire Relations in California. Environment and Society 14:142–161. https://doi.org/10.3167/ares.2023.140109

Martin-Pozas T, Cuezva S, Fernandez-Cortes A, et al (2022) Role of subterranean microbiota in the carbon cycle and greenhouse gas dynamics. Science of The Total Environment 831:154921. https://doi.org/10.1016/j.scitotenv.2022.154921

Martin-Pozas T, Jurado V, Fernandez-Cortes A, et al (2024) Bacterial communities forming yellow biofilms in different cave types share a common core. Science of The Total Environment 956:177263. https://doi.org/10.1016/j.scitotenv.2024.177263

Matchado MS, Lauber M, Reitmeier S, et al (2021) Network analysis methods for studying microbial communities: A mini review. Computational and Structural Biotechnology Journal 19:2687–2698. https://doi.org/10.1016/j.csbj.2021.05.001

McAuliffe JR (2016) Perennial Grass-dominated Plant Communities of the Eastern Mojave Desert Region. Desert Plants 32:8–92

McGonigle TP, Miller MH, Evans DG, et al (1990) A new method which gives an objective measure of colonization of roots by vesicular—arbuscular mycorrhizal

fungi. New Phytologist 115:495–501. https://doi.org/10.1111/j.1469-8137.1990.tb00476.x

McKenney MC, Lindsey DL (1987) Improved Method for Quantifying Endomycorrhizal Fungi Spores from Soil. Mycologia 79:779–782. https://doi.org/10.1080/00275514.1987.12025458

McMullan-Fisher SJ, May TW, Keane PJ (2002) The macrofungal community and fire in a Mountain Ash forest in southern Australia. Fungal Diversity 57–76

McMurdie PJ, Holmes S (2013) phyloseq: An R Package for Reproducible Interactive Analysis and Graphics of Microbiome Census Data. PLOS ONE 8:e61217. https://doi.org/10.1371/journal.pone.0061217

Meinshausen N, Bühlmann P (2006) High-dimensional graphs and variable selection with the Lasso. Annals of Statistics 34:

Meng L, Zhang A, Wang F, et al (2015) Arbuscular mycorrhizal fungi and rhizobium facilitate nitrogen uptake and transfer in soybean/maize intercropping system. Front Plant Sci 6:339. https://doi.org/10.3389/fpls.2015.00339

Mino L, Kolp MR, Fox S, et al (2021) Watershed and fire severity are stronger determinants of soil chemistry and microbiomes than within-watershed woody encroachment in a tallgrass prairie system. FEMS Microbiology Ecology 97:fiab154. https://doi.org/10.1093/femsec/fiab154

Miriti MN, Rodríguez-Buriticá S, Wright SJ, Howe HF (2007) Episodic Death Across Species of Desert Shrubs. Ecology 88:32–36. https://doi.org/10.1890/0012-9658(2007)88%255B32:EDASOD%255D2.0.CO;2

Moura JB, Souza RF, Vieira-Júnior WG, et al (2022) Effects of a megafire on the arbuscular mycorrhizal fungal community and parameters in the Brazilian Cerrado ecosystem. Forest Syst 31:e001–e001. https://doi.org/10.5424/fs/2022311-18557

Mu Y, Zhou L, Zeng X-C, et al (2016) Arsenicitalea aurantiaca gen. nov., sp. nov., a new member of the family Hyphomicrobiaceae, isolated from high-arsenic sediment. International Journal of Systematic and Evolutionary Microbiology 66:5478–5484. https://doi.org/10.1099/ijsem.0.001543

Mummey DL, Rillig MC (2006) The invasive plant species Centaurea maculosa alters arbuscular mycorrhizal fungal communities in the field. Plant Soil 288:81–90. https://doi.org/10.1007/s11104-006-9091-6

Muñoz-Rojas M, Erickson TE, Martini D, et al (2016) Soil physicochemical and microbiological indicators of short, medium and long term post-fire recovery in semi-arid ecosystems. Ecological Indicators 63:14–22. https://doi.org/10.1016/j.ecolind.2015.11.038

Neary DG, Klopatek CC, DeBano LF, Ffolliott PF (1999) Fire effects on belowground sustainability: a review and synthesis. Forest Ecology and Management 122:51–71. https://doi.org/10.1016/S0378-1127(99)00032-8

Nelson AR, Narrowe AB, Rhoades CC, et al (2022a) Wildfire-dependent changes in soil microbiome diversity and function. Nat Microbiol 7:1419–1430. https://doi.org/10.1038/s41564-022-01203-y

Nelson AR, Narrowe AB, Rhoades CC, et al (2022b) Wildfire-dependent changes in soil microbiome diversity and function. Nat Microbiol 7:1419–1430. https://doi.org/10.1038/s41564-022-01203-y

Nelson AR, Rhoades CC, Fegel TS, et al (2024) Wildfire impact on soil microbiome life history traits and roles in ecosystem carbon cycling. ISME Commun 4:ycae108. https://doi.org/10.1093/ismeco/ycae108

Neuenkamp L, Moora M, Öpik M, et al (2018) The role of plant mycorrhizal type and status in modulating the relationship between plant and arbuscular mycorrhizal fungal communities. New Phytologist 220:1236–1247. https://doi.org/10.1111/nph.14995

Nguyen NH, Song Z, Bates ST, et al (2016) FUNGuild: An open annotation tool for parsing fungal community datasets by ecological guild. Fungal Ecology 20:241–248. https://doi.org/10.1016/j.funeco.2015.06.006

Norman JS, King GM, Friesen ML (2017) Rubrobacter spartanus sp. nov., a moderately thermophilic oligotrophic bacterium isolated from volcanic soil. International Journal of Systematic and Evolutionary Microbiology 67:3597–3602. https://doi.org/10.1099/ijsem.0.002175

NPS. (2020) Dome Fire - Mojave National Preserve (U.S. National Park Service). https://www.nps.gov/moja/learn/nature/dome-fire.htm. Accessed 7 May 2021

Oksanen J, Kindt R, Legendre P, et al (2008) The vegan Package. http://vegan.r-forge.r-project.org/. Accessed 22 Aug 2021

Oksanen J, Simpson GL, Blanchet FG, et al (2022) vegan: Community Ecology Package

Öpik M, Vanatoa A, Vanatoa E, et al (2010) The online database MaarjAM reveals global and ecosystemic distribution patterns in arbuscular mycorrhizal fungi

(Glomeromycota). New Phytologist 188:223–241. https://doi.org/10.1111/j.1469-8137.2010.03334.x

Packard EE, Durall DM, Jones MD (2023) Successional changes in fungal communities occur a few weeks following wildfire in a mixed Douglas-fir-ponderosa pine forest. Fungal Ecology 63:101246. https://doi.org/10.1016/j.funeco.2023.101246

Pascual J, García-López M, Bills GF, Genilloud O (2016) Longimicrobium terrae gen. nov., sp. nov., an oligotrophic bacterium of the under-represented phylum Gemmatimonadetes isolated through a system of miniaturized diffusion chambers. International Journal of Systematic and Evolutionary Microbiology 66:1976–1985. https://doi.org/10.1099/ijsem.0.000974

Pausas JG, Keeley JE (2021) Wildfires and global change. Frontiers in Ecology and the Environment 19:387–395. https://doi.org/10.1002/fee.2359

Paz C, Öpik M, Bulascoschi L, et al (2021) Dispersal of Arbuscular Mycorrhizal Fungi: Evidence and Insights for Ecological Studies. Microb Ecol 81:283–292. https://doi.org/10.1007/s00248-020-01582-x

Pepe A, Giovannetti M, Sbrana C (2018) Lifespan and functionality of mycorrhizal fungal mycelium are uncoupled from host plant lifespan. Sci Rep 8:10235. https://doi.org/10.1038/s41598-018-28354-5

Pérez-Valera E, Goberna M, Faust K, et al (2017) Fire modifies the phylogenetic structure of soil bacterial co-occurrence networks. Environmental Microbiology 19:317–327. https://doi.org/10.1111/1462-2920.13609

Pérez-Valera E, Verdú M, Navarro-Cano JA, Goberna M (2018) Resilience to fire of phylogenetic diversity across biological domains. Molecular Ecology 27:2896–2908. https://doi.org/10.1111/mec.14729

Pérez-Valera E, Verdú M, Navarro-Cano JA, Goberna M (2018) Resilience to fire of phylogenetic diversity across biological domains. Molecular Ecology 27:2896–2908. https://doi.org/10.1111/mec.14729

Pinheiro J, Bates D, DebRoy S, et al (2017) Package 'nlme.' Linear and nonlinear mixed effects models, version 3:274

Placella SA, Brodie EL, Firestone MK (2012) Rainfall-induced carbon dioxide pulses result from sequential resuscitation of phylogenetically clustered microbial groups. Proceedings of the National Academy of Sciences 109:10931–10936. https://doi.org/10.1073/pnas.1204306109

Põlme S, Abarenkov K, Henrik Nilsson R, et al (2020) FungalTraits: a user-friendly traits database of fungi and fungus-like stramenopiles. Fungal Diversity 105:1–16. https://doi.org/10.1007/s13225-020-00466-2

Pombubpa N, Pietrasiak N, De Ley P, Stajich JE (2020) Insights into dryland biocrust microbiome: geography, soil depth and crust type affect biocrust microbial communities and networks in Mojave Desert, USA. FEMS Microbiology Ecology 96:fiaa125. https://doi.org/10.1093/femsec/fiaa125

Porras-Alfaro A, Herrera J, Natvig DO, Sinsabaugh RL (2007) Effect of long-term nitrogen fertilization on mycorrhizal fungi associated with a dominant grass in a semiarid grassland. Plant Soil 296:65–75. https://doi.org/10.1007/s11104-007-9290-9

Powell JR, Parrent JL, Hart MM, et al (2009) Phylogenetic trait conservatism and the evolution of functional trade-offs in arbuscular mycorrhizal fungi. Proceedings of the Royal Society B: Biological Sciences 276:4237–4245. https://doi.org/10.1098/rspb.2009.1015

Powell JR, Rillig MC (2018) Biodiversity of arbuscular mycorrhizal fungi and ecosystem function. New Phytologist 220:1059–1075. https://doi.org/10.1111/nph.15119

Power ME, Tilman D, Estes JA, et al (1996) Challenges in the quest for keystones: identifying keystone species is difficult—but essential to understanding how loss of species will affect ecosystems. BioScience 46:609–620

Pressler Y, Moore JC, Cotrufo MF (2019) Belowground community responses to fire: meta-analysis reveals contrasting responses of soil microorganisms and mesofauna. Oikos 128:309–327. https://doi.org/10.1111/oik.05738

Prober SM, Leff JW, Bates ST, et al (2015) Plant diversity predicts beta but not alpha diversity of soil microbes across grasslands worldwide. Ecol Lett 18:85–95. https://doi.org/10.1111/ele.12381

Pulido-Chavez MF (2023) Measuring the Succession, Functions and Resilience of Soil Microbes After a Chaparral Wildfire. Ph.D., University of California, Riverside

Pulido-Chavez MF, Randolph JWJ, Zalman C, et al (2023) Rapid bacterial and fungal successional dynamics in first year after chaparral wildfire. Molecular Ecology 32:1685–1707. https://doi.org/10.1111/mec.16835

Quast C, Pruesse E, Yilmaz P, et al (2013) The SILVA ribosomal RNA gene database project: improved data processing and web-based tools. Nucleic Acids Research 41:D590–D596. https://doi.org/10.1093/nar/gks1219

R Core Team (2020) R: A language and environment for statistical computing. https://www.R-project.org/. Accessed 22 Aug 2021

Ramond J-B, Cowan DA (2022) Microbial Ecology of Hot Desert Soils. In: Ramond J-B, Cowan DA (eds) Microbiology of Hot Deserts. Springer International Publishing, Cham, pp 89–110

Ravi S, Law DJ, Caplan JS, et al (2022) Biological invasions and climate change amplify each other's effects on dryland degradation. Global Change Biology 28:285–295. https://doi.org/10.1111/gcb.15919

Rawstern AH, Hernandez DJ, Afkhami ME (2025) Central Taxa Are Keystone Microbes During Early Succession. Ecology Letters 28:e70031. https://doi.org/10.1111/ele.70031

Revillini D, David AS, Menges ES, et al (2022) Microbiome-mediated response to pulse fire disturbance outweighs the effects of fire legacy on plant performance. New Phytologist 233:2071–2082. https://doi.org/10.1111/nph.17689

Ripley B, Venables B, Bates DM, et al (2024) MASS: Support Functions and Datasets for Venables and Ripley's MASS

Risely A (2020) Applying the core microbiome to understand host–microbe systems. Journal of Animal Ecology 89:1549–1558. https://doi.org/10.1111/1365-2656.13229

Rodríguez J, González-Pérez JA, Turmero A, et al (2018) Physico-chemical and microbial perturbations of Andalusian pine forest soils following a wildfire. Science of The Total Environment 634:650–660. https://doi.org/10.1016/j.scitotenv.2018.04.028

Royer AM, Streisfeld MA, Smith CI (2016) Population genomics of divergence within an obligate pollination mutualism: Selection maintains differences between Joshua tree species. American Journal of Botany 103:1730–1741. https://doi.org/10.3732/ajb.1600069

Rundel PW, Gibson AC (1997) Ecological Communities and Processes in a Mojave Desert Ecosystem. The New Phytologist 137:703–707. https://doi.org/10.1046/j.1469-8137.1997.00872-4.x

Sáenz de Miera LE, Pinto R, Gutierrez-Gonzalez JJ, et al (2020) Wildfire effects on diversity and composition in soil bacterial communities. Science of The Total Environment 726:138636. https://doi.org/10.1016/j.scitotenv.2020.138636

Salazar G (2015) EcolUtils: Utilities for community ecology analysis

Sánchez-Castro I, Ferrol N, Cornejo P, Barea J-M (2012) Temporal dynamics of arbuscular mycorrhizal fungi colonizing roots of representative shrub species in a semi-arid Mediterranean ecosystem. Mycorrhiza 22:449–460. https://doi.org/10.1007/s00572-011-0421-z

Sari E, Enright DJ, Ordonez M, et al (2025) Gene Duplication, Horizontal Gene Transfer, and Trait Trade-offs Drive Evolution of Post-Fire Resource Acquisition in Pyrophilous Fungi. 2025.07.17.665399

Schlesinger WH, Reynolds JF, Cunningham GL, et al (1990) Biological feedbacks in global desertification. Science 247:1043–1048

Schloss PD (2024) Rarefaction is currently the best approach to control for uneven sequencing effort in amplicon sequence analyses. mSphere 9:e00354-23. https://doi.org/10.1128/msphere.00354-23

Schoch CL, Seifert KA, Huhndorf S, et al (2012) Nuclear ribosomal internal transcribed spacer (ITS) region as a universal DNA barcode marker for Fungi. PNAS 109:6241–6246. https://doi.org/10.1073/pnas.1117018109

Schoen C, Montibeler M, Costa MD, et al (2021) Inter and intra-specific variability in arbuscular mycorrhizal fungi affects hosts and soil health. Symbiosis 85:273–289. https://doi.org/10.1007/s13199-021-00812-1

Schultz BB (1985) Levene's Test for Relative Variation. Systematic Biology 34:449–456. https://doi.org/10.1093/sysbio/34.4.449

Schussman H, Enquist C, List M (2006) Historic fire return intervals for Arizona and New Mexico: A regional perspective for southwestern land managers. The Nature Conservancy: Phoenix, AZ, USA

Seaver FJ (1909) Studies in Pyrophilous Fungi—I. The Occurrence and Cultivation of Pyronema. Mycologia

Semenova-Nelsen TA, Platt WJ, Patterson TR, et al (2019) Frequent fire reorganizes fungal communities and slows decomposition across a heterogeneous pine savanna landscape. New Phytologist 224:916–927. https://doi.org/10.1111/nph.16096

Senés-Guerrero C, Schüßler A (2016) A conserved arbuscular mycorrhizal fungal core-species community colonizes potato roots in the Andes. Fungal Diversity 77:317–333. https://doi.org/10.1007/s13225-015-0328-7

Sepp S-K, Davison J, Jairus T, et al (2019) Non-random association patterns in a plant–mycorrhizal fungal network reveal host–symbiont specificity. Molecular Ecology 28:365–378. https://doi.org/10.1111/mec.14924

Shade A, Peter H, Allison SD, et al (2012) Fundamentals of Microbial Community Resistance and Resilience. Front Microbiol 3:. https://doi.org/10.3389/fmicb.2012.00417

Shapiro SS, Wilk MB (1965) An analysis of variance test for normality (complete samples). Biometrika 52:591–611. https://doi.org/10.1093/biomet/52.3-4.591

Smith CI, Godsoe WKW, Tank S, et al (2008) Distinguishing Coevolution from Covicariance in an Obligate Pollination Mutualism: Asynchronous Divergence in Joshua Tree and Its Pollinators. Evolution 62:2676–2687. https://doi.org/10.1111/j.1558-5646.2008.00500.x

Smith CI, Sweet LC, Yoder J, et al (2023) Dust storms ahead: Climate change, green energy development and endangered species in the Mojave Desert. Biological Conservation 277:109819. https://doi.org/10.1016/j.biocon.2022.109819

Smith SE, Read DJ (2010) Mycorrhizal Symbiosis. Academic Press

Soria R, Tortosa A, Rodríguez-Berbel N, et al (2023) Short-Term Response of Soil Bacterial Communities after Prescribed Fires in Semi-Arid Mediterranean Forests. Fire 6:145. https://doi.org/10.3390/fire6040145

Stanton RL, Nusink BC, Cass KL, et al (2023) Fire frequency effects on plant community characteristics in the Great Basin and Mojave deserts of North America. Fire Ecology 19:60. https://doi.org/10.1186/s42408-023-00222-2

Stark JM, Firestone MK (1995) Mechanisms for soil moisture effects on activity of nitrifying bacteria. Applied and Environmental Microbiology 61:218–221. https://doi.org/10.1128/aem.61.1.218-221.1995

Steven B, Phillips ML, Belnap J, et al (2021) Resistance, Resilience, and Recovery of Dryland Soil Bacterial Communities Across Multiple Disturbances. Front Microbiol 12:. https://doi.org/10.3389/fmicb.2021.648455

Stinson KA, Campbell SA, Powell JR, et al (2006) Invasive Plant Suppresses the Growth of Native Tree Seedlings by Disrupting Belowground Mutualisms. PLOS Biology 4:e140. https://doi.org/10.1371/journal.pbio.0040140

Stürmer SL, Bever JD, Schultz PA, Bentivenga SP (2021) Celebrating INVAM: 35 years of the largest living culture collection of arbuscular mycorrhizal fungi. Mycorrhiza 31:117–126. https://doi.org/10.1007/s00572-020-01008-z

Stürmer SL, Heinz KGH, Marascalchi MN, et al (2022) Wildfire does not affect spore abundance, species richness, and inoculum potential of arbuscular mycorrhizal fungi (Glomeromycota) in ferruginous Canga ecosystems. Acta Bot Bras 36:e2021abb0218. https://doi.org/10.1590/0102-33062021abb0218

Su W, Tang C, Lin J, et al (2022) Recovery patterns of soil bacterial and fungal communities in Chinese boreal forests along a fire chronosequence. Science of The Total Environment 805:150372. https://doi.org/10.1016/j.scitotenv.2021.150372

Sweet LC, Green T, Heintz JGC, et al (2019) Congruence between future distribution models and empirical data for an iconic species at Joshua Tree National Park. Ecosphere 10:e02763. https://doi.org/10.1002/ecs2.2763

Tagestad J, Brooks M, Cullinan V, et al (2016) Precipitation regime classification for the Mojave Desert: Implications for fire occurrence. Journal of Arid Environments 124:388–397. https://doi.org/10.1016/j.jaridenv.2015.09.002

Taniguchi T, Isobe K, Imada S, et al (2023) Root endophytic bacterial and fungal communities in a natural hot desert are differentially regulated in dry and wet seasons by stochastic processes and functional traits. Science of The Total Environment 899:165524. https://doi.org/10.1016/j.scitotenv.2023.165524

Tawaraya K (2003) Arbuscular mycorrhizal dependency of different plant species and cultivars. Soil Science and Plant Nutrition 49:655–668. https://doi.org/10.1080/00380768.2003.10410323

Taylor DL, Walters WA, Lennon NJ, et al (2016) Accurate Estimation of Fungal Diversity and Abundance through Improved Lineage-Specific Primers Optimized for Illumina Amplicon Sequencing. Appl Environ Microbiol 82:7217–7226. https://doi.org/10.1128/AEM.02576-16

Thomma BPHJ (2003) Alternaria spp.: from general saprophyte to specific parasite. Molecular Plant Pathology 4:225–236. https://doi.org/10.1046/j.1364-3703.2003.00173.x

Timóteo S, Albrecht J, Rumeu B, et al (2023) Tripartite networks show that keystone species can multitask. Functional Ecology 37:274–286. https://doi.org/10.1111/1365-2435.14206

Titus JH, Nowak RS, Smith SD (2002a) Soil resource heterogeneity in the Mojave Desert. Journal of Arid Environments 52:269–292. https://doi.org/10.1006/jare.2002.1010

Titus JH, Titus PJ, Nowak RS, Smith SD (2002b) Arbuscular mycorrhizae of Mojave Desert plants. Western North American Naturalist 62:327–334

Tourna M, Stieglmeier M, Spang A, et al (2011) Nitrososphaera viennensis, an ammonia oxidizing archaeon from soil. Proceedings of the National Academy of Sciences 108:8420–8425. https://doi.org/10.1073/pnas.1013488108

Traveset A, Tur C, Eguíluz VM (2017) Plant survival and keystone pollinator species in stochastic coextinction models: role of intrinsic dependence on animal-pollination. Sci Rep 7:6915. https://doi.org/10.1038/s41598-017-07037-7

Turco M, Abatzoglou JT, Herrera S, et al (2023) Anthropogenic climate change impacts exacerbate summer forest fires in California. Proceedings of the National Academy of Sciences 120:e2213815120. https://doi.org/10.1073/pnas.2213815120

Vachula RS, Russell JM, Huang Y (2019) Climate exceeded human management as the dominant control of fire at the regional scale in California's Sierra Nevada. Environ Res Lett 14:104011. https://doi.org/10.1088/1748-9326/ab4669

Vale T (2013) Fire, Native Peoples, and the Natural Landscape. Island Press

Vamstad MS, Rotenberry JT (2010) Effects of fire on vegetation and small mammal communities in a Mojave Desert Joshua tree woodland. Journal of Arid Environments 74:1309–1318. https://doi.org/10.1016/j.jaridenv.2010.04.002

Van Der Heijden MGA, Bardgett RD, Van Straalen NM (2008) The unseen majority: soil microbes as drivers of plant diversity and productivity in terrestrial ecosystems. Ecology Letters 11:296–310. https://doi.org/10.1111/j.1461-0248.2007.01139.x

van der Spuy JE (1975) The heat resistance of moulds Penicillium vermiculatum Dangeard and Penicillium brefeldianum Dodge in apple juice. Phytophylactica 7:105–108

Varela-Cervero S, Vasar M, Davison J, et al (2015) The composition of arbuscular mycorrhizal fungal communities differs among the roots, spores and extraradical mycelia associated with five Mediterranean plant species. Environmental Microbiology 17:2882–2895. https://doi.org/10.1111/1462-2920.12810

Vasar M, Davison J, Sepp S-K, et al (2021) Arbuscular Mycorrhizal Fungal Communities in the Soils of Desert Habitats. Microorganisms 9:229. https://doi.org/10.3390/microorganisms9020229

Vega-Cofre MV, Williams W, Song Y, et al (2023) Effects of grazing and fire management on rangeland soil and biocrust microbiomes. Ecological Indicators 148:110094. https://doi.org/10.1016/j.ecolind.2023.110094

Wang G, Mayes MA, Gu L, Schadt CW (2014) Representation of Dormant and Active Microbial Dynamics for Ecosystem Modeling. PLOS ONE 9:e89252. https://doi.org/10.1371/journal.pone.0089252

Wang J, Chen C, Ye Z, et al (2018) Relationships Between Fungal and Plant Communities Differ Between Desert and Grassland in a Typical Dryland Region of Northwest China. Front Microbiol 9:. https://doi.org/10.3389/fmicb.2018.02327

Wang L, Jiao W, MacBean N, et al (2022a) Dryland productivity under a changing climate. Nat Clim Chang 12:981–994. https://doi.org/10.1038/s41558-022-01499-y

Wang S, Zuo X, Awada T, et al (2021) Changes of soil bacterial and fungal community structure along a natural aridity gradient in desert grassland ecosystems, Inner Mongolia. CATENA 205:105470. https://doi.org/10.1016/j.catena.2021.105470

Wang X, Liang C, Mao J, et al (2023) Microbial keystone taxa drive succession of plant residue chemistry. ISME J 17:748–757. https://doi.org/10.1038/s41396-023-01384-2

Wang X-B, Azarbad H, Leclerc L, et al (2022b) A Drying-Rewetting Cycle Imposes More Important Shifts on Soil Microbial Communities than Does Reduced Precipitation. mSystems 7:e00247-22. https://doi.org/10.1128/msystems.00247-22

Wang Z, Na R, Koziol L, et al (2020) Response of bacterial communities and plant-mediated soil processes to nitrogen deposition and precipitation in a desert steppe. Plant Soil 448:277–297. https://doi.org/10.1007/s11104-020-04424-4

Warcup JH (1990) Occurrence of ectomycorrhizal and saprophytic discomycetes after a wild fire in a eucalypt forest. Mycological Research 94:1065–1069. https://doi.org/10.1016/S0953-7562(09)81334-8

Warren SD, Clair LL, Stark LR, et al (2019) Reproduction and Dispersal of Biological Soil Crust Organisms. Front Ecol Evol 7:. https://doi.org/10.3389/fevo.2019.00344

Weber SE, Diez JM, Andrews LV, et al (2019) Responses of arbuscular mycorrhizal fungi to multiple coinciding global change drivers. Fungal Ecology 40:62–71. https://doi.org/10.1016/j.funeco.2018.11.008

Wei X-Y, Zhu H-Y, Song L, et al (2022) Yeast Diversity in the Qaidam Basin Desert in China with the Description of Five New Yeast Species. Journal of Fungi 8:858. https://doi.org/10.3390/jof8080858

Weiss S, Xu ZZ, Peddada S, et al (2017) Normalization and microbial differential abundance strategies depend upon data characteristics. Microbiome 5:27. https://doi.org/10.1186/s40168-017-0237-y

Whitman T, Whitman E, Woolet J, et al (2019) Soil bacterial and fungal response to wildfires in the Canadian boreal forest across a burn severity gradient. Soil Biology and Biochemistry 138:107571. https://doi.org/10.1016/j.soilbio.2019.107571

Whitman T, Woolet J, Sikora M, et al (2022) Resilience in soil bacterial communities of the boreal forest from one to five years after wildfire across a severity gradient. Soil Biology and Biochemistry 172:108755. https://doi.org/10.1016/j.soilbio.2022.108755

Whitman T, Woolet J, Sikora MC, et al (2025) Resilience not yet apparent in soil fungal communities of the boreal forest from one to five years after wildfire across a severity gradient. 2025.03.29.646032

Wilkening JL, Hoffmann SL, Sirchia F (2022) Examining the past, present, and future of an iconic Mojave Desert species, the Joshua tree (Yucca brevifolia, Yucca jaegeriana). The Southwestern Naturalist 65:. https://doi.org/10.1894/0038-4909-65.3-4.216

Wilkin KM, Ponisio LC, Fry DL, et al (2017) Decade-Long Plant Community Responses to Shrubland Fuel Hazard Reduction. fire ecol 13:105–136. https://doi.org/10.4996/fireecology.130210513

Willms IM, Rudolph AY, Göschel I, et al (2020) Globally Abundant "Candidatus Udaeobacter" Benefits from Release of Antibiotics in Soil and Potentially Performs Trace Gas Scavenging. mSphere 5:10.1128/msphere.00186-20. https://doi.org/10.1128/msphere.00186-20

Woolet J, Whitman E, Parisien M-A, et al (2022) Effects of short-interval reburns in the boreal forest on soil bacterial communities compared to long-interval reburns. FEMS Microbiol Ecol 98:fiac069. https://doi.org/10.1093/femsec/fiac069

Woolet J, Whitman T (2020) Pyrogenic organic matter effects on soil bacterial community composition. Soil Biology and Biochemistry 141:107678. https://doi.org/10.1016/j.soilbio.2019.107678

Wu J, Liu Y, Sui H, et al (2019) Using network analysis to identify keystone species in the food web of Haizhou Bay, China. Mar Freshwater Res 71:469–481. https://doi.org/10.1071/MF18417

Yang M, Luo X, Cai Y, et al (2024) Effect of fire and post-fire management on soil microbial communities in a lower subtropical forest ecosystem after a mountain fire. Journal of Environmental Management 351:119885. https://doi.org/10.1016/j.jenvman.2023.119885

Yang T, Tedersoo L, Liu X, et al (2022) Fungi stabilize multi-kingdom community in a high elevation timberline ecosystem. iMeta 1:e49. https://doi.org/10.1002/imt2.49

Zeng N, Yoon J (2009) Expansion of the world's deserts due to vegetation-albedo feedback under global warming. Geophysical Research Letters 36:. https://doi.org/10.1029/2009GL039699

Zhang Y, Du Y, Mu Z, et al (2025) Response of Soil Microbial Communities in Extreme Arid Deserts to Different Long-Term Management Methods. Forests 16:306. https://doi.org/10.3390/f16020306

Zheng W, Morris EK, Rillig MC (2014) Ectomycorrhizal fungi in association with *Pinus sylvestris* seedlings promote soil aggregation and soil water repellency. Soil Biology and Biochemistry 78:326–331. https://doi.org/10.1016/j.soilbio.2014.07.015

Zhou G, Eisenhauer N, Du Z, et al (2025) Fire-driven disruptions of global soil biochemical relationships. Nat Commun 16:1190. https://doi.org/10.1038/s41467-025-56598-z

Zuo Y, Hu Q, Liu J, He X (2022) Relationship of root dark septate endophytes and soil factors to plant species and seasonal variation in extremely arid desert in Northwest China. Applied Soil Ecology 175:104454. https://doi.org/10.1016/j.apsoil.2022.104454